THE SYNTHESIS AND ENZYMATIC EVALUATION OF BIOLOGICALLY RELEVANT SUGAR 1-PHOSPHONATES

By

Gaia Ashlee Aish

Submitted in partial fulfillment of the requirements

for the degree of Master of Science

at

Dalhousie University

Halifax, Nova Scotia

August 2013

~ for Derrick and Stella ~

Do you think that the caterpillar knows
that one day it will become a butterfly?
Or does the butterfly know
that once it was a caterpillar.

Table of Contents

List of Tables

List of Figures

List of Schemes

Abstract

Phosphonates are commonly used as hydrolytically stable phosphate mimics to explore a multitude of biological processes. This general approach has lead to the development of enzyme inhibitors, antifungals, antibiotics, and anticancer agents. Physiologically, sugar 1-phosphates are utilized by nucleotidylyltransferases which catalyze the condensation of sugar 1-phosphates with nucleotides to generate sugar nucleotides. These enzymes can be exploited to generate novel sugar nucleotides, including phosphonate analogues of sugar 1-phosphates. Inhibiting these enzymes with phosphonate analogues may also lead to novel therapeutic opportunities. To explore these enzymes there is a need to generate novel sugar 1-phosphate analogues; however, access to these analogues is limited by the lack of synthetic methodologies.

A library of *galacto*-configured ketose phosphonates was synthesized, generating analogues that included mono and difluorination at the methylene functionality alpha to the phosphorus. Methods were explored to generate *gluco*-configured alpha hydroxy phosphonates. The interactions of these compounds with a series of enzymes were studied, including the thymidylyltransferase Cps2L and the uridylyltransferases GalT and AtUSP. Studies included investigating the substrate specificity of these enzymes, as well as enzyme-ligand binding experiments using WaterLOGSY NMR spectroscopy. In addition, the synthesis of prodrug analogues of the *galacto*-configured ketose phosphonates were also explored.

List of Abbreviations and Symbols Used

α	alpha
Å	angstrom
β	beta
δ	chemical shift
ε	molar absorptivity
λ	wavelength
Ac	acetyl
amu	atomic mass unit
aq	aqueous
ATP	adenosine triphosphate
Bn	benzyl
n-Bu	normal-butyl
COSY	COrrelation SpectroscopY
d	doublet
DAST™	*N*,*N*-diethylaminosufluor trifluoride
DBU	1,8-diazabicyclo[5.4.0]unde-7-ene
DCM	dichloromethane
dd	doublet of doublets
ddd	doublet of doublet of doublets
DEPT	distortionless enhancement by polarization transfer
DMF	dimethylformamide
DMP	Dess-Martin periodinane
DMSO	dimethyl sulfoxide
DNA	deoxyribonucleic acid

dTTP	deoxythymidine 5′-triphosphate
E	trans
E2	bimolecular elimination
EC	Enzyme Commission (number)
equiv	equivalent(s)
ESI	electrospray ionization
Et	ethyl
EtOAc	ethyl acetate
EU	enzyme unit(s)
Gal*f*	α-D-galactofuranose
Gal*p*	α-D-galactopyranose
Glc*p*	α-D-glucopyranose
h	hour(s)
HMDS	bis(trimethylsilyl)azanide
HPLC	high performance liquid chromatograph
HRMS	high-resolution mass spectrometry
HSQC	heteronuclear single quantum coherence
Hz	Hertz
J	coupling constant
LCMS	liquid chromatography mass spectrometry
LDA	lithium diisopropylamide
LOGSY	Ligand Observed via Gradient SpectroscopY
LRMS	low-resolution mass spectrometry
M	molar
m	multiplet

Me	methyl
MeOH	methanol
min	minute(s)
MHz	megahertz
mol	mole(s)
mmol	milimole(s)
NDP	nucleoside 5′-diphosphate
NOE	nuclear Overhauser effect
NMR	nuclear magnetic resonance
NFSI	*N*-fluorobenzenesulfonimide
NTP	nucleoside 5′-triphosphate
Ph	phenyl
POM	pivaloyloxymethyl
PP_i	inorganic pyrophosphate
ppm	parts per million
psi	pounds per square inch
q	quartet
R	organic substituent
R_f	retention factor
RNA	ribonucleic acid
rt	room temperature
s	singlet
Selectfluor™	1-chloromethyl-4-fluoro-1,4-diazobicyclo[2.2.2]octane bis(tetrafluoroborate)
S_N2	substitution nucleophilic bimolecular

t	triplet
TFAA	trifluoroacetic anhydride
THF	tetrahydrofuran
TLC	thin layer chromatography
TMSI	trimethylsilyl iodide
TOF	time-of-flight
Tris	2-amino-2-hydroxymethyl-propane-1,3-diol
UDP	uridine 5′-diphosphate
UDP-Gal*p*	uridine 5′-diphosphate-α-D-galactopyranose
UDP-Gal*f*	UDP-α-D-galactofuranose
UDP-Glc	uridine 5′-diphosphate-α-D-glucopyranose
UGM	uridine diphosphate galactopyranose mutase
UMP	uridine 5′-monophosphate
UTP	uridine 5′-triphosphate
Z	cis

Acknowledgments

First and foremost, I would like to thank my supervisor, Dr. David Jakeman for his continued support since I arrived at Dalhousie as a completely inexperienced second year undergraduate chemist. He provided me the opportunity to develop my skills as a chemist and researcher, which opened many doors for me and for that I am very grateful. I would also like to thank my lab mates, past and present, for their positive attitudes and for building a constructive research environment. Current colleagues include Andrew Robertson, Matt Loranger, Stephanie Forget, Nicole McCormick, Camilo Martinez-Farina, Alison Jee, and Dr. Ramprasad Ghosh. I would like to thank past members Stephen Beaton, Thomas Veinot, Steph Dupuis, Dr. Debarata Bhattasali, Dr. Ali Sadeghi-Khomami, Dr. Shannon Timmons, Malcolm Huestis, and Cathy Graham.

I would like to acknowledge my thesis committee members, Dr. D. Jean Burnell, Dr. Norman P. Schepp, and Dr. Alison Thompson for their advice and support throughout the course of this work. Next, I would like to acknowledge my peers, as well as the staff, for making the department a great place to work. Special thanks are due to Dr. Ray Syvitski and Dr. Nadine Merkley at the Biomolecular Magnetic Resonance Facility National Research Council of Canada in Halifax, for their help and insight while conducting 700 MHz NMR experiments, and Dr. Stan Cameron, at DALX, for X-ray crystallographic work.

I would like to thank my friends and family for their patience and encouragement. Lastly Travis, thank you for being by my side through the many ups and downs of graduate school.

CHAPTER 1. INTRODUCTION

1.1 Phosphorus in Living Systems

Phosphorous plays a pivotal role in the chemistry of living systems wherein phosphate mono- and di-esters are at the core of the biological world. The chemist Alexander Todd was among the first to appreciate the importance and remarkability of phosphorous in living systems during his work in the 1940s.[1] In nature, phosphate esters have evolved to be either stable, as exhibited by the stable biopolymers of ribonucleic acid (RNA) and deoxyribonucleic acid (DNA), or very labile, as observed in the phosphates that can undergo phosphoryl transfer. Phosphoryl transfer is central to many enzymatic processes, for example the storage and transfer of energy as adenosine triphosphate (ATP). The presence of two types of phosphates, with different chemical stabilities, is an important natural accomplishment. The underlying mechanism of this accomplishment in biological systems is the process by which enzymes can recognize and cleave P−O−C and P−O−P bonds in a very specific and accurate manner in a wide array of biological settings. The diverse range of the cellular roles that utilize phosphates, and the sizeable enzymatic rate acceleration of phosphoryl transfer enzymes, make them some of the most proficient, evolutionarily diverse, and ubiquitous enzymes in living systems.[2]

1.2 Phosphonates as Analogues of Phosphates

Since the 1960s phosphonates have been investigated as hydrolytically stable phosphate mimics for exploring a multitude of biological processes.[3] A phosphonate has a carbon atom in the place of the phosphoester oxygen of the phosphate, as shown in Figure 1, creating a bond that is not normally hydrolyzed enzymatically.

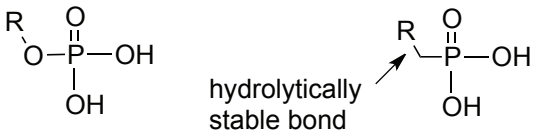

Figure 1. Comparison of phosphate and phosphonate bonds.

In general, the resulting interruption of enzyme function can be pharmaceutically advantageous.[4] This approach has led to the development of enzyme inhibitors, antifungals, antibiotics, and anticancer agents.[5,6] Vistide, a potent antiviral phosphonate-based medication, is shown as an example in Figure 2.

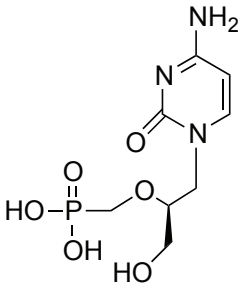

Figure 2. Vistide™; A phosphonate drug currently on the market.

The general strategy used for the development of these agents is the replacement of the natural phosphate, involved in phosphoryl transfer in biological systems, with a phosphonate analogue. Phosphonates are not a universal substitute for phosphates and may not interact with their intended target.[7,8] For this reason phosphonate analogues must be synthesized and studied on a case-by-case basis. In some situations, phosphonates are

used as analogues of other functional groups, as shown in Figure 3, where a phosphonate was found to inhibit gamma-glutamyl transpeptidase (GGT), an enzyme involved in glutathione metabolism.[5]

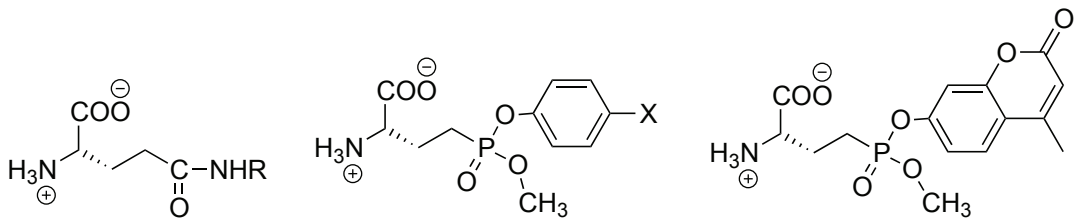

Figure 3. Developing phosphonate analogues of natural substrates.

To compare, phosphonates and phosphates have a general shared geometry,[3] although phosphonate analogues vary compared to the corresponding phosphates chemically and physically. Physically, the bond lengths between C−C−P are longer (10%) than in C−O−P, and the bond angles created by the C−C−P are smaller (6%) than those in the C−O and O−P of phosphate.[6] Chemically, the methylene unit of the phosphonate causes a decrease in the acidity of the phosphoric acid group compared to the phosphoric acid group in the phosphate.[9] The first pK_a for both phosphates and phosphonates is ~ 2.0 and will not be of significance when considering biological reactivity at physiological pH. However, the pK_a2 of both functional groups are different. The pK_a2 for phosphates is ~ 6.4, while for phosphonates the pK_a2 is ~ 7.7-8.2.[3] Given that these values are close to physiological pH (7.4), these differences lead to changes in the state of dissociation that can in turn affect the desired biological effect. For this reason, functionalization at the methylene unit is a strategy used to try to better mimic the acidity of the natural phosphate.

A common bioisostere of hydrogen is fluorine, and it has been shown that in some systems fluorination at the phosphonate α-methylene unit can improve biological activity.[10,11] This is maybe due to the fact that fluorine can participate in hydrogen bonding, and the electron-withdrawing nature of the fluorine atom causes a decrease in the pK_a2 of the phosphonate.[12] The ability to participate in hydrogen bonding makes it much like the lone pair of electrons on the oxygen atom of the parent phosphate and the decrease in pK_a2 also makes it a better phosphate mimic. A comparison is shown in Figure 4.

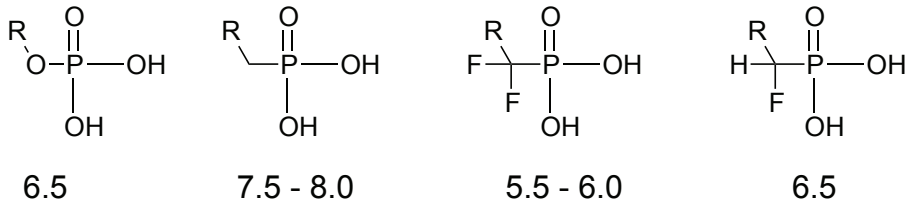

Figure 4. pK_a2 comparison for phosphates, phosphonates, and the potential effect of fluorination.

1.3 Biological Relevance of Sugar 1-Phosphates

In nature, sugar phosphates are the primary precursor of the glycosyl donors that feed into the biosynthesis of glycoconjugates, and are regulators of some biosynthetic processes.[13] While the development of hydrolytically stable phosphate isosteric analogues is a validated avenue of drug research, the differences in physiochemical properties of phosphonates and phosphates, mandate that these analogues must be synthesized and analyzed for any true comparison, and should include functionalization of the α-carbon (with respect to phosphorous) to best mimic the acidity of the physiological substrate.[2]

An important drawback of therapeutic phosphonates is that they are deprotonated at physiological pH. This limits their potential for oral administration. For example, Vistide™, which was previously mentioned, must be given as an injection. Other drawbacks include the limitation for cellular membrane permeability, and in turn cleavage by extracellular phosphatases. To tackle these problems, phosphonates can be designed as prodrugs, wherein the phosphonic acid can be masked by protecting groups that promote absorption and distribution of the prodrug. Once the molecule is absorbed, esterases can cleave the protecting groups and release the drug molecule. This approach has lead to the development of novel antiviral therapeutics, for example Hepsera™ and Viread™ (Figure 5).[14] Nucleotide prodrugs are also being developed.[15] Exploring sugar 1-phosphate prodrugs is an attractive avenue towards designing therapeutic agents and developing in-cell studies.

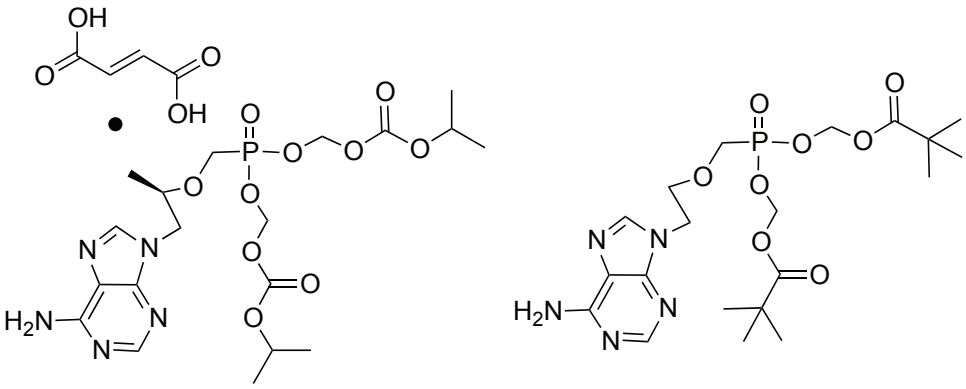

Figure 5. Prodrugs currently on the market, Hepsera™ and Viread™ to treat hepatitis B infections. Hepsera™ also treats herpes simplex virus.

1.3.1 Generating Novel Carbohydrates

The development of biologically relevant sugar 1-phosphate analogues remains an underexplored field of chemistry due to a lack of synthetic methodologies. These analogues have potential applications as probes and inhibitors of carbohydrate metabolism. Carbohydrates present a synthetic challenge due to their polyhydroxylated backbone and numerous stereocenters, yet they deserve our attention due to their dominance in nature, wherein over half of human proteins are glycoproteins, and many of the secondary metabolites of bacteria are glycosylated.[16] Those secondary metabolites are currently a supply of natural products being studied for their intrinsic antibiotic, anticancer, or other biological properties.

1.4 The Medicinal Importance of Carbohydrates and Phosphonates

The medical benefit of the carbohydrate moiety was initially recognized to be the improvement of pharmacokinetic properties, which include absorption, distribution, metabolism, and excretion of the therapeutic agents. These improvements are generally attributed to the increase in hydrophilicity of the molecule compared to its aglycon relative.[17] However, many natural product therapeutic agents have now been shown to require the glycol moiety for the desired biological activity.[18]

1.4.1 Nucleotidylyltransferases Substrates

Sugar 1-phosphate nucleotidylyltransferases are important precursor enzymes to glycosylation in biological systems. Nucleotidylyltransferases couple sugar 1-phosphates with nucleoside 5′-triphosphates (NTP), generating glycosylated nucleoside 5′-

diphosphates (NDP). The resultant activated sugars are substrates for glycosyltransferases that transfers the sugar to glycosyl acceptors, as summarized in Scheme 1. In this way, designing novel nucleotidylyltransferase substrates can allow exploration of a multitude of biological systems. Additionally, nucleotidylyltransferases can be utilized as synthetic tools to synthesize sugar nucleotides,[19] often in higher yields and with increased regioselectivity compared to current chemical coupling routes.[20]

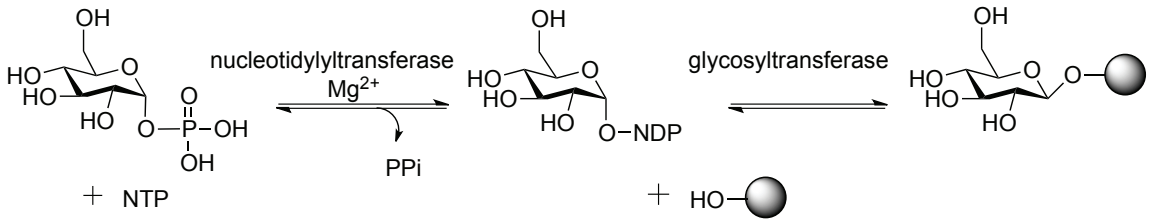

Scheme 1. The biological pathway for a sugar 1-phosphate.

1.5 Previous Synthetic Strategies to Generate α-Fluorinated Sugar Phosphonates

Numerous approaches to generate sugar phosphonates have been reported[21,22,8] and the Jakeman lab has expanded the library of novel sugar analogues, including the development of phosphonate and keto-phosphonate analogues, as well as subsequent fluorinated derivatives. The incorporation of fluorine at the methylene center of glucose 1-phosphonate was also investigated previously in the Jakeman lab.[23] This was accomplished by treating globally protected glucose 1-phosphonate with *N*-fluorobenzenesulfonimide (NFSI) in the presence of hexamethyldisilazane. After optimization, the yield was 9% and the product was exclusively the difluoro derivative (Scheme 2). Despite diligent exploration of alternative solvents, equivalents of NFSI,

reaction temperature, and variation of bases, no monofluorinated material was isolated. This was due to the fact the once the monofluorinated was generated the presence of the fluorine made that center more reactive then the methylene unit of the unreacted starting material.

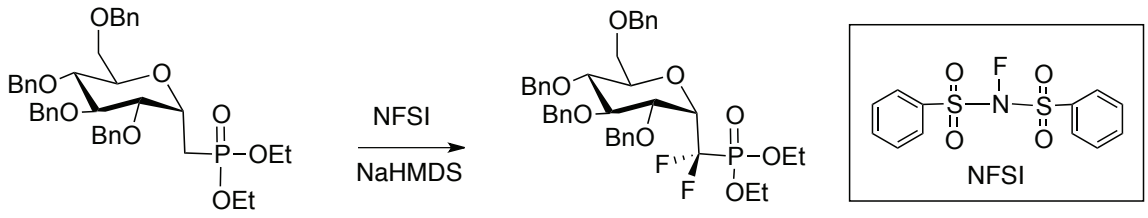

Scheme 2. Fluorination of glucose 1-phosphonate using NFSI.

A small library of *gluco*-ketose phosphonates was previously prepared in the Jakeman lab, including mono- and difluoro- analogues.[7] An intermediate exoglycal was generated using *N*,*N*-diethylaminosufluor trifluoride (DAST™) but also lead to formation of a side product, as shown in Scheme 3. The resultant exoglycal was then reacted with Selectfluor™ to generate a diastereomeric monofluorinated mixture, as shown in Scheme 3. Formation of only the exoglycal could potentially be accomplished using treatment with triflouroacetic anhydride (TFAA).[24]

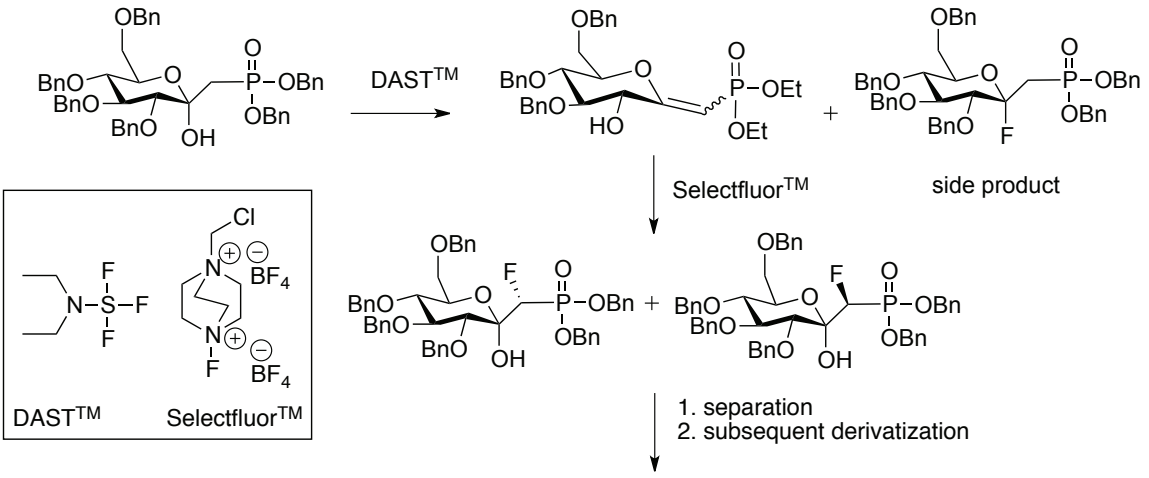

Scheme 3. Synthesis of monofluorinated gluco-configured ketose phosphonates.[7]

Currently, a major aim of the Jakeman lab is the design and synthesis of novel sugar 1-phosphate analogues, specifically the mono- and difluorinated phosphonate derivatives, and to use these to as enzyme probes. Using these compounds as probes will be expanded in future chapters.

1.6 Project Objectives

The objectives for this project are:

- To synthesize *galacto*-ketose phosphonates, including the non-fluorinated, monofluorinated diastereomers, as well as the difluorinated compounds and to evaluate their properties as enzyme probes.
- To synthesize a *gluco*-configured alpha hydroxy phosphonate and explore the monofluorination of this compound.
- To explore synthetic routes toward sugar prodrugs.

CHAPTER 2. RESULTS AND DISCUSSION: SYNTHESIS

The syntheses of phosphonate analogues of galactose and glucose 1-phosphates were explored. In this work, different functionalities were installed at the α-methylene unit, with respect to the phosphorous, using different synthetic approaches. One aim was to learn more about how these classes of analogues might be generated. Synthetic avenues toward galactose prodrugs were also explored.

2.1 *Galacto*-Ketose Phosphonates as Analogues of Galactose 1-Phosphate

2.1.1 Introduction

An enzyme of potential medicinal importance is UDP galactopyranose mutase (UGM) because it is involved in the biosynthesis of the cell wall in many pathogenic microorganisms, for example *Mycobacterium tuberculosis*. UGM utilizes UDP-Gal*p* and catalyzes the isomerization to UDP-α-D-galactofuranose (UDP-Gal*f*), shown in Scheme 4.

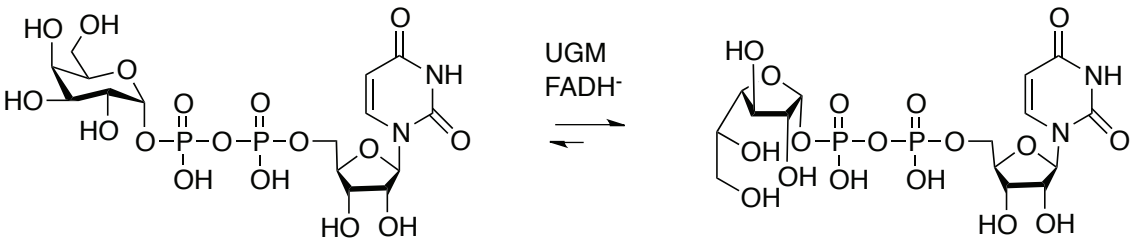

Scheme 4. Isomerization of UDP-Gal catalyzed by UGM.

The furanosyl form is the precursor to galactofuranose residues in cell walls. Targeting α-D-galactofuranose (Gal*f)* biosynthesis is an attractive antibiotic target as it is

not found in human cells. There is significant conjecture regarding the mechanism of this enzyme;[17] however, isotope-exchange experiments have deduced that the cleavage of the anomeric C-O takes place during catalysis.[25] Therefore, replacement of this bond with an enzymatically non-hydrolyzable bond could generate inhibitors of UGM. Previous work by Sanders and Jakeman showed that a phosphonate analogue of UDP-Gal*p*, wherein the C-O bond was replaced with a C-C methylene bond, generated a moderate inhibitor that was a better inhibitor than the phosphonate analogue of UDP-gal*f*.[26] Based on this, novel UDP-Gal*p* analogues are of great interest. For this reason, four novel galactose 1-phosphate analogues were synthesized.

2.2 The Synthesis of *Galacto*-Ketose Analogues

The synthesis of four novel *galacto*-ketose analogues of galactose 1-phosphate was achieved as outlined in Scheme 5. The treatment of commercially available 2,3,4,6-tetrabenzyl-D-galactopyranose with DMSO and acetic anhydride afforded the requisite lactone **1** via an Albright-Goldman oxidation.[27] Freshly prepared dibenzyl methylphosphonate[28] was lithiated with *n*-BuLi and reacted with the protected lactone **1** at -78 °C to produce hexabenzylated α-hydroxy *galacto*-ketose phosphonate **2** in high yield (94%) generating an (*R)*-configured stereocenter at the anomeric center, where the phosphoryl substituent is in the equatorial position.

The ketose phosphonate **2** was then globally deprotected via hydrogenolysis (Pd-C) under atmospheric pressure[29,30] to yield the novel *galacto*-analogue **3.** Alternatively, compound **2** was further functionalized. To access the α-monofluorinated analogues **5** and **6**, compound **2** was treated with TFAA in the presence of pyridine to facilitate

elimination which generated intermediate **4** in good yield as a single isomer about the double bond, which is proposed to be the (*E*)-exoglycal.[24] The exoglycal **4** was monofluorinated using Selectfluor™, an electrophilic fluorine donor, in the presence of water to generate the α-fluoro ketose phosphonates in a diastereomeric mixture of **5** and **6**, the (*R*) and (*S*) isomers (*R*:*S,* 1:0.39), with yields of 46% and 18%, respectively; which is a diastereomeric excess of 44% towards the (***R***)- isomer.[7] The reaction was highest yielding when performed on a 0.65 mmol scale. The separation and isolation of the minor (*S*)-configured diastereomer was difficult and at times unachievable. However this compound was successfully purified when two column chromatography steps were employed during purification. The first column was used to separate the diastereomeric mixture from the reaction mixture; while the second column allowed for some separation of the diastereomers when one milliliter fractions were collected. Compounds **5** and **6** were globally deprotected using hydrogenolysis to yield the α-fluoro-analogues **7** and **8**, respectively, with modest yields. It was not clear why the hydrogenolysis of **6** was lower yielding then that of **5**.

To generate the α,α-difluorinated derivative **9**, lithium diisopropylamide (LDA) was generated *in situ* by treating diisopropylamine with *n*-BuLi. The resultant solution was reacted with diethyl difluoromethyl phosphonate at –78 °C, then charged with a solution of lactone **1** generating compound **9** in a yield of 52%. The α,α-difluorinated product (**9**) was then globally deprotected by treatment with iodotrimethylsilane (TMSI) to yield the novel difluorinated ketose analogue **10** with a yield of 44%.

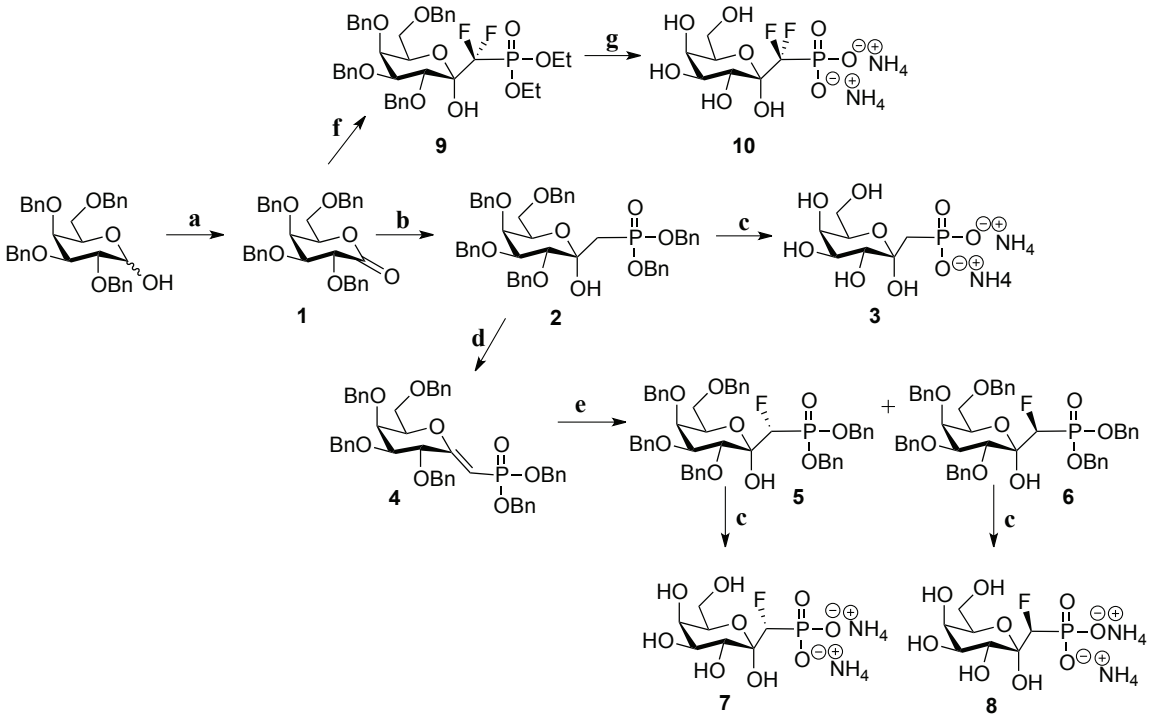

Scheme 5. Synthetic strategy for generating *galacto*-ketose phosphonates.

(a) Ac_2O, DMSO, rt, 12 h, 90%; (b) $MePO(OBn)_2$, *n*-BuLi, THF, -78 °C, 2 h, 94%; (c) i) H_2, Pd-C (10% w/w), 18 h, rt, 14.7 psi, MeOH:EtOAc (1:1), ii) NH_4OH, pH 7.5, **3** (63%), **7** (73%), **8** (35%); (d) TFAA, Py, 4Å molecular sieves, THF, 0 °C, 61%; (e) i) SelectFluor™, CH_3CN, rt, 12 h, ii) H_2O, reflux, 3 h, 46% (*R*)-**5** and 18% (*S*)-**6**; (f) $F_2CHPO(OEt)_2$, LDA, THF, -78 °C, 30 min, 52%; (g) i) TMSI, DCM, rt, 4 h; ii) NH_4OH, pH 8, 44%.

There was substantial difficulty during the deprotection step for these compounds, and it was necessary to remove impurities using a size exclusion column (Sephadex® LH-20). At times, small amounts of mono and dibenzylated material was still present after reaction times of 18 hours; however, it was found that if reactions were continued for longer, increased decomposition occurred, as observed using ^{31}P NMR spectroscopy. The separation of fully deprotected product and residual protected material was possible using chromatography. However, the extra chromatography step and incomplete deprotection contributed to lower product yields.

To explore other deprotection avenues (Scheme 6), lactone **1** was reacted with dimethyl methyl phosphonate to generate a differentially protected analogue of **2**. First, dimethyl methylphosphonate was lithiated with *n*-BuLi and reacted with the protected lactone **1** at -78 °C to produce *galacto*-ketose phosphonate **11** in reasonable yield (60%). Lower yields during this reaction, compared to the reaction using dibenzyl methylphosphonate, may have been due to using the phosphorylating reagent without adequate drying or distillation. However, reaction yields during phosphorylation, using either phosphite reagent, varied greatly (between 50% and 90%) and lower yields to synthesize **11** were deemed acceptable when generating material for preliminary investigations with this compound. Next, a TMSI deprotection of **11** was explored to generate **3**; however, after 30 minutes at 0 °C only decomposition was observed using TLC and ^{31}P NMR spectroscopy of the crude reaction mixture.

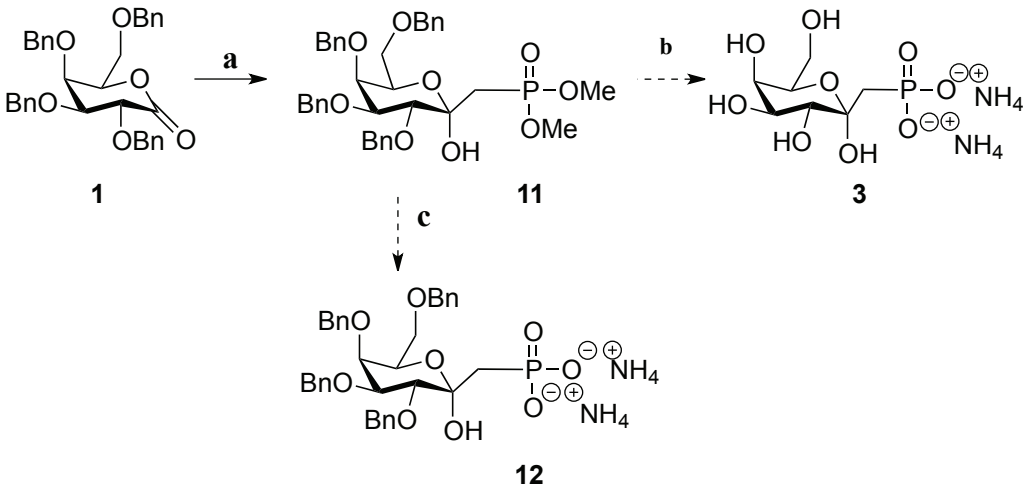

Scheme 6. Methyl protected ketose phosphonate and attempted selective deprotection.

(a) $MePO(OMe)_2$, *n*-BuLi, THF, -78 °C, 2 h, 60%; (b) i) TMSI, ii) Amberlite resin, NH_4OH, pH 8; (c) i) HCl (1.0 M), ii) NH_4OH, pH 7.5.

The prospect of removing only the phosphonyl protecting groups to generate **12** was also of interest as this could allow for chemical coupling of benzylated sugar moieties to nucleosides, generating novel nucleotide analogues while alleviating the need to handle unstable and water-soluble sugar 1-phosphate analogues during investigation of coupling strategies. To remove the methyl protecting groups, compound **11** was stirred with 1.0 M HCl at reflux temperature. After 4 hours a new compound was detected using TLC. Analysis using HRMS suggested that this new compound was potentially the mono-methyl protected compound, wherein $C_{36}H_{40}O_9P$ $(M + H)^-$ requires 647.2420, 647.2415 was found. When the reaction mixture was concentrated, heated, or left for longer time intervals, decomposition was observed. Further investigations into selective deprotection or alternative deprotection strategies were abandoned at this point. The chemical coupling of these compounds to form sugar nucleotide analogues was not an immediate aim of the project. With the fully deprotected *galacto*-configured compounds **3**, **7**, **8**, and **10** in hand we next investigated their chemical and biological properties.

2.2.1 Determination of Stereochemistry

1D NOE NMR spectroscopy[31] was used to assign stereochemistry of the benzylated compounds. This included assigning the configuration at the anomeric center in compound **2.** as shown in Figure 6; the tentative configuration of the exocyclic double bond in **4** (Figure 7); and the stereochemistry at the CHF center in compound **5** as follows: an n*O*e was observed between H-2 and one of the exocyclic methylene protons H-1′ in **2** (Figure 8). This observation was anticipated with an equatorial methylene phosphonate and is in agreement with the X-ray structure that was determined (Figure 9) and the observations for related *gluco*-ketose phosphonates.[7] The configuration of the

CHFP chiral centers generated in **5** and **6** were elucidated by comparing the observed n*O*e of the methylene proton in the fluorinated derivatives to the n*O*e of the parent compound **2**. This assumes that the monofluoromethylene compounds **5** and **6**, Figure 10 and Figure 11 respectively, adopt the same conformations as the methylene derivative **2,** and assignment was possible because each of the methylene protons had a unique n*O*e to either H-2 or the anomeric OH, exclusively (Figure 8). Because we were able to distinguish which methyl proton interacted with either H-2 or the anomeric OH in **2**, the absence of such an n*O*e interaction in the fluorinated material determined which proton was replaced with a fluorine atom (Figure 12). In molecule **4,** an n*O*e between the exocyclic proton H-1′ and the methylene group from a phosphonyl benzyl group was observed; wherein, in the (*Z*)-exoglycal, an n*O*e between H-1′ and H-2 would be anticipated as was observed during the synthesis of related *gluco*-configured exoglycals.[32] The lack of an n*O*e between H-1′ and H-2 suggests that the configuration of the exoglycal is (*E*) (Figure 13). However, without access to the (*Z*)-exoglycal for NMR comparison, the assignment of **4** remains tentative. At this time, attempts to acquire meaningful 1D or 2D spectrum of compound **6** to assign the CHF stereochemistry have been unsuccessful. However, tentative assignments of **5** and **6** are in agreement with the assignments from previous work on the *gluco*-configured ketose phosphonates.[7]

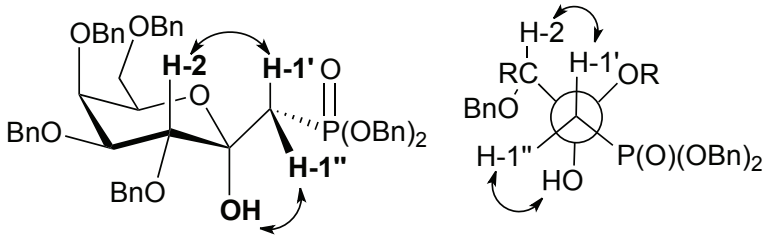

Figure 6. Observed n*O*e in compound **2**.

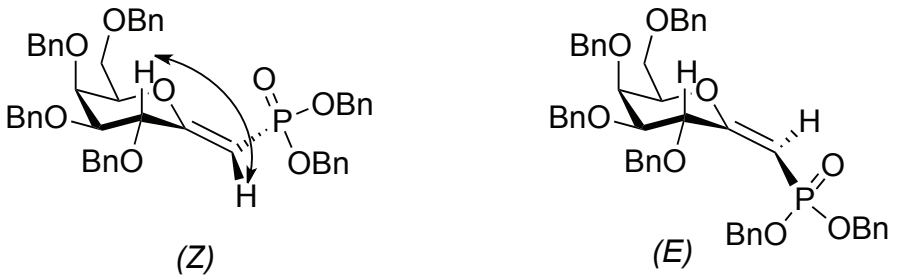

Figure 7. Expected n*O*e of proton H-1′ to H-2 in compound **4**.

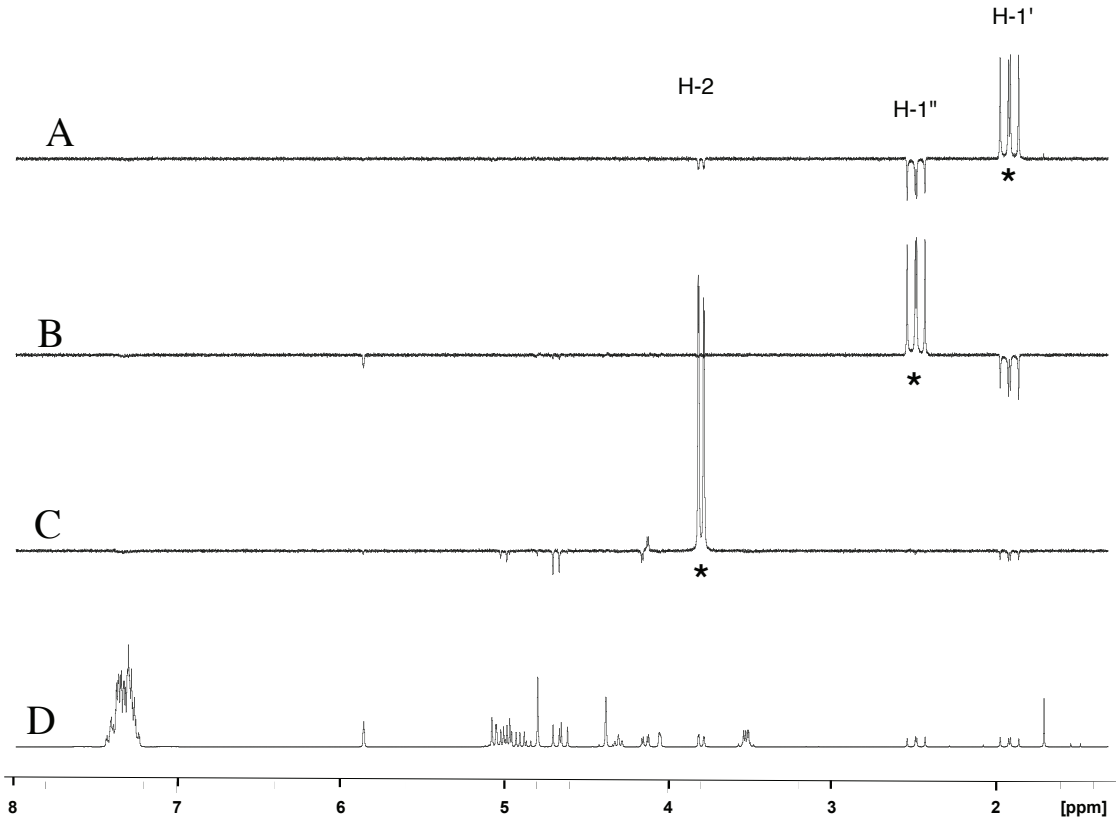

Figure 6. 1D NOESY of compound **2** (in $CDCl_3$).

The spectrum shows an n*O*e between two protons, where the proton that was irradiated is marked with *. (A) H-1′ irradiated, an n*O*e between H-1′ and H-1′′ as well as H-1′and H-2 is observed. (B) H-1′′ is irradiated, an n*O*e between H-1′′ and H-1′ as well as H-1′′ the anomeric OH (5.85 ppm) is observed. (C) H-2 is irradiated, an n*O*e between H-2 and H-1′ is observed. (D) ^{1}H NMR.

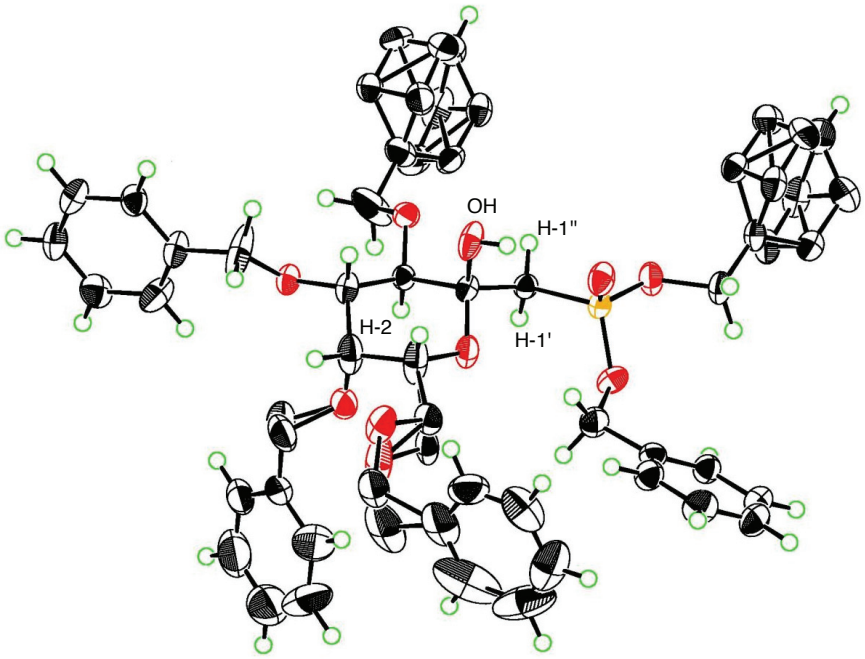

Figure 9. X-ray structure of compound **2**.

Protons H-2, H-1′, H-1″, and the anomeric OH are labeled. The crystal structure supports the geometry, and nOe observed during the NMR experiments on the molecule in solution (Figure 8).

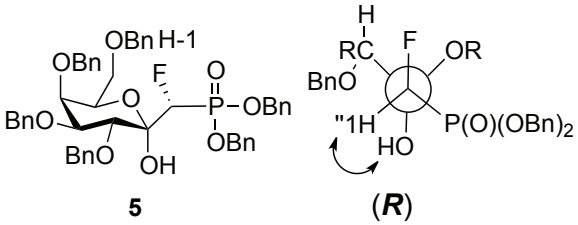

Figure 10. Expected n*O*e in compound **5**.

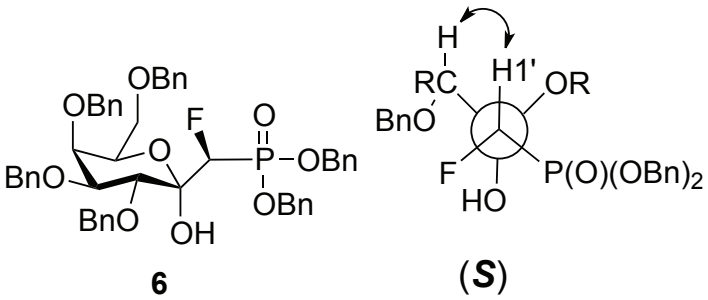

Figure 11. Expected n*O*e of compound **6**.

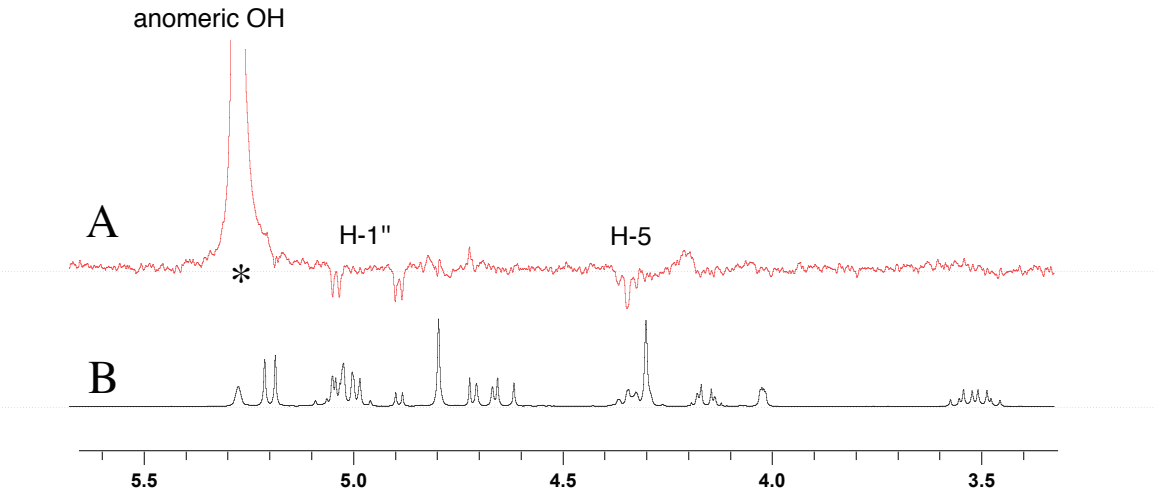

Figure 7. 1D NOESY NMR of compound **5**.

The spectrum shows an n*O*e between the α-phosphonate proton (H-1′′) and the OH at the anomeric center where the proton that was irradiated is marked with *. (A) Shows an n*O*e between OH and H-1. (B) The ^{1}H NMR spectrum, shown for comparison. Note that one side of the H-1′′ doublet of doublets is overlapping with benzyl methylene units; however, it clearly emerges during the experiment.

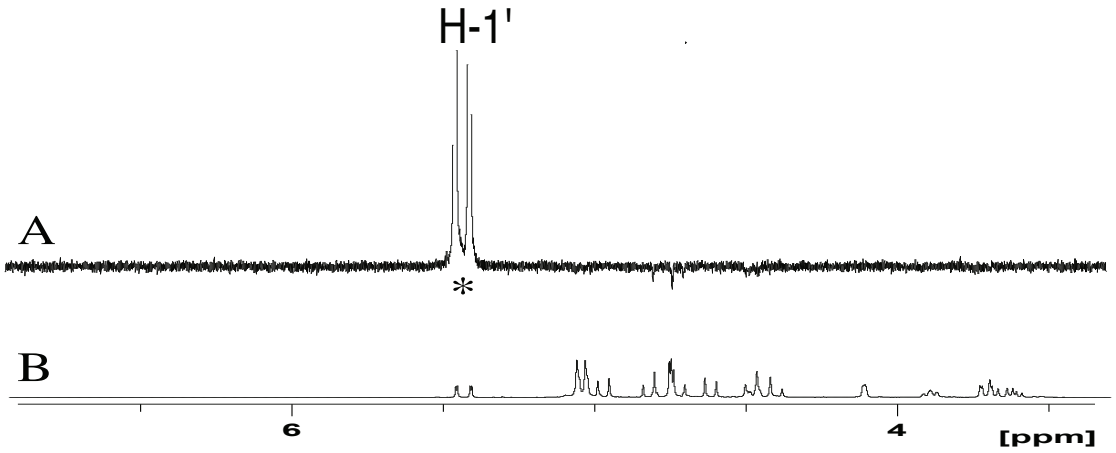

Figure 13. 1D NOESY of compound **4** showing (*Z*) isomer.

The spectrum shows an n*O*e between one of the α-phosphonate protons (H-1′) and the CH_2 of the phosphonyl benzyl groups, where the proton that was irradiated is marked with *****. (A) Shows a lack n*O*e between H-1′ and the H-2 proton. (B) The ^{1}H NMR specta, shown for comparison.

2.2.2 Exchange of the Methylene Protons in MeOD

Compound **2** exhibited exchange of both protons on the α-methylene unit, with respect to the phosphorous, in deuterated methanol. This was observed during ^{1}H NMR spectroscopy studies whereby the signals at 2.48 and 2.38 ppm diminish over time and after 24 hours the integration changed from 1.00 for each hydrogen signal to 0.37 and 0.27, respectively, as shown in Figure 14, suggesting these protons are highly acidic. Surprisingly, when compound **5** was treated in the same manner, no deuterium exchange was noted after 24 hours.

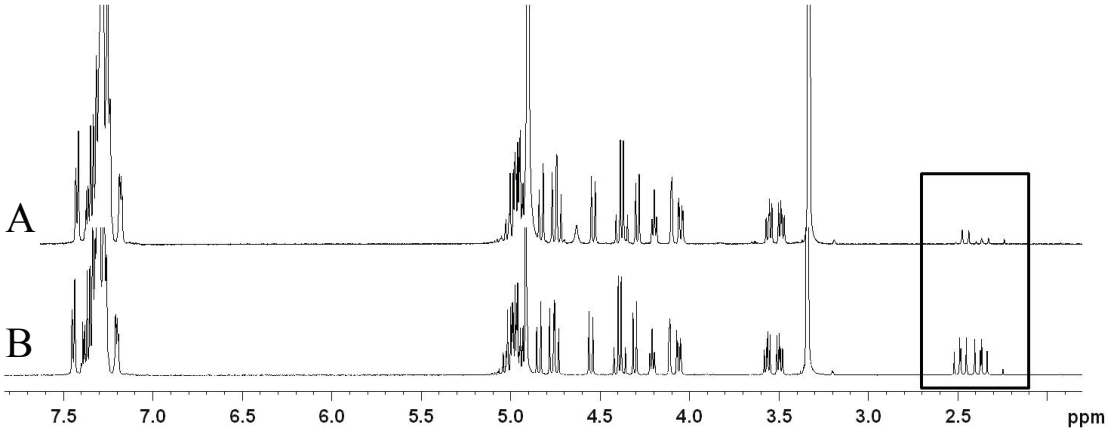

Figure 8. ^{1}H NMR experiment showing proton-deuterium exchange at methylene carbon.

A) ^{1}H NMR spectrum after 24 hours at room temperature compared to B) which is the same NMR sample at only one hour in MeOD. The box to the right highlights the clear loss of hydrogen at the methylene unit.

2.2.3 Potential Mutarotation of Ketose Phosphonates

In aqueous solutions, it is reasonable to anticipate that the isolated *galacto*-ketose phosphonates exhibit interconversion and mutarotation to the pyranosyl, furanosyl, and straight-chain forms, as well as α- and β-anomeric configurations (Figure 15). In a previous study, it was shown that the thymidylyltransferase Cps2L catalyzes the conversion of the dynamic equilibrium species of the *gluco*-configured ketose phosphonates to access sugar nucleotides.[7] Compounds **3**, **7**, and **8** were also found to be

unstable in solution or at room temperature which mandated that they be dried and stored at -20° C whenever possible. By contrast **10** was stable under these conditions.

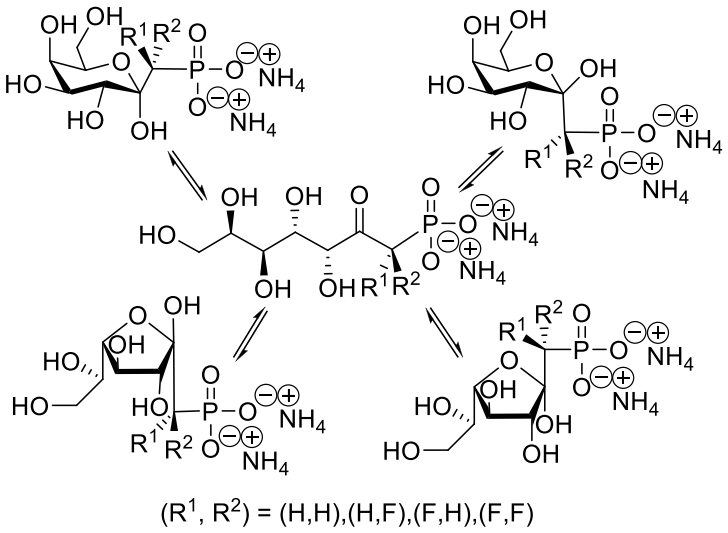

Figure 9. Proposed mutarotation in aqueous environments of ketose phosphonates.

^{31}P and ^{19}F NMR experiments at pH 8 show multiple peaks consistent with a mutarotation hypothesis, wherein multiple equilibrium species are clearly observed in Figure 16. The phosphorous NMR spectrum of compound **3** (entry **A**) shows five singlets, with two major species. It is likely that these species are the α- and β-pyranose forms as they are the thermodynamically stable forms of the sugars. However, assignment of the forms has not been achieved due to difficulty handling these compounds and convoluted NMR spectra. In the fluorine NMR spectra of **7**, **8**, and **10,** two bond F-P splitting is observed ($^2J_{F\text{-}P} \sim$ 68-78 Hz) giving rise to clear doublet patterns (spectra **B**, **C**, **D**). In contrast to **A**, the phosphorous NMR spectra of **7**, **8**, and **10** (**B1**, **C1**, and **D1**) do not show five species and were difficult to interpret due to signal overlap. However, the fluorine NMR spectra provide a clearer picture with well resolved signals: in **B** and **C** five doublets are observed, suggesting five species are present for **7** and **8**. In

spectrum **D**, there are two major compounds observed (likely the α- and β-pyranose forms again) giving rise to four fluorine signals, each are experiencing geminal F-F splitting on a magnitude of 300 Hz add F-P coupling.

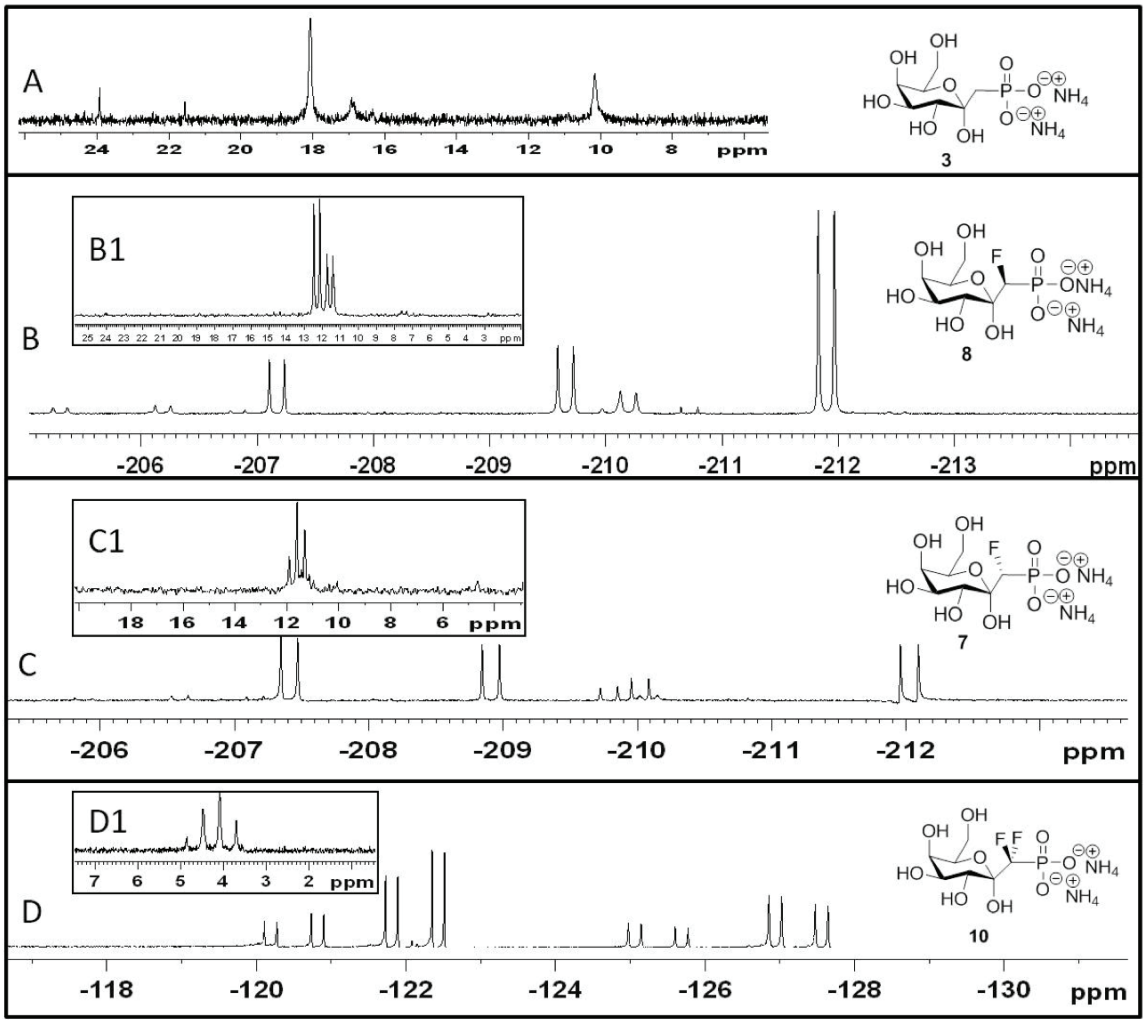

Figure 10. Proton-decoupled NMR spectra of compounds **3**, **7**, **8** and **10** in D_2O at pH 8.

(A) ^{31}P NMR (121 MHz); (B) and (C) ^{19}F NMR (282 MHz); (D) ^{19}F NMR showing geminal fluorine splitting ($^{2}J_{F,F}$ = 300 Hz). (B1), (C1), and (D1) corresponding ^{31}P NMR NMR (121 MHz).

2.2.4 Determination of pK_a2 Values

The pK_a2 of these compounds was determined experimentally using titration, and calculated by fitting the data points to a model using non-linear regression software. The results are summarized in Table 1, and follows. The previously discussed expected trend, wherein the replacement of the exocyclic oxygen atom, in galactose 1-phosphate, with a carbon atom increases the pK_a2. Further monofluorination at the carbon provides better pK_a2 mimicry. A pK_a2 value of 6.21 was determined for galactose 1-phosphate, which had not been previously reported in the literature. The monofluorinated compounds **7** and **8** appear to most closely mimic the parent compound (6.14 and 6.15), whereas the difluorinated material has a lower pK_a2 of 5.66. To ensure consistency of the method, the pK_a2 of glucose 1-phosphate was determined experimentally, and it was shown to be in good agreement with the literature value (6.13).[33] An example graph generated using this protocol is shown (Figure 17). These results suggest that the acidities of the monofluorinated compounds **7** and **8** best mimic the physiological substrates and that may be beneficial for the interactions with enzymes in order to for these compounds to act as substrates.

Table 1. Determination of pK_a2 values for Gal*p* and the ketose phosphonates.

Compound	pK_a2 Value
Glucose 1-phosphate	6.15[A]
Galactose 1-phosphate	6.21
3	6.58
7	6.15
8	6.14
10	5.66

[A] experimental value; in agreement with literature.

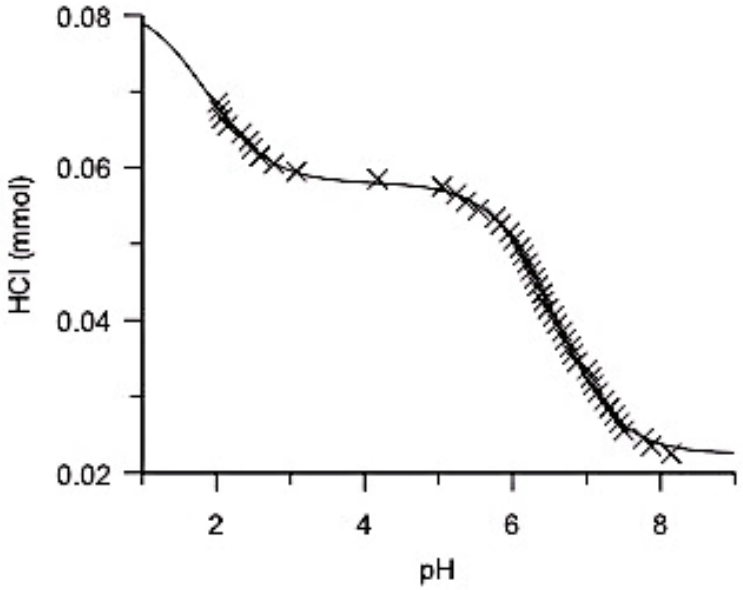

Figure 11. Example graph from pK_a2 determination for compound **3** generated using GraFit linear regression software.

2.3 Toward the Synthesis of Galacto-Phosphonate Prodrugs

The development of prodrugs to improve the bioavailability of phosphonate drugs has led to the development of biolabile protecting groups for the phosphonate.[14,15] This allows the phosphonate, which exists in an ionized form at physiological pH, to be delivered to tissue in the neutral ester form of the compound. The prodrug functionality can then be cleaved releasing the drug molecule.

The protection of compound **11** with pivaloyloxymethyl (POM) esters was explored because methyl protected phosphonates have been shown to generate the POM protected product with good yield in 48 hours.[34] Previous work in the Jakeman lab generated *gluco*-configured POM compounds in good yield.[32] It was proposed that the use of literature reaction conditions would be suitable for generation of a POM protected ketose phosphonate (**13**) as shown in Scheme 7, which could then be deprotected to yield compound **14**. This compound could then deliver the *galacto*-ketose phosphonate to tissues upon cleavage by cellular esterases. This would allow for in-cell studies with sugar 1-phosphonates. In addition, acetylation of compound **14** could allow for further tailoring of the hydrophobicity for these compounds.

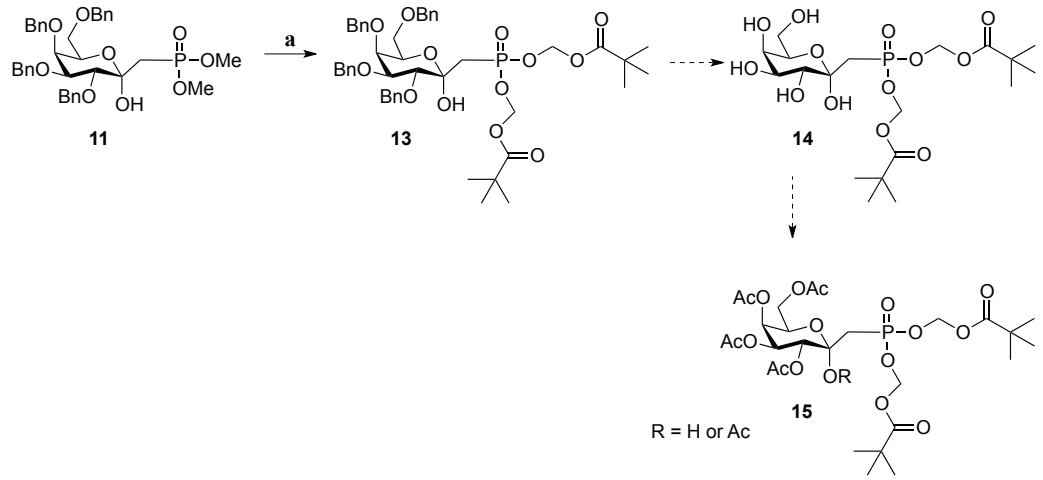

Scheme 7. Proposed synthesis of *galacto*-phosphonate prodrugs.

(a) NaI, POMCl, CH_3CN, reflux temperature, 48 h.

The reaction was explored over a range of reaction conditions as outlined in Table 2. The reaction generated a mixture of mono-POM protected diastereomers (isolated using chromatography), as well as the di-POM protected product **13**. The di-POM product was observed during ^{31}P NMR spectroscopy experiments, and an example spectrum is shown in Figure 18. In **Method A** no reaction occurred with the use of acetonitrile as solvent due to the insolubility of compound **11**. The solvent was changed to an acetonitrile:THF (1:1) mixture and this lead to some product formation (9%) according to analysis of the ^{31}P NMR spectrum of the crude reaction mixture and new compounds using TLC (**Method B**). When this reaction was left longer, the starting material was not still consumed and decomposition was observed using TLC. After 48 hours at reflux temperature the reaction had not gone to completion and was stopped (**Method C**). Next, a lower reaction temperature was explored in hopes that this may reduce decomposition over time. The reaction mixture was stirred overnight at 40°C (**Method D)** and the reaction was shown to proceed, generating some mono-POM

protected product at the lower temperature. However, when this reaction mixture was allowed to proceed longer, decomposition was still observed and only mono-POM protected material was generated (**Method E**). The equivalents of POMCl were doubled in order to ensure that the reaction was not being limited by the amount of POMCl available (where 2.0 equivalents of POMCl were required per equivalent of phosphonate) and analysis using NMR spectroscopy showed an increase in the amount of product generated, from 9% to 19%. With the increase in POMCl, the previous temperatures were revisited (**Method F**, **Method G**, **Method H**), but this lead to no notable increase in product formation (monitoring with ^{31}P NMR spectroscopy). Lastly, an intermediate temperature of 75°C was explored but the formation of product compared to the generation of multiple compounds using TLC was only somewhat improved, and a 40% conversion was noted using ^{31}P NMR (**Method I**). However, this reaction also generated numerous other phosphorus-containing compounds using NMR. Attempts to isolate compound **13** from the reaction mixtures were complicated by the number of compounds generated during the reaction. It remains unclear why the reaction fails to proceed to completion.

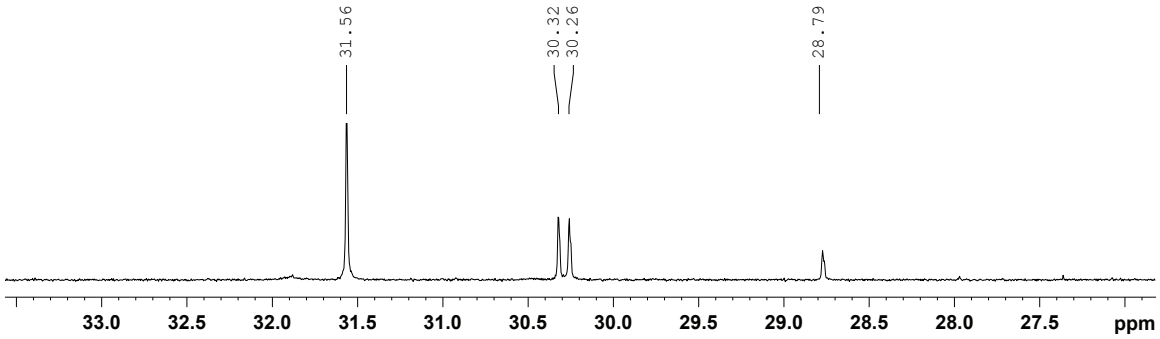

Figure 12. ^{31}P NMR of POM reaction progress on compound **11** (**Method F**).

The spectrum shows the starting material (31.56 ppm), the mono-POM protected intermediates (30.32 & 30.26 ppm), and product (28.79 ppm). The reaction ratio was 1:0.82:0.19, respectively.

Table 2. POMCl reaction conditions explored to generate compound **13**.

Method	**Temp** (°C)	**Time** (h)	**Solvent**	**POMCl equivalents**	**Observations** (Starting material:Product)[A]
A	90	5	CH_3CN	2.5	low solubility of **11** (1:0)
B	90	10	CH_3CN/ THF	2.5	(1:0.09)
C	90	48	CH_3CN/ THF	2.5	decomposition
D	40	18	CH_3CN/ THF	2.5	(1:0)
E	40	48	CH_3CN/ THF	2.5	(1:0.58[B]:0)
F	90	10	CH_3CN/ THF	5.0	(1:0.82[B]:0.19)
G	90	48	CH_3CN/ THF	5.0	decomposition
H	40	10	CH_3CN/ THF	5.0	(1:0)
I	75	18	CH_3CN/ THF	5.0	(1:0.4)

[A] according to ^{31}P NMR experiments.

[B] mono-POM protected product.

2.4 *Gluco*-α-Hydroxy Phosphonates as Analogues of Glucose 1-Phosphate

2.4.1 Introduction

Given that previous attempts to generate monofluorinated glucose 1-phosphonates had been unsuccessful,[23] the synthesis was revisited because developing these molecules as probes for nucleotidylyltransferase is of great interest in the Jakeman Lab. Previous work had generated the glucose 1-phosphonate via an Arbuzov reaction upon tetrabenzylated glucopyranosyl iodomethane (**18**). In resuming this project, efforts were focused on phosphonylation of **18** to generate an α-hydroxy phosphonate that could then be further functionalized via reagents that react with alcohols. This allowed for alternative fluorination avenues to be explored.

2.5 The Synthesis of *Gluco*-α-Hydroxy Phosphonates

The synthetic strategy employed to synthesize a diastereomeric mixture of α-hydroxyl *gluco*-phosphonates was first attempted upon a tetrabenzylated glucopyranosyl iodomethane derivative (**18**), which was prepared according to literature procedures as shown in Scheme 8.[35,8] A solution of 2,3,4,6-tetra-*O*-benzyl-D-glucopyranose was reacted with a methylene ylide (as a lithiated suspension in THF) via a Wittig reaction to generate the α-olefin **16**, thus delivering the requisite chain extension. Mercuration at the α-olefin of **16** exclusively generated the organomercury compound **17,** via an anti-Markovnikov addition, which was collected as the chloride salt. The electrophilic salt activates the olefin and promotes cyclization.[35] The ring closure is stereospecific, orienting the methylene mercuric unit in the axial position as predicted by the anomeric effect.

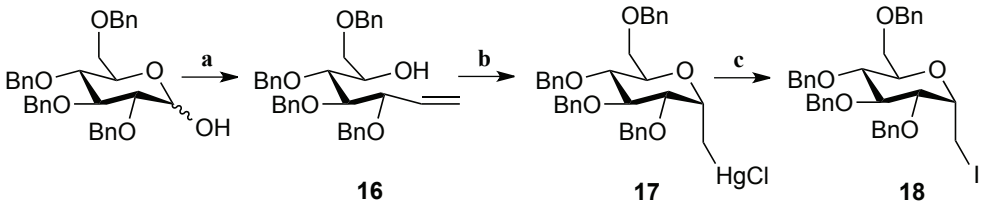

Scheme 8. The synthesis of compound **18**.

(a) $MePPh_3Br$, *n*-BuLi (2.5 M), THF, −78 °C, 30 min, followed by 45 °C, 3 h, 90%; (b) i) $Hg(CF_3COO)_2$, THF, rt, 18h, ii) KCl, 2 h, 60%; (c) I_2, DCM, rt, 2 h, 70%.

2.5.1 Revised Synthesis

The strategy pursued was to first accomplish a DMSO oxidation[36,37] on the aliphatic iodide compound **18,** and was attempted because it was expected that this reaction would yield the corresponding aldehyde (**19**) by an S_N2-type displacement with an immediate E2 elimination.

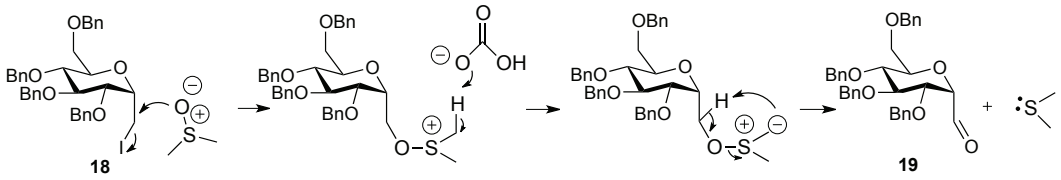

Scheme 9. The DMSO oxidation of the iodomethane sugar **18**.

Compound **19** could then be reacted with a nucleophilic phosphite under Pudovik conditions (Scheme 10).[38] The global deprotection of the separated diastereomers would then generate novel α-hydroxy glucose 1-phosphonates **21** (shown as a diastereomeric mixture for simplicity). The intermediate **20** could also be explored to generate a library

of derivatives, including the desired α-monofluorinated glucose 1-phosphonates (diastereomeric mixture **22**).

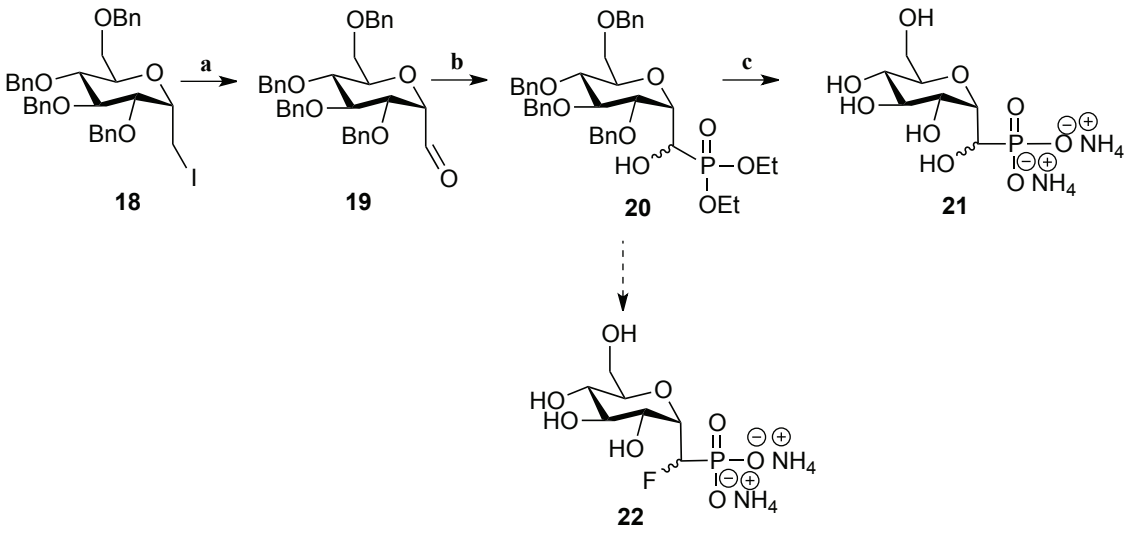

Scheme 10. The proposed scheme for the synthesis of α-hydroxy and monofluoro-Glc*p*.

(a) DMSO, $NaHCO_3$, 150 °C; (b) $PH(O)(OEt)_2$, NEt_3, 100 °C; (c) i) H_2, Pd-C (10% w/w), 5 h, rt, 55 psi, MeOH:EtOAc (1:1), ii) NH_4OH, pH 7.5.

After DMSO oxidation for six minutes at 150 °C, **18** was consumed. The resultant aldehyde **19** was not very stable, but a ^1H NMR spectrum of the reaction mixture was successfully collected by diluting the reaction mixture into 3 mL of water, extracting the solution with two milliliters of $CDCl_3$, and immediately acquiring the spectrum, which clearly showed the presence of the expected aldehyde signal at 10.10 ppm (Figure 19). However, attempts to work-up this material lead to decomposition, as did efforts to condense the material to dryness. Further purification was not possible.

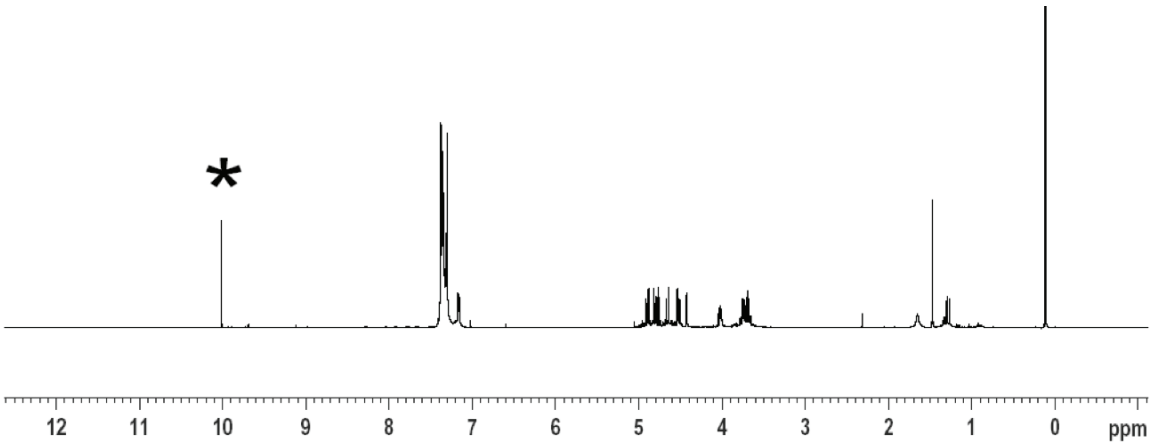

Figure 13. ^{1}H NMR spectrum of the crude reaction product showing the generation of an aldehyde **19**.

2.5.2 One-Pot Oxidation and Pudovik Reaction

Given that the aldehyde was formed, but not stable to work-up conditions, an alternative synthetic avenue was explored, wherein the Pudovik reaction was performed *in situ.* The generation of the α-hydroxy phosphonate would then be formed via a one-pot reaction sequence starting from the requisite alkyl halide as shown in Scheme 11.

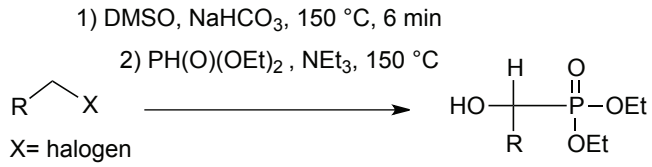

Scheme 11. Proposed one-pot Pudovik reaction an alkyl halides.

R = tetrabenzyl glucopyranosyl, octyl, 3-methylpentanyl, benzyl.

This one-pot strategy was tested on a series of readily available alkyl halides in trial reactions as summarized in Table 3. The synthetic strategy was shown to work on simple alkyl halides (**1A**, **1B**, **1C**, **1D**, **1E**), but the reactions were not high yielding.

Table 3. Oxidation with *in situ* Pudovik phosphonylation.

Reactant	Reaction Time	Result
Iodooctane **1A**	20 minutes	81% material recovered after work-up 44% yield
Bromooctane **1B**	35 minutes	66% material recovered after work-up 51% yield
Chlorooctane **1C**	> 2 hours; stopped at 2 hours	35% material recovered after work-up product not purified further
1-bromo-2-ethyl butane **1D**	1 hour	50% material recovered after work-up product was not purified further
Benzyl bromide **1E**	15 minutes	Trace after work-up product was not purified further

It is reasonable to assume that low yields may have been partially due to a competing E2 elimination reaction, but there was no attempt to collect such side-products. In addition, water solubility of the desired products caused product loss during aqueous work-up. The mass remaining, after work-up only, were low for **1A** and **1B**. For example, the mass was 66% of what would be expected from the theoretical yield in the case of the **1B** reaction, and product was detected in the water layer using ^{31}P NMR. Compound **1C** reacted much more slowly than the other halides. Compounds **1D** and **1E** were found to result in less than 50% mass recovery after work-up and were not purified further. When the coupled reaction on the corresponding sugar halide (**15**) was attempted, no product was detected using ^{31}P NMR spectroscopy.

Reaction conditions were evaluated to produce and collect the desired aldehyde **19,** as it would allow for a new approach to compound **20**. Treatment of compound **18**

with potassium superoxide in the presence of crown ether[39] was explored en route to **19**. The reaction resulted in the formation of a literature α-olefin (**25**)[40] in a yield of 42% as outlined in Scheme 12.

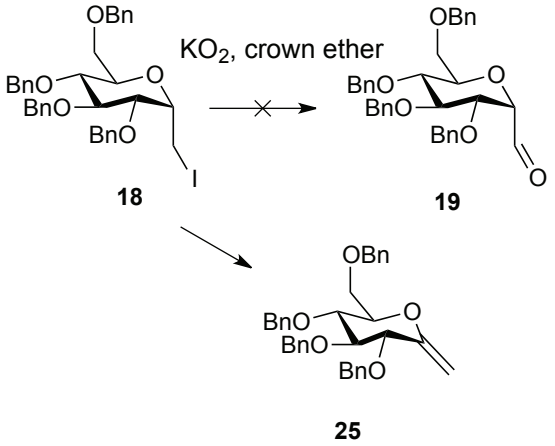

Scheme 12. The reaction of potassium superoxide on compound **18**.

An alternative strategy to access the desired aldehyde **19** was devised, as outlined in Scheme 13. Instead of forming the iodo-compound **18,** the mercuric(II) chloride precursor (**17**) was purified and subjected to an oxidative demercuration using oxygen gas and sodium borohydride.[35,41] This reaction was optimized to generate novel compound **26** with a modest, yet reproducible, yield of 45%. The oxidation of **26** was achieved using Dess-Martin periodinane (DMP).[42] Compound **19** was partially purified by work-up only with high yields (> 90%).

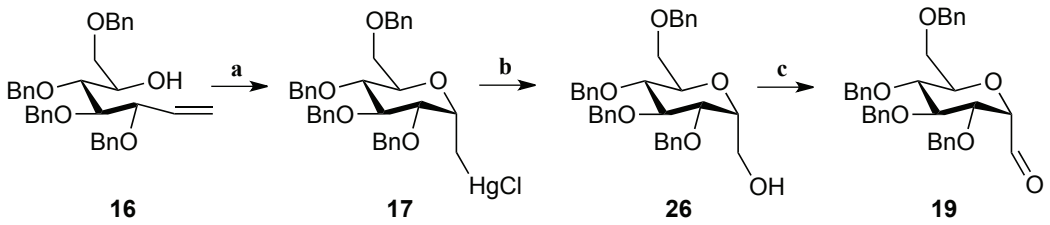

Scheme 13. A route to α-hydroxy phosphonates via compound **17**.

(a) i) $Hg(CF_3COO)_2$, THF, rt, 18 h, ii) KCl, 2 h, 90%; (b) $O_{2\,(g)}$, $NaBH_4$, DCM, DMF, rt, 2 h, 46%; (c) DMP, $NaHCO_3$, DCM, rt, 1.5 h, quant.

The successful synthesis and collection of requisite aldehyde **19** allowed for phosphorylation conditions to be revisited as summarized in Table 4. In the interest of avoiding the collection and storage of **19**, an *in situ* approach (**Method A**) was attempted whereby the reagents for phosphorylation where added directly to the oxidation. Monitoring using ^{31}P NMR spectroscopy indicated no product signals. Next, a neat method (**Method B**) was attempted, according to a literature protocol,[43] which again showed no product using ^{31}P NMR spectroscopy. **Method C** was an analogous reaction but included the addition of toluene and stoichiometric amounts of diethyl phosphite. Again no product was observed when monitoring using ^{31}P NMR spectroscopy. Phosphorylation was achieved at lower temperatures using more sophisticated bases as outlined in **Method D**[44] and **Method E**.[45]

Table 4. Pudovik conditions explored toward the generation of **20**.

Method	Phosphorylation conditions	Result
A	*In situ* addition 1.5 eq. diethyl phosphite, 1.5 eq. NEt_3 to DMP reaction. rt.	No product
B	4 mL diethyl phosphite, and 1.25 eq. NEt_3, 100 °C	No product
C	2 eq. diethyl phosphite, 2 eq. NEt_3, toluene, 120 °C	No product
D	1.1 eq. diethyl phosphite, 1.1 eq. LiHMDS, THF, -78 °C, 15 min	Complete consumption using TLC 21% yield diastereomeric mixture
E	1.1 eq. diethyl phosphite, 1.1 eq. DBU, THF, 0 °C-rt., 30 min	Complete consumption using TLC 34% yield diastereomeric mixture

Both methods **D** and **E** were shown to produce diastereomeric mixtures of α-hydroxy phosphonates with a maximum yield of 34% (combined diastereomeric mixture). ^{31}P NMR spectroscopy was used to determine a diastereomeric ratio of 1:1.34 (22.6 ppm and 21.8 ppm respectively) based on integration (Figure 20). Attempts to separate the diastereomers were unsuccessful due to overlapping elution during chromatography. Preparative TLC on silica was employed to separate the compounds, which resulted in a small amount (4.3 mg) of one highly enriched diastereomer as shown in Figure 20.

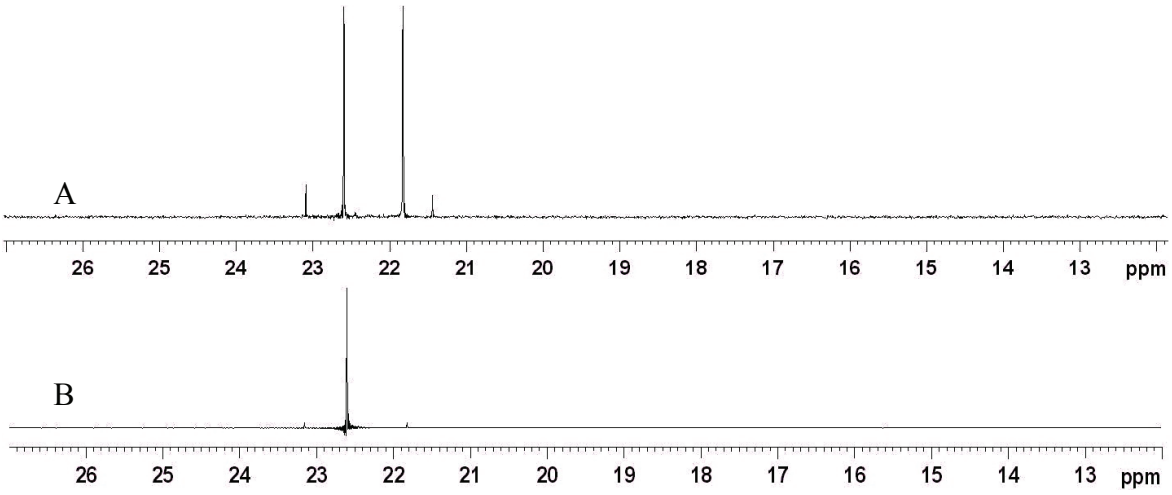

Figure 14. ^{31}P NMR spectroscopy after column chromatography and preparative TLC. (A) ^{31}P NMR spectroscopy after column chromatography, used to assign diastereomeric ratio. (B) ^{31}P NMR spectroscopy of the single diastereomer collected from preparative TLC.

The product was collected as the diastereomeric mixture (**20**) because attempts to separate the diastereomers were unsuccessful and resulted small amounts of pure

compounds, but the collection of one diastereomer allowed for the collection and partial characterization of one anomer. The yields of the reaction were widely variable and ^{31}P NMR spectroscopy showed the formation of numerous other phosphorous-containing compounds. The diastereomeric mixture was deprotected using hydrogenolysis to yield a mixture (**21**) with a good yield (70%).

2.5.3 Attempted Synthesis of *Gluco*-Configured α-Fluoro Phosphonates

Fluorination with DAST™[44] on a small amount (8.0 mg) of the mixture of protected diastereomers (**21**) was attempted. Compound **21** was reacted with DAST™, an electrophilic fluorine donor, at 0 °C. The mixture was allowed to warm to rt and react for one hour. However, ^{19}F NMR spectroscopy data showed no generation of fluorinated analogue **22**.

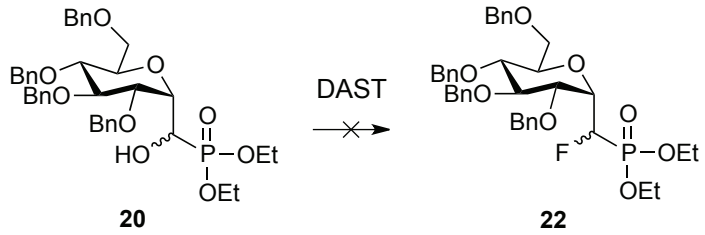

Scheme 14. The attempted fluorination with DAST™ on compound **20**.

Typically, DAST™ reacts readily with alcohols at low temperatures.[44] However, the bulky benzyl protecting groups may be sterically limiting access to the α-hydroxy group. To investigate the effect of steric hindrance at this site, the synthetic scheme could be revised with acetyl protecting groups on the sugar moiety and the phosphorylating

reagent could be substituted for commercially available dimethyl phosphite. Further fluorination strategies were not attempted at this point due to the difficulty in generating compound **20**, and also given that trial reactions conducted during the same time frame, on a related *galacto*-configured analogue had resulted in no reaction or starting material decomposition.[46]

In 2011 a review paper was published by Haudrechy and coworkers[47] which drew attention to previous work on mannose bearing the same exocyclic aldehyde moiety. In the work of Zou and coworkers[48] it was shown that treatment of the aldehyde with base (for example 4% MeONa) caused the molecule to rearrange to the beta-configuration (α/β = 1/8) at the anomeric center via interconversion with the straight chain form. It is likely that the basic conditions used during the phosphonylation may be causing the rearrangement of compound **19** at the same time as the desired reaction. Therefore, ring opening and rearrangement could have contributed to product yields less then 34% and the formation of multiple other phosphorous-containing products.

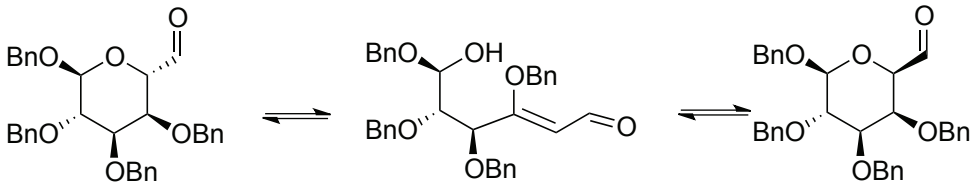

Scheme 15. Ring-opening and equilibration of the exocyclic aldehyde **19**.

CHAPTER 3. RESULTS AND DISCUSSION: ENZYMATIC ANALYSIS

3.1 Introduction

A major research aim in the Jakeman lab is to explore, understand, and utilize nucleotidylyltransferases. In general, these enzymes catalyze a reaction between a sugar 1-phosphate and a nucleoside 5′-triphosphate, wherein the nucleophilic sugar 1-phosphate attacks the α-phosphorous nucleoside atom from one face, while cleavage of the phosphodiester bond occurs on the opposite side (Scheme 16).[49, 50]

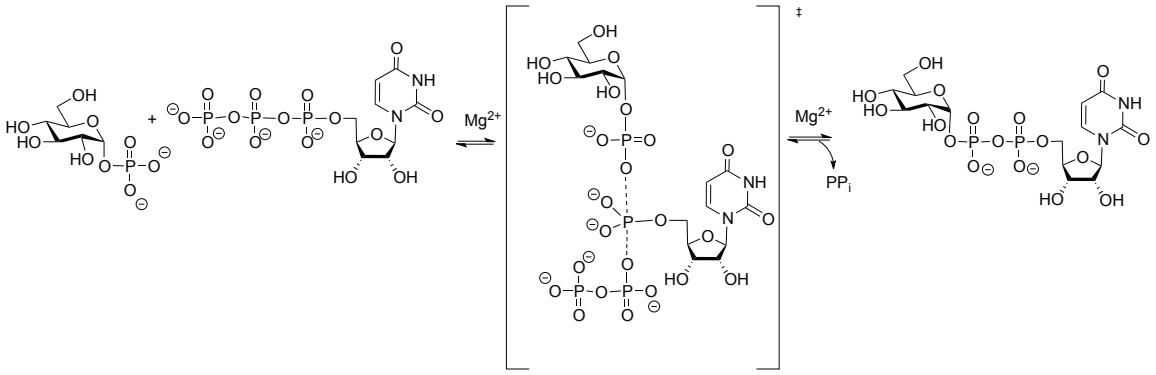

Scheme 16. General mechanism of a nucleotidylyltransferases.
Shown is a reaction between glucose 1-phosphate and UTP as an example.

The common mechanism of these enzymes is proposed to be an ordered bi-bi pathway wherein each substrate is required to bind in a specific order for catalysis, after which each product is released in a particular order (Figure 21). The bi-bi mechanism was first supported during nucleotidylyltransferase studies in the 1960s.[51,52] Since those preliminary studies, further kinetic and crystallographic evidence involving numerous nucleotidylyltransferases has determined that the ordered bi-bi mechanism is central to the function of many of these enzymes.[49, 50, 53]

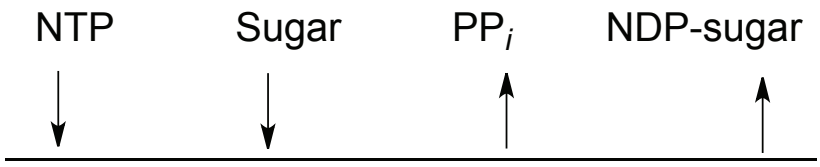

Figure 15. The ordered bi-bi mechanism of a mucleotidylyltransferase.

3.1.1 Cps2L a prototypical thymidylyltransferase

Cps2L, a thymidylyltransferase with broad substrate specificity,[8] naturally catalyzes the coupling of α-D-glucose 1-phosphate with deoxythymidine 5′-triphosphate (dTTP) to generate dTDP-Glc. It is found in the Gram-positive bacterium *Streptococcus pneumonia* R6 and is a component of natural primary metabolism, coupling sugar 1-phosphates and nucleoside triphosphates as described previously in Scheme 16. Cps2L also follows the ordered bi-bi mechanism as shown in Figure 21. Cps2L has been cloned, expressed, and purified in the Jakeman laboratory, and the substrate specificity has been explored in numerous studies employing commercially available and synthesized novel sugars.[54, 55, 56] Furthermore, studies have shown that the enzyme also catalyzes the reaction when phosphonyl,[8] ketose-phosphonyl,[7] or *galacto*-configured[56] substrates are used. Similarly, the nucleoside triphosphates have been successfully varied.[56] Cps2L was not a good catalyst to prepare UDP-α-D-Gal due to its lack of tolerance for the axial hydroxy configuration at C4.

3.1.2 AtUSP

AtUSP is a urididylyltransferase that naturally catalyzes the reaction between galactose 1-phospate and UTP. It is found in the plant *Arabidopsis thaliana* but the mechanism of this enzyme is not known. AtUSP was expressed, cloned, and provided by Toshihisa Kotake at Saitama University, Japan. It has not been studied in as great detail as Cps2L in the

Jakeman lab because it degrades. Recently it was found that freezing aliquots in MOPS buffer maintained the efficacy of the enzyme. This renders it suitable for this work.

In previous work, AtUSP was shown to catalyze the coupling of α-configured galactose 1-phosphonate with UTP, with 100% conversion to the corresponding sugar nucleotide observed within three hours.[26] AtUSP also exhibited 100% conversion within three hours for the coupling of glucose 1-phosphonate with UTP. In that case, the change in stereochemistry at C-4 showed no effect on turnover efficiency. Given the results of the previous studies, AtUSP was a promising avenue for exploring novel nucleotide synthesis with our novel *galacto*-configured compounds.

3.1.3 GalT

GalT is a galactose 1-phosphate uridylyltransferase that does not follow the common ordered bi-bi mechanism. Instead, it functions by a ping-pong double displacement mechanism, during which UDP-glucose acts as the first substrate and UMP is bound covalently to the enzyme via a histidine residue (Scheme 17), releasing glucose 1-phosphate.[57] Next, galactose 1-phosphate binds to the altered enzyme, allowing for the transfer of UMP to galactose 1-phosphate, which results in the formation of UDP-Gal*p* (Figure 22). GalT from the Gram-negative bacterium *Escherichia coli* was supplied by the Lowary lab and studied in the Jakeman lab for this project.[58]

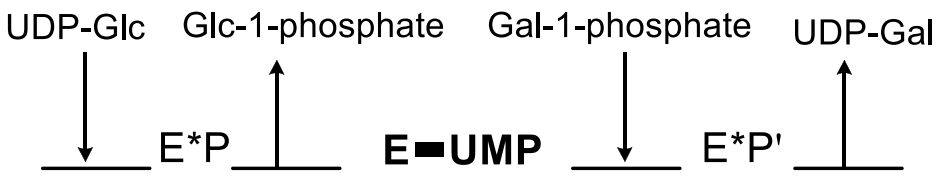

Figure 16. The ping-pong double displacement mechanism of GalT.

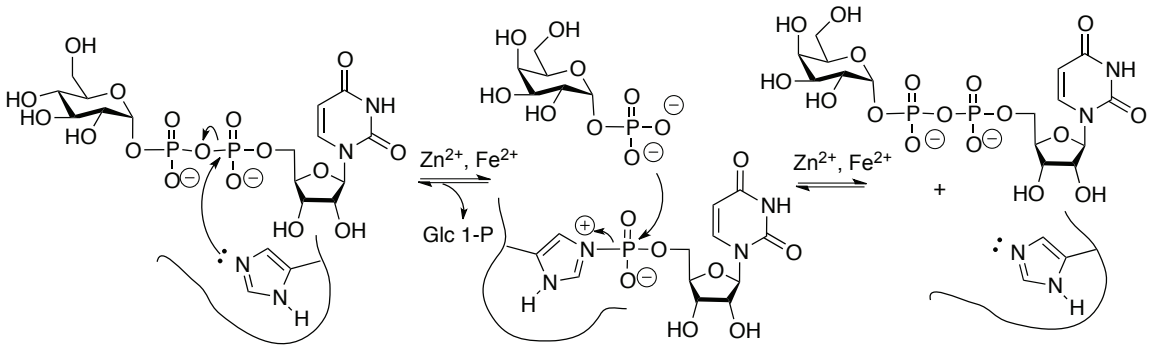

Scheme 17. The mechanism of UMP transfer by a histidine residue in the active site of GalT.

3.2 Enzymatic Analysis

Nucleotidylyltransferases are used as synthetic tools in the Jakeman laboratory for conducting enzymatic reactions that have all the necessary reagents present for catalysis.[56,8] The reactions are typically monitored using HPLC, which generates a trace that is integrated to allow for the formation of product and consumption of nucleoside to be compared. The HPLC analysis of nucleotidylyltransferase reactions and the retention times are well standardized and the traces are indicative of reaction progress as shown in Figure 23.

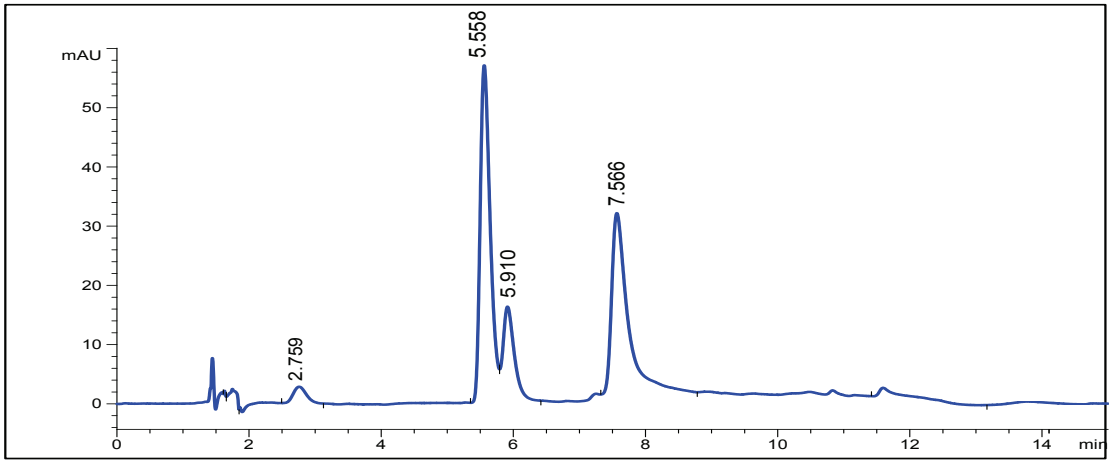

Figure 17. An example HLPC trace of an enzymatic assay generating UDP-Glc.

UTP elutes at 7.566 min, UDP at 5.910 min, and UMP at 2.759, wherein UDP and UMP is due to the breakdown of UTP. A peak at 5.6 minutes is due to UDP-Glc.

3.2.2 Enzymatic Analysis of α-Hydroxy Glucose 1-Phosphonate Mixture

The diastereomeric mixture **21** was explored for potential substrates or inhibitors of Cps2L. The reaction was performed with dTTP as the nucleotide source. After incubation for 40 minutes at 37 °C the percent conversion to sugar nucleotide was 32% according to analysis using HPLC.

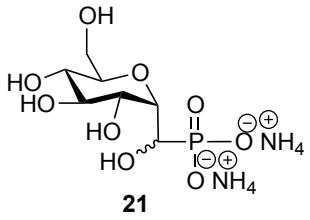

21

Figure 18. The novel Cps2L substrate diastereomeric mixture **21**.

Given that at least one of these diastereomers is a substrate for Cps2L, this project should be revised so that the diastereomers are separated, and their individual substrate activities studied. Cps2L could then be a method of generating the corresponding novel sugar nucleotides.

3.2.3 Enzymatic Assays of Novel Galactose 1-phosphate Analogues

Compounds **3**, **7**, **8,** and **10** (Figure 25) were explored as potential substrates for Cps2L, GalT, and AtUSP which have been shown to utilize α-configured sugar phosphonate as substrates.[8,26] In this work, the potential substrates are generated by mutarotation as shown in Figure 26. As substrates these enzymatic reactions would yield the desired sugar nucleotides of the novel *galacto*-analogues. The reactions were monitored using HPLC. A series of *gluco*-ketose phosphonates were previously shown to be good substrates for Cps2L.[7]

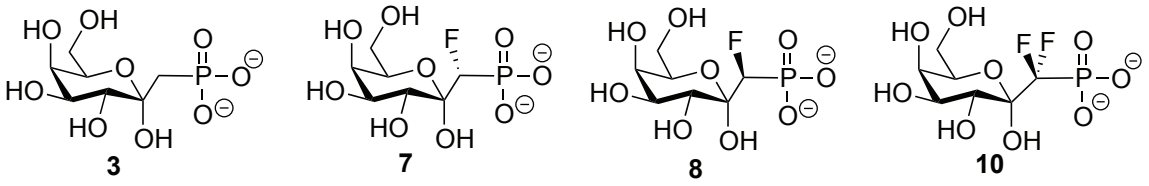

Figure 19. Potential substrates or inhibitors of nucleotidylyltransferases**.**

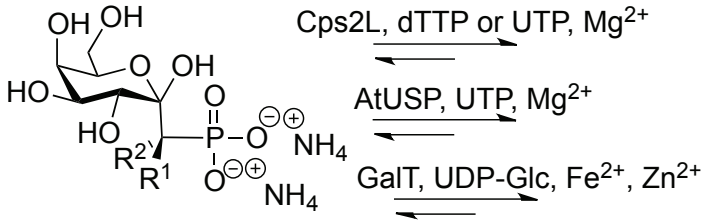

Figure 20. Mutarotation generated probes for enzymatic analysis**.**

3.2.4 Cps2L Assays Containing Novel Galactose Analogues

These molecules were first tested with Cps2L as this enzyme has been extensively studied in the Jakeman lab. Previous work demonstrated that Cps2L couples galactose 1-phosphonate and dTTP. However, activity was attenuated when UTP was substituted as the NTP. Interestingly, coupling of **3**, **7**, **8**, or **10** to UTP or dTTP to give the desired UDP-Gal*p* analogues was unsuccessful in each case. This is in stark contrast to the *gluco*-configured analogues.[3] These results suggest that the axial hydroxyl group of the *galacto*-configured analogues is effecting the tolerance of Cps2L for these compounds.

3.2.5 GalT Assays

GalT is an enzyme that naturally accepts α-configured galactose 1-phosphate and generates galactose-UDP. To do so, GalT utilizes glucose-UDP as a uridine source and yields glucose 1-phosphate in the process. Thus, the physiological substrates and products of this enzyme have identical molecular weights, as shown in Scheme 18. Also, the retention times of Glc-UDP and Gal-UDP are essentially the same. These two factors made it difficult to monitor enzyme activity because mass spectrometry and HPLC were not useful for observing the physiological reaction.

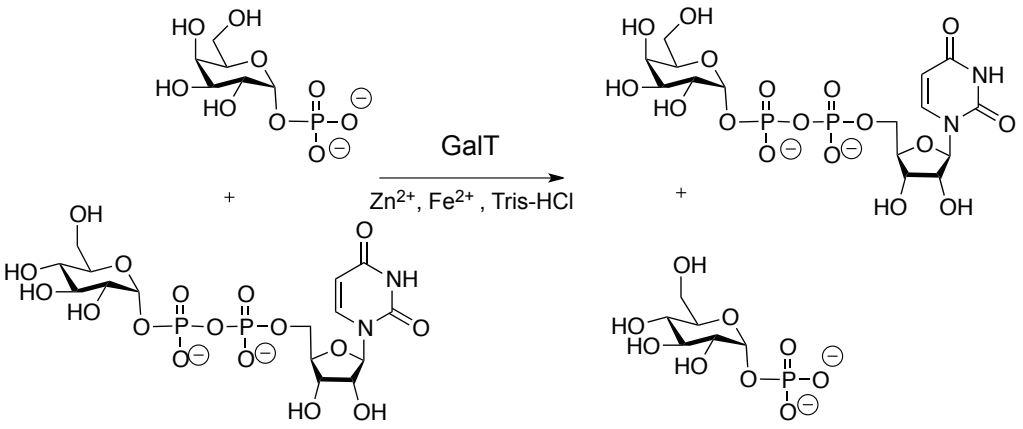

Scheme 18. GalT reaction substrates and products.

3.2.5.1 Monitoring GalT Activity

A new method of monitoring the activity of GalT was developed which coupled a Cps2L reaction with the GalT reaction. Two equivalents of UTP were added. The first equivalent was consumed by the Cps2L reaction within a one hour incubation period at 37 °C, to generated UDP-glc, the substrate for GalT. An aliquot of the reaction mixture was quenched and analyzed using HPLC, wherein the conversion of UTP to UDP-glc was observed via the difference in retention times of these two compounds. After an hour the percent consumption of UTP was seen to be within 45-49% (1 equivalent) as predicted by previous Cps2L studies.[56] At this point, galactose 1-phosphate, $ZnCl_2$, $FeCl_2$, and GalT were added. Within fifteen minutes all the UTP was consumed. Since the GalT reaction released glucose 1-phosphate as a product, any remaining UTP was consumed in a second reaction cycle, as shown in Scheme 19. Therefore, any consumption of UTP beyond 50% is due to the GalT activity with the galactose 1-phosphate. In trials with the novel galactose 1-phosphate analogues the differences in molecular weights allowed for monitoring by mass spectrometry (Figure 27).

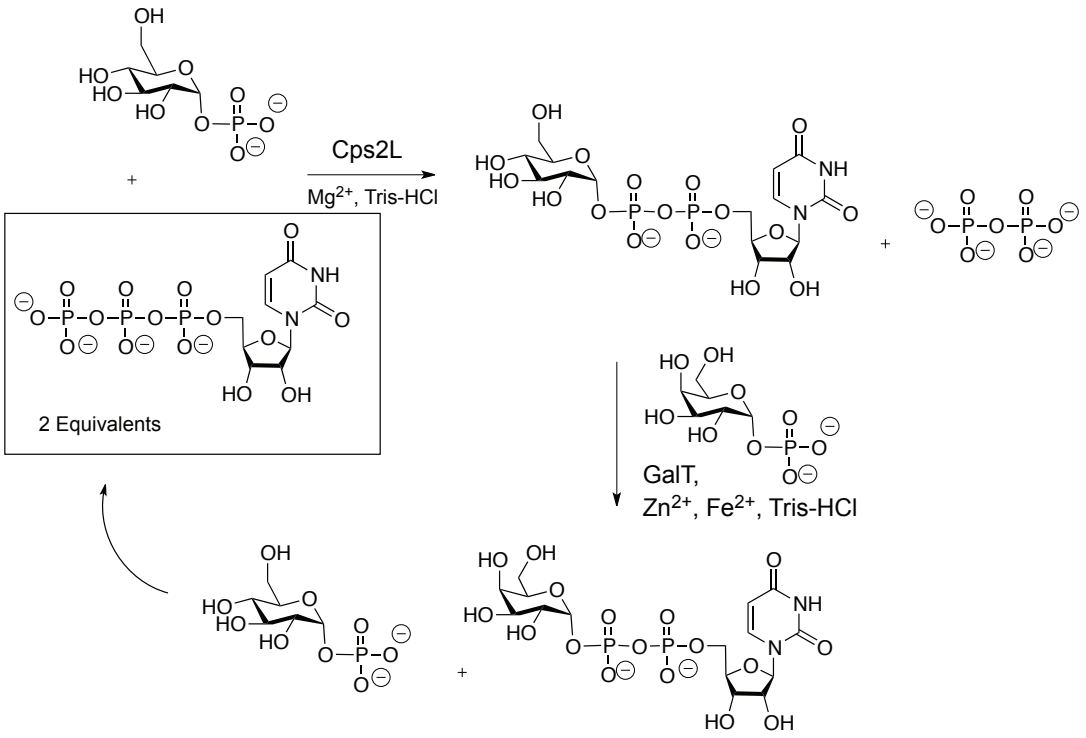

Scheme 19. Cps2L and GalT coupled assay for the generation of UDP-Galp.

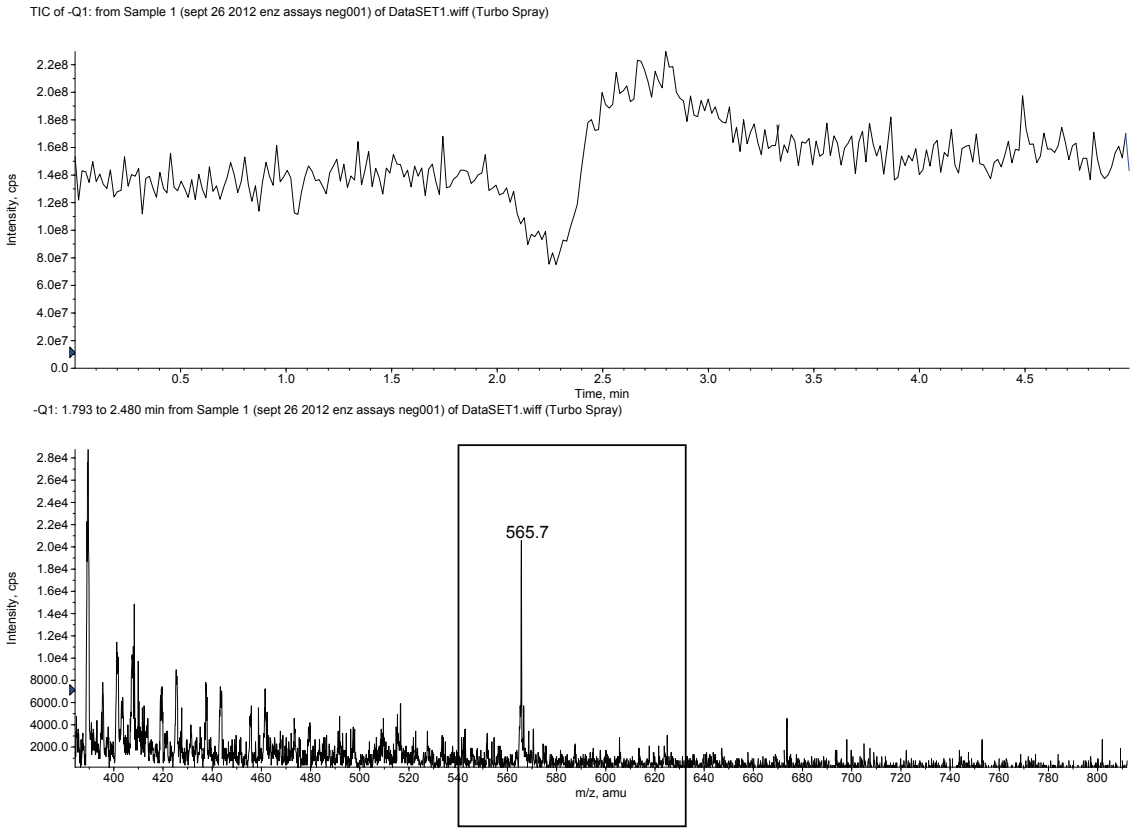

Figure 21. Mass spectrometry monitoring of the GalT assay.

Q1 ESI mass spectrometry in negative mode was used to monitor any generation of the enzymatic product when treated with compounds **3**, **7**, **8**, or **10**. Shown is an example spectrum showing that after 24 hours only starting UDP-glc is detectable (M = 566.3017 amu, chemical formula: $C_{15}H_{24}N_2O_{17}P_2$).

3.2.5.1 GalT Assays Containing Novel Galactose Analogues

The method of the GalT assay was demonstrated to work well with the physiological substrates, so the novel substrates were explored. Reactions were carried out via the coupled Cps2L reaction as well the uncoupled method using purchased UDP-glc. No

generation of sugar nucleotide resulted from assays containing **3**, **7**, **8**, or **10** after incubation at room temperature for 48 hours. Reactions were monitored using HPLC and low-resolution mass spectrometry at various time points.

3.2.6 AtUSP Assays Containing Novel Galactose Analogues

The method used for the AtUSP assay was demonstrated to work well with galactose 1-phosphate, the physiological substrate, so the novel substrates were explored. No generation of sugar nucleotide resulted from assays containing **3**, **7**, **8**, or **10** after incubation at 37 °C for 48 hours. Reactions were monitored using HPLC and low-resolution mass spectrometry at various time points. In previous work, AtUSP was shown to catalyze the coupling of α-configured galactose 1-phosphonate with UTP, with 100% conversion to the corresponding sugar nucleotide observed within three hours.[6] However, this research concluded that the addition of an anomeric OH completely attenuates AtUSP activity.

3.3 WaterLOGSY NMR Experiments to Examine Binding of Compound to AtUSP, GalT, or Cps2L

WaterLOGSY was employed to look for any enzyme substrate binding between GalT, AtUSP, or Cps2L with known substrates and novel substrate analogues. WaterLOGSY NMR detects the binding of small molecules to enzymes. This process was summarized by Peng and coworkers in a review article in 2004.[59] Peng summarized the process as follows: first the bulk water molecules in solution are irradiated, followed by magnetization passing from water to the receptor (enzyme) and then to ligands bound in the receptor (enzyme). Next, ligands that return to solution have differing differential

cross-relaxation properties compared to non-binding ligands which will have created WaterLOGSY NMR signals with opposite signs that phase in opposite directions. WaterLOGSY NMR can show interactions for substrate, inhibitors, as well as non-competitive binders. When no interaction is seen, the compound is either not interacting with the enzyme, the compound could be binding tightly, or the parameters of the WaterLOGSY NMR experiment may not suitable for the given enzyme.[59]

During the WaterLOGSY NMR experiments, initial spectra were collected with 1.0 mmol sugar (while maintaining the requisite reagent ratios) instead of 5.0 mmol, which was used in previous work,[7] in efforts to conserve enzyme and the synthesized substrates. However, it was found that this concentration gave inconsistent results and at times showed no binding, when the reaction was repeated with 5.0 mmol sugar binding was observed and results were reproducible.

3.3.1 Cation effect on ^{1}H NMR of GalT

WaterLOGSY NMR experiments were run in the presence and absence of Fe^{2+} and Zn^{2+} in the case of GalT. In samples with cations present line broadening was observed. ^{1}H NMR spectrum were obtained separately for the mixture of galactose 1-phosphate and UDP-glucose in the presence of each cation. It was found that the line broadening was due to the effects of Fe^{2+}. The resultant spectra are compared in Figure 28.

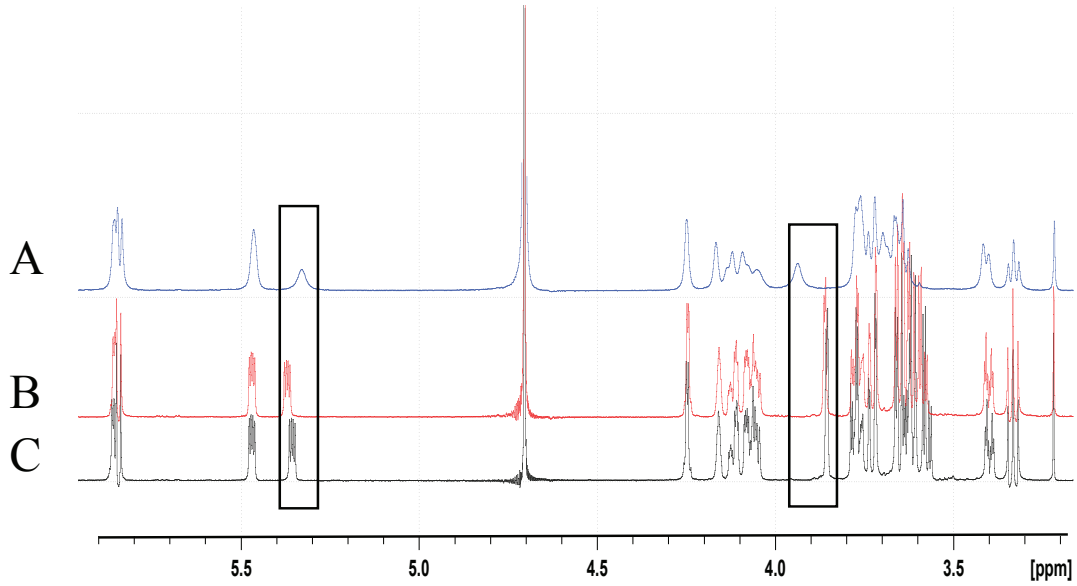

Figure 22. The effects of cations on the ^{1}H NMR signal of Gal*p* and UDP-glc.

All spectra included galactose 1-phosphate and UDP-glucose (1:1, 0.1M), (pH 7.5), in D_2O. (A) only $FeCl_2$ is present. (B) only $ZnCl_2$ is present. (C) no cations are present.

In **B** and **C**, signals at 5.37 ppm and 3.85 ppm (the anomeric proton and H-2 proton, respectively) on galactose 1-phosphate, were shielded. The difference in line broadening and direction of deshielding is due to the differences in magnetism of iron and zinc, where the paramagnetism of iron has a much stronger effect on NMR spectrum.[60] The shielding indicates that the divalent cation is coordinating to, or is in close proximity to, those protons in solution. Due to the line broadening caused by iron, it was omitted henceforth during NMR studies.

3.3.2 The Dependence of GalT Activity on Divalent Metal Cations

The dependence of GalT efficacy on Fe^{2+} and Zn^{2+} cations was explored because of inconsistency in the primary literature. Studies in 2002[61] involving *E. coli* GalT provide an Enzyme Commission (EC) number for Human GalT that only requires Mg^{2+} as a cation. However, a study from 1996 reported that *E. coli* GalT requires Fe^{2+} or Zn^{2+}.[62] In that work, it was shown that the enzyme, in its natural dimeric form, contains ~ 0.67 mol of Fe^{2+} and ~1.21 mol Zn^{2+} and that at least one mole of divalent cation is required for catalysis per mole of enzyme subunit. When the cation was replaced with other divalent cations the enzymatic activity was only partially restored. However, if two equivalents of either Fe^{2+} or Zn^{2+} were used the full activity of the enzymes was maintained. The coupled Cps2L and GalT assay was run with and without Fe^{2+} and Zn^{2+} in parallel. After fifteen minutes, the GalT reaction with cations consumed 90% UTP while the reaction without the cations consumed only 42%. The HPLC traces are provided in an overlay in Figure 29, for comparison. After an additional thirty minutes, the reaction without $ZnCl_2$ and $FeCl_2$ was incomplete. Given that the use of Fe^{2+} as a cofactor during NMR experiments caused severe line broadening, it was fortuitous that if only 2 equivalents Zn^{2+} was present during enzyme assays the efficiency of GalT was not affected as predicted.[62]

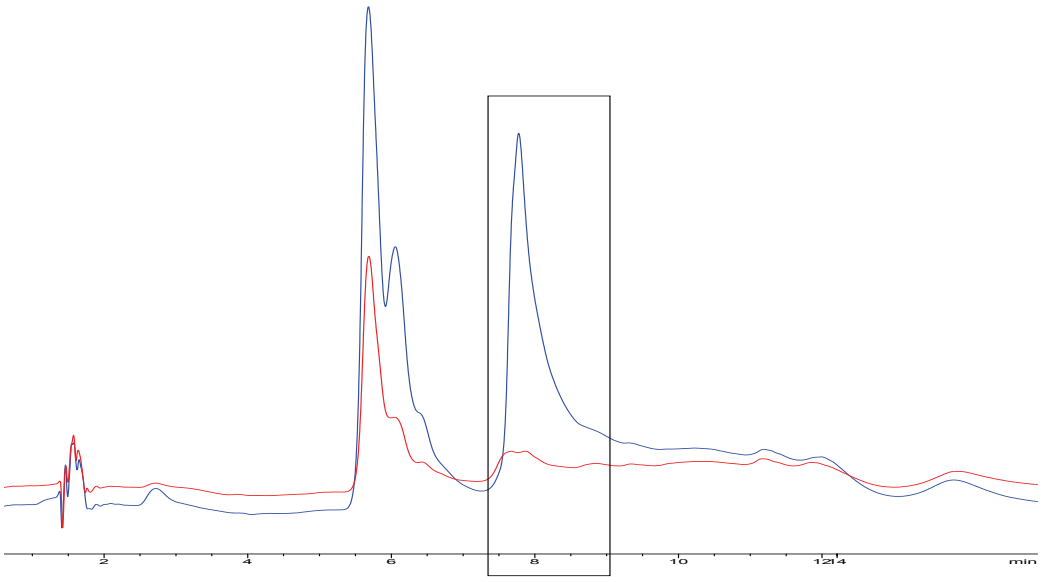

Figure 23. HPLC of GalT activity dependence on Fe^{2+} and Zn^{2+}.

The box highlights the change in UTP consumption over five minutes, with and without cations.

3.3.3 WaterLOGSY NMR Experiments: AtUSP

Given that the four *galacto*-ketose phosphonates were not substrates for AtUSP, WaterLOGSY NMR binding experiments with AtUSP and **3**, **7**, **8,** or **10** were observed in the absence of UTP, with benzoic acid as a non-binding control. Galactose 1-phosphate showed binding by NMR to AtUSP in the absence of UTP, suggesting that UTP is not required to bind before the sugar 1-phosphate. NMR results suggest that the *galacto*-configured ketose phosphonates do bind AtUSP (Figure 30). Further inhibition studies were not conducted because the inhibition of AtUSP of not an objective of this project.

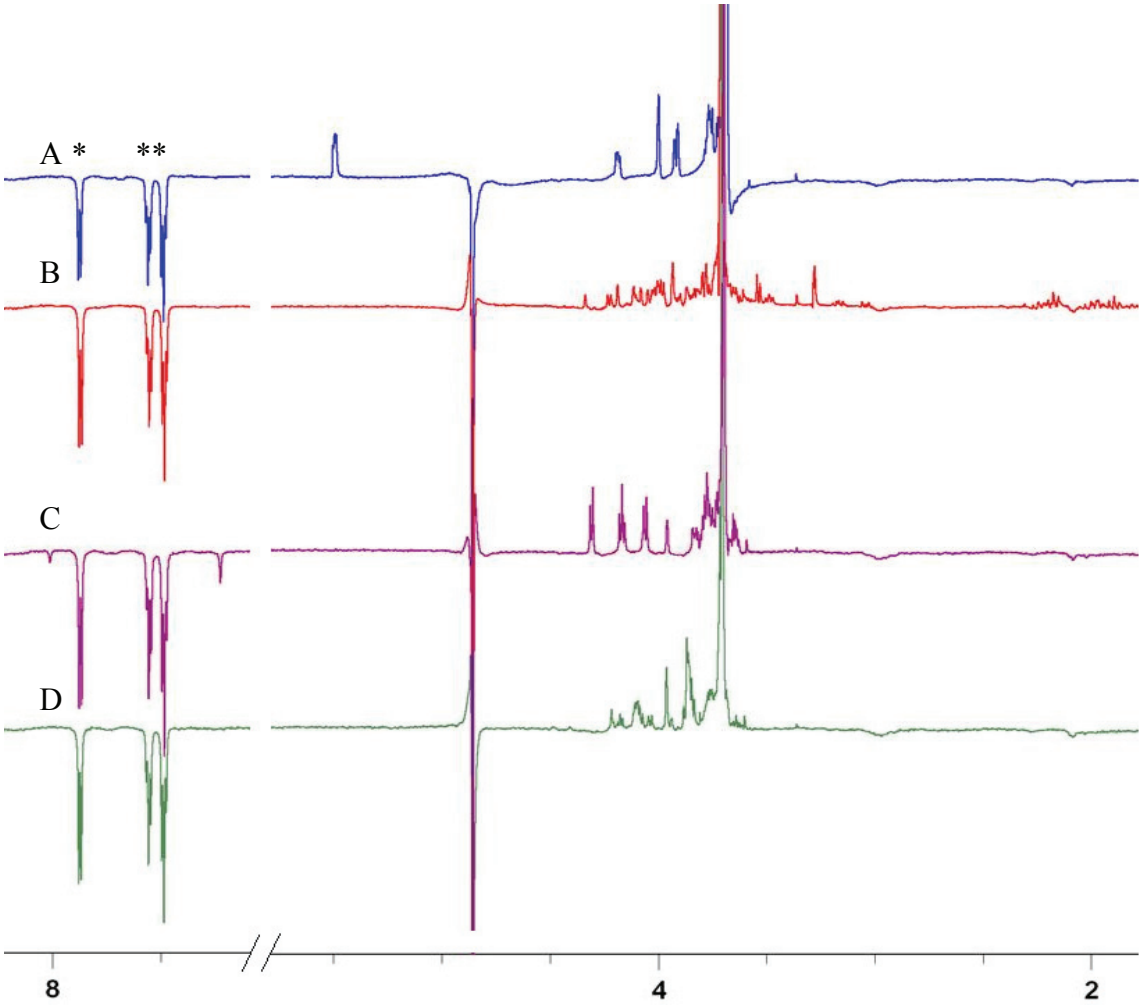

Figure 24. WaterLOGSY NMR spectra from assay with AtUSP.

(700 MHz, 1:9 D_2O:H_2O) showing ligand binding above the baseline and non-binding phased in the opposite phase. (A) 5.0 mmol galactose 1-phosphate. (B) 5.0 mmol compound **3**. (C) 5.0 mmol compound **10**. (D) 5.0 mmol compound **8**. *Benzoic acid, added as a negative control. The peak at 3.65 ppm is Tris-HCl buffer.

3.3.4 WaterLOGSY NMR Experiments: GalT

Given that the four *galacto*-ketose phosphonates were not substrates for GalT, WaterLOGSY NMR binding experiments with GalT and **3**, **7**, **8,** or **10** were observed in the presence and absence of UDP-Glc. In the case of GalT, it was found that benzoic acid binds GalT, and during these assays benzoic acid functioned as a binding control.

Attempts were made to screen other non-binders. However, acetic acid, ethyl acetate, phenol, and cyclohexanol were all found to bind GalT as shown in Figure 31.

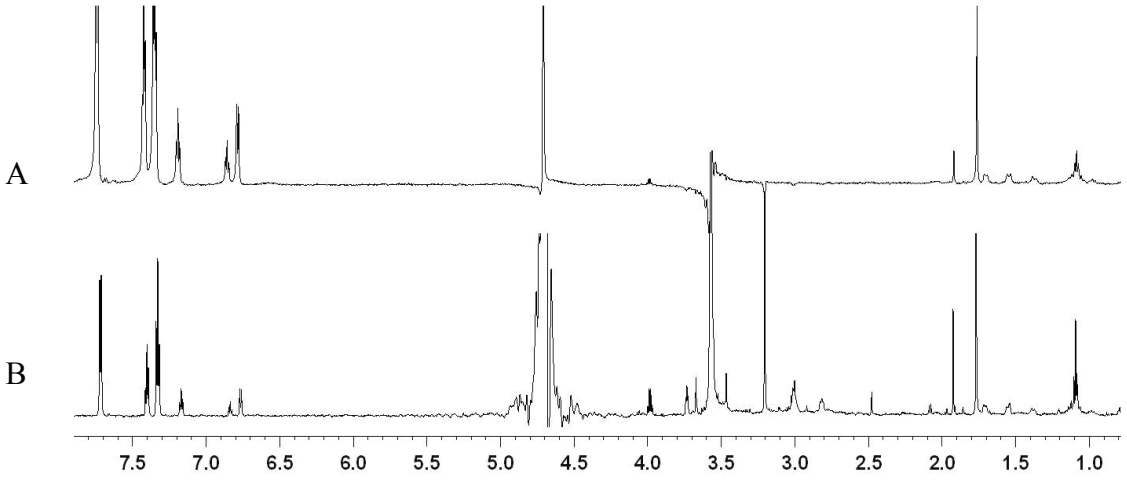

Figure 25. GalT WaterLOGSY NMR non-binding screen.

(700 MHz NMR, 9:1 H_2O:D_2O), containing acetic acid, ethyl acetate, phenol, cyclohexanol, and benzoic acid showing ligand binding phased above the baseline. (A) WaterLOGSY NMR spectrum. (B) ^{1}H NMR spectrum of the same sample.

Binding was observed using waterLOGSY NMR to monitor the physiological reaction, whereby it shows the generation of products (Figure 32), NMR binding studies show binding to the substrates and products. Binding interactions in the WaterLOGSY experiments with **3**, **7**, **8,** or **10** were observed in the presence or absence of UDP-Glc. Figure 33 shows this with compound **10** as an example. Results suggest that the *galacto*-configured ketose phosphonates do bind GalT. However, the ketose phosphonates were shown not to be substrates, these results suggests that the ketose phosphonates were not able to act as nucleophiles and react with the UMP bound in the active site

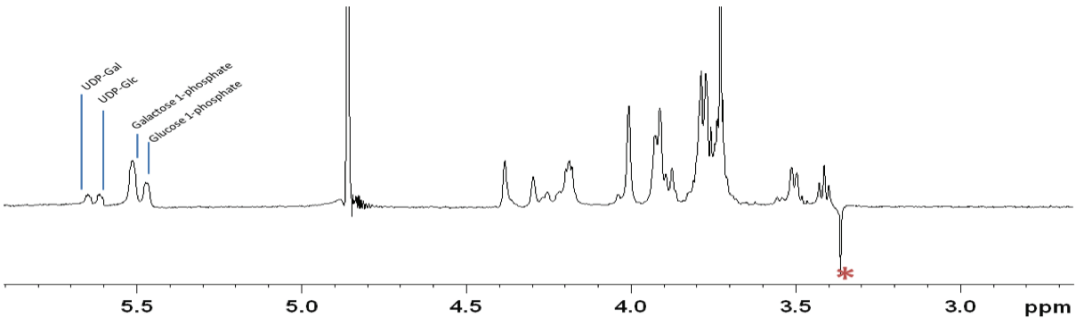

Figure 26. WaterLOGSY NMR spectrum of the physiological GalT reaction.

Shown is the reaction in progress where the anomeric protons on all four sugar containing compounds are clearly resolved (labeled above). During this experiment, UDP-Gal and glucose 1-phosphate are being generated by GalT catalysis. *Tris HCl buffer, non-binding.

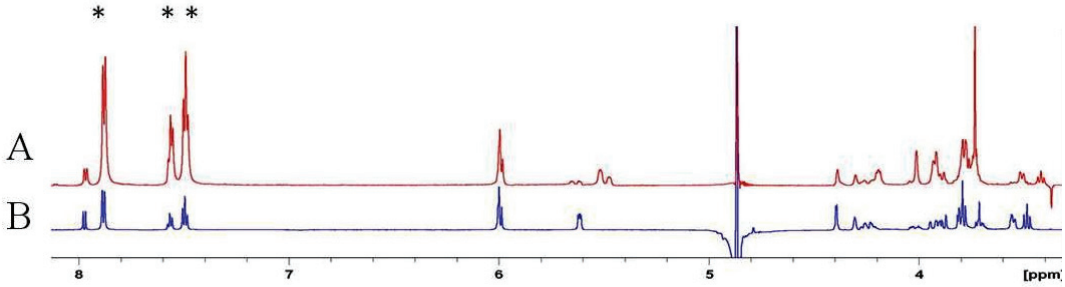

Figure 27. WaterLOGSY NMR comparison of reactions with substrates or non-substrates.

(700 MHz, 1:9 D_2O:H_2O) showing ligand binding above the baseline and non-binding phased in the opposite phase. (A) a reaction in progress with galactose 1-phospate and UDP-Glc. (B) no reaction observed between UDP-Glc and **3**. *Benzoic acid, positive binding control.

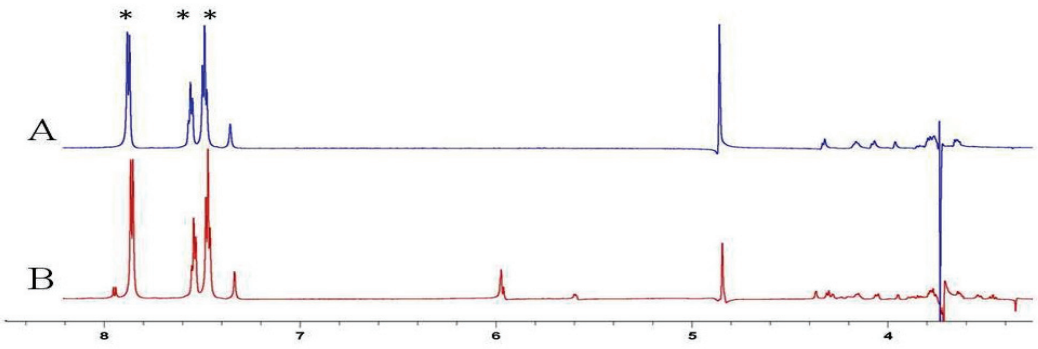

Figure 28. WaterLOGSY of Compound **10** in the presence and absence of UDP-Glc. (700 MHz, 1:9 D_2O:H_2O) showing ligand binding above the baseline and non-binding phased in the opposite phase. (A) Compound **10**. (B) Compound **10** and UDP-Glc. *Benzoic acid, positive binding control.

3.3.5 WaterLOGSY NMR Experiments: Cps2L

The coupling of **3**, **7**, **8**, or **10** with UTP to give the desired UDP-Gal*p* analogues was unsuccessful. In an attempt to better understand the binding interactions between **3**, **7**, **8,** or **10** with Cps2L, WaterLOGSY NMR binding experiments were performed in the absence of NTP because Cps2L has an ordered bi-bi mechanism as previously described, where the nucleoside must bind first, followed by the sugar 1-phosphate.

In the case of *gluco*-configured ketose phosphonate analogues, binding was observed in the absence of NTP.[7] This suggests that these analogues could function via a different enzymatic mechanism. In the WaterLOGSY NMR experiment with **3**, **7**, or **10** in the absence of NTP, no binding was observed. This suggests that the *galacto*-configured ketose phosphonates do not bind Cps2L in the same manner as the *gluco*-configured phosphonates. Interestingly, the (*S*)-monofluorinated ketose phosphonate

shows binding to Cps2L. Figure 35 shows the WaterLOGSY spectra. This result suggests that binding of this diastereomer does not follow the ordered bi-bi mechanism and could be further explored for potential inhibition of Cps2L, as this compound appears to be acting via an alternative mechanism.

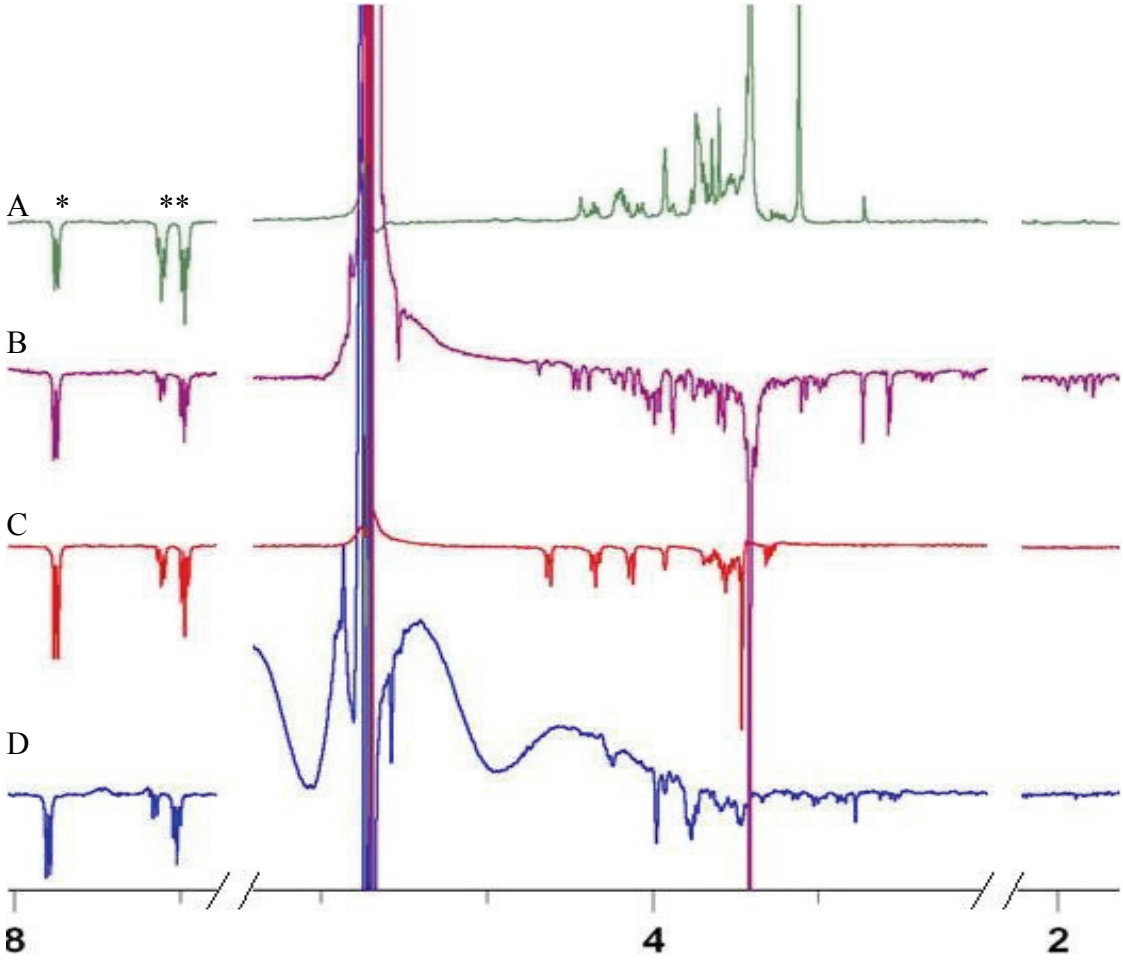

Figure 29. WaterLOGSY NMR spectra showing Cps2L and the novel *galacto*-ketose phosphonates binding.

(700 MHz, 1:9 D_2O:H_2O) showing ligand binding above the baseline and non-binding phased in the opposite phase. (A) 5.0 mmol compound **8**. (B) 5.0 mmol compound **3**. (C) 5.0 mmol compound **10**. (D) 4.0 mmol compound **7**; the spectrum shows poor water suppression, likely as a result of using an alternative 3.0 mm NMR tube in efforts to maintain an appropriate concentration of compound. *Benzoic acid, added as a negative control. The peak at 3.65 ppm is Tris-HCl buffer.

During binding studies the concentration was found to play an important role while observing binding. Initial studies using 1.0 mmol of these sugars gave dispersive spectra where little to no sugar proton character was observable. However, recent experiments at 5.0 mmol of **8** showed binding. At this time, data has been collected for compound **7** at 4.0 mmol, in a 3.0 mm NMR tube to determine if increasing the reagent concentrations will generate similar results. It was found that **7** does not show binding at this concentration. However, the water suppression was poor during this experiment (Figure 35, entry D) as a 3.0 mm NMR tube was used.

CHAPTER 4. CONCLUSIONS

4.2 Conclusions

A series of *galacto*-configured ketose phosphonates were synthesized and evaluated as substrates for GalT, AtUSP, and Cps2L. WaterLOGSY NMR binding studies showed that the (*S*)-configured monofluorinated *galacto*-ketose phosphonate interacted with Cps2L in the absence of NTP which is not in-line with the ordered bi-bi mechanism of this enzyme. WaterLOGSY NMR studies showed binding of gal*p* to AtUSP in the absence of NTP demonstrating that the binding order of this enzyme does not require NTP to bind before the sugar substrate. WaterLOGSY NMR studies of the synthetic substrate analogues also showed binding to AtUSP. WaterLOGSY studies with GalT demonstrated that the substrates gal*p* and UDP-glc, as well as the synthetic substrate analogues, bound GalT. However, non-specific binding to other small molecules was also observed.

The synthesis of *gluco*-configured α-hydroxy phosphonates was achieved. The diastereomeric mixture of this material was shown to include a novel Cps2L substrate. The protected *gluco*-configured α-hydroxy phosphonate in a diastereomeric mixture was found to be unreactive with DAST™.

4.2 Future Work

Currently, efforts are focused on generating sufficient material for future inhibition studies with UGM for our collaborators. Generating more material will also allow for WaterLOGSY NMR experiments with the (*R*)-monofluoro ketose phosphonate to be

reexamined with sufficient concentration. With sufficient material, Cps2L inhibition could also be explored. Chemical coupling approaches to the sugar nucleotide analogues should also be developed.

Inhibition assays with Cps2L have been standardized within the Jakeman lab and may allow for the determination of inhibition parameters for Cps2L with the (*S*)-monofluorinated *galacto*-ketose phosphonates. At this time, a strategy for exploring GalT inhibition within the Jakeman lab has not been established. Given that non-specific binding was observed for all ligands studied during the enzyme-ligand binding experiments, those experiments did not aid in generating any predictions regarding potential binding, or narrow the library of compounds that should be investigated for inhibition of GalT. An avenue of inhibition experiments that could be considered would be NMR analysis of the reaction progress in the presence and absence of the novel *galacto*-ketose phosphonates.

CHAPTER 5. EXPERIMENTAL

5.1 General Synthetic Methods

Reagents and anhydrous solvents were purchased from Sigma-Aldrich and used without further purification. All other solvents were used without further purification. Unless otherwise stated, all reactions were performed under a nitrogen atmosphere and in oven-dried glassware (>100 °C). Molecular Sieves were activated before use by drying in an oven (>100 °C, >12 h). Thin layer chromatography and low-resolution LCMS were used to monitor the progress of all reactions. Glass Silicycle™ precoated silica gel plates (250 μm thickness) were utilized and visualized with ultraviolet light (λ = 254 nm), and a potassium permanganate dip solution (3.0 g potassium permanganate, 20.0 g potassium carbonate, 5.0 mL 5% aqueous sodium hydroxide, 300 mL distilled water) or a *p*-anisaldehyde dip solution (*p*-anisaldehyde 3.4%, sulfuric acid 2.2%, and acetic acid 1.1% in ethanol), followed by warming with a heat gun. Evaporations were performed using a Büchi rotary evaporator. Lyophilizations were performed using an Edward Freeze-Dryer.

Normal-phase silica gel chromatography was performed using a bench-top glass column or using a Biotage SP1™ high performance flash chromatography system using Silicycle™ ultra pure silica (230-400 mesh) or Silicycle™ Siliasep™ cartridges, respectively. Compounds were dried onto Biotage™ Isolute HM-N for chromatography. Water-soluble compounds were purified with LH-20 size exclusion resin. Yields are reported for chromatographically and analytically pure compounds, unless otherwise discussed.

NMR spectra were acquired using a Bruker AV-300 and AV-500 spectrometers at the Nuclear Magnetic Resonance Research Resource, Dalhousie University, or using a Bruker AV-700 spectrometer at the Biomolecular Magnetic Resonance Facility, National Research Council of Canada, Halifax. Chemical shift data were measured relative to TMS (0.00 ppm) for ^{1}H, $CDCl_3$ (77.16 ppm) for ^{13}C or methanol-d_4 (3.31 ppm for ^{1}H). Proton assignments were based on COSY experiments, coupling constants, and 1D NOE NMR, and H-P HSQC. High-resolution mass spectra were recorded using a microTOF instrument (Bruker Dalton) with an electrospray (ESI) source.

5.2 pK_a2 Determinations

10 mM solutions of the diammonium salt of the ketose phosphonates (**3**, **8**, **7**, or **10**) were adjusted to pH 9 with 0.2 M NaOH and titrated with 2 μL aliquots of 0.2 M HCl to pH 1.5. The pH was measured using a Hach waterproof microelectrode (model H160). pK_a values were then determined by fitting the data, moles of HCl added against pH, in GraFit 5.0.5 (Erithacus Software Limited).

5.3 WaterLOGSY Sample preparation

In general, WaterLOGSY NMR experiments were composed of 1:1:0.1 sugar:UTP:enzyme using either 5 mM or 1 mM sugar and 0.2 mM cation(s). An equimolar amount of benzoic acid to sugar was used as a non-binding control (except for experiments with GalT). Each sample was buffered with deuterated Tris and run in 10% D_2O/ 90% H_2O on the AV 700 MHz NMR spectrometer.

5.4 Enzymatic Assay Methods

Unless otherwise noted, enzymatic reaction were incubated at 37 °C with aliquots taken at various time points analyzed via HPLC using methods previously described.[56] Enzymatic reactions were analyzed using HPLC with Hewlett Packard Series 1050 instrument with an Agilent Zorbax 5 μM Rx-C18 column (150 cm × 4.6 mm) as well as low resolution mass spectrometry, where beneficial, using an Applied Biosystems hybrid triple quadrupole linear ion trap (Qtrap2000) mass spectrometer with an electrospray (ESI) source. The enzymes used were over-expressed and purified in the lab using methods that were previously described.[56,63,26,61] The enzyme concentrations were determined spectrophotometrically at 280 nm using the respective extinction coefficients (Cps2L $\varepsilon = 29\ 340\ M^{-1}cm^{-1}$, *At*UPS $\varepsilon = 83\ 685\ M^{-1}cm^{-1}$, GalT $\varepsilon = 71\ 765\ M^{-1}cm^{-1}$)[7, 26]

5.4.1 Assays Containing Cps2L or AtUSP

Assays containing sugar analogues (2 mmol), NTP (1 mmol), $MgCl_2$ (2.2 mmol), inorganic pyrophosphatases (0.5 EU), and enzyme (2 EU or up to the maximum enzyme concentration based on volume) were made up to 50 or 100 μL final volume with Tris·HCl buffer (50 mM, pH 7.5) and incubated at 37 °C. Aliquots (5 μL) of the reaction mixtures were quenched with MeOH (15 μL), centrifuged (4 minutes, 13 000 rpm), and analyzed using HPLC.

5.4.2 Assays Containing GalT

Cps2L coupled reaction assays containing glucose 1-phosphate (2 mmol), UTP (4 mmol), $MgCl_2$ (2.2 mmol), inorganic pyrophosphatases (0.5 EU), and Cps2L (4 EU) were made up to 50 μL final volume with Tris·HCl buffer (50 mM, pH 7.5) and incubated at 37 °C for 1 hour, at which point an aliquot (5 μL) of the reaction mixture was quenched with MeOH (15 μL), centrifuged (4 minutes, 13 000 rpm), and analyzed using HPLC to confirm consumption of approximately half of the UTP. Next, the galactose 1-phosphate analogue (2 mmol), $FeCl_2$ (2.2 mmol), $ZnCl_2$ (2.2 mmol) were added, followed by GalT (24 μL GalT in Tris-HCl buffer), for a final volume of 100 μL which was allowed to react at rt. Aliquots (5 μL) of the reaction mixture were quenched with MeOH (15 μL), centrifuged (4 minutes, 13 000 rpm), and analyzed using HPLC.

Alternatively, reaction assays containing galactose 1-phosphonate analogues (2 mmol), UDP-glc (2 mmol), $ZnCl_2$ (2.2 mmol), $FeCl_2$ (2.2 mmol), and GalT were made up to a final volume of 100 μL with Tris·HCl buffer (50 mM, pH 7.5) and allowed to stand at rt. Aliquots (10 μL) of the reaction mixture were quenched with MeOH (30 μL), centrifuged (4 minutes, 13 000 rpm), and analyzed using low resolution mass spectrometry.

5.5 Compound Preparation and Characterization Data

2,3,4,6-Tetra-O-benzyl-D-galactonolactone (1)

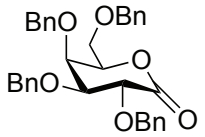

1

To a stirring solution of 2,3,4,6-tetra-*O*-benzyl-D-galactopyranose (10.00 g, 18.5 mmol) in anhydrous DMSO (60 mL) was added acetic anhydride (46.0 mL) at rt. The reaction mixture was stirred for 18 h before being poured into H_2O (200 mL). The resultant solution was then extracted with EtOAc (2 × 50 mL). The combined organic fractions washed further with H_2O (3 × 150 mL) to remove residual DMSO, then dried with anhydrous Na_2SO_4, filtered and concentrated. The residue was purified using silica gel flash chromatography (1:3 EtOAc:hexanes) to afford **2** as a colourless oil (4:6 EtOAc:hexanes, R_f product = 0.83) (9.26 g, 17.2 mmol, 92%); spectroscopic data were consistent with literature.[64,65]

2,3,4,6-Tetra-*O*-benzyl-C-(1′-dibenzylphosphonomethyl)-α-D-galactopyranose (2)

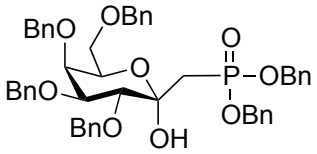

2

To a stirring solution of freshly prepared dibenzyl methylphosphate (11.99 g, 43.3 mmol) in anhydrous THF (55 mL) at –78 °C, was added *n*-BuLi (18.0 mL, 43.3 mol, 2.5 M in hexanes) dropwise. The reaction mixture was stirred for 30 min before **1** was added (8.32

g, 15.5 mmol, in 15.0 mL THF) dropwise. The resultant solution was then allowed to warm to rt with stirring for 2 h. The reaction was quenched with saturated NH_4Cl (50 mL). The organic layer was then washed with H_2O (100 mL). The aqueous layers were combined and extracted with DCM (2 × 50 mL). the organic extracts were combined dried with anhydrous Na_2SO_4, filtered and concentrated. The remaining residue was purified using silica gel flash chromatography (35:65 EtOAc:hexanes) to afford **2** as a white solid (4:6 EtOAc:hexanes, $R_f$product = 0.64) (12.6 g, 14.5 mol, 94%); ^{1}H NMR (500 MHz, $CDCl_3$) δ =7.45-7.22 (m, 30H, 6 × Ph), 5.90 (s, 1H, anomeric OH), 5.11, 5.07 (ABq, 2H, J_{AB} = 4.5 Hz, CH_2Ph), 5.03, 5.00 (ABq, 2H, J_{AB} = 10 Hz , CH_2Ph), 4.96,4.88 (ABq, 2H, J_{AB} = 8.5 Hz, CH_2Ph), 4.80 (s, 2H, CH_2Ph), 4.70, 4.65 (ABq, 2H, J_{AB} = 11.5 Hz, CH_2Ph), 4.41, 4.38 (ABq, 2H, J_{AB} = 11.5 Hz, CH_2Ph), 4.32 (dd, $J_{5,6a}$ = 7.4 Hz, $J_{4,5}$ = 1.4 Hz, 1H, H-5) 4.16 (dd, $J_{3,4}$ = 2.7 Hz, $J_{2,3}$ = 10.3 Hz, 1H, H-3), 4.06 (dd, $J_{4,5}$ = 1.4 Hz, $J_{3,4}$ = 2.7 Hz, 1H, H-4) 3.81 (d, $J_{2,3}$ = 10.3 Hz, 1H, H-2), 3.56 (dd, $J_{5,6a}$ = 7.5 Hz, $J_{6a,6b}$ = 5.4 Hz 2H, H-6a, H-6b), 2.55 (dd, $^2J_{H,P}$ = 17.2 Hz, $J_{1a,1b}$ = 15.3 Hz, 1H, H-1′a), 1.95 (dd, $^2J_{H,P}$ = 18.5 Hz, $J_{1a,1b}$ = 15.3 Hz, 1H, H-1′b); ^{13}C NMR (125 MHz, $CDCl_3$) δ =140.0, 139.7, 139.4, 139.2 (4 quaternary aromatic C), 137.8 (d, $^3J_{C,P}$ = 6.4 Hz), 137.2(d, $^3J_{C,P}$ = 6.4 Hz), 127.9-126.8 (30C, Ph × 6), 98.7 (d, $^2J_{C,P}$ = 9.1 Hz, C-1), 81.6 (d, $^3J_{C,P}$ = 4.0 Hz, C-2), 80.3 (d, $^4J_{C,P}$ = 13.6 Hz, C-5), 76.5 (C-4), 76.3, 76.0, 74.4, 74.0 (CH_2Ph × 4), 71.4 (C-3), 70.3 (C-6), 69.5 (d, $^2J_{C,P}$ = 5.3 Hz, Ph*C*H_2OP), 68.1 (d, $^2J_{C,P}$ = 8.2 Hz, Ph*C*H_2OP), 32.4 (d, $^1J_{C,P}$ = 137.5 Hz, C-1′); ^{31}P{^{1}H} NMR (202.5, $CDCl_3$) δ =29.98 (s, 1P) ppm; HRMS (ESI, positive mode): found $(M + Na)^+$ 837.3173. $C_{49}H_{51}O_9P$ requires $(M + Na)^+$ 837.3168.

Dibenzyl (Z)-C-(1′-deoxy-2,3,4,6-tetra-*O*-benzyl-D-galactopyranosyl-2-ylidene) methanephosphonate (4)

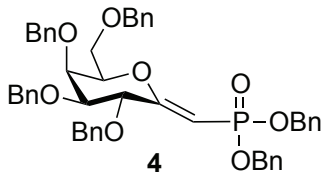

4

To a stirring solution of **2** (4.02 g, 4.93 mmol) in anhydrous THF (50 mL) over molecular sieves (4Å) at 0 °C, was added pyridine (4.38 mL, 49.3 mmol). After 20 min, TFAA (3.50 mL, 24.7 mmol) at 0 °C was added dropwise. The resultant solution was then stirred for 4 h at 0 °C. The reaction was quenched with saturated $NaHCO_3$ (50 mL) and extracted with EtOAc (3 × 100 mL). The combined organic extracts were dried with anhydrous Na_2SO_4, filtered and concentrated. The remaining residue was purified using silica gel flash chromatography (35:65 EtOAc:hexanes) to afford **4** as a colourless oil (4:6 EtOAc:hexanes, R_f product = 0.49) (2.39 g, 3.01 mmol, 61%); ^{1}H NMR (700 MHz, $CDCl_3$) δ =7.32-7.28 (m, 30H, 6 × Ph), 5.44 (dd, $^2J_{H,P}$ = 13.65 Hz, $^1J_{1',2}$ = 1.9 Hz, 1H, H-1′), 5.01-4.99 (m, 2H, CH_2Ph), 5.00, 4.94 (ABq, 2H, J_{AB} = 11.5 Hz, CH_2Ph), 4.78, 4.69 (ABq, 2H, J_{AB} = 11 Hz, CH_2Ph), 4.71, 4.59 (ABq, 2H, J_{AB} = 11 Hz, CH_2Ph), 4.43, 4.36 (ABq, 2H, J_{AB} = 11.5 Hz, CH_2Ph) 4.42 (dd, $J_{4,5}$ = 1.4 Hz, $J_{5,6a}$ = 3.2 Hz, 1H, H-5), 4.07 (d, $J_{4,5}$ = 1.4 Hz, 1H, H-4), 3.81 (dd, $J_{2,3}$ = 5.5 Hz, $J_{2,1'}$ = 1.9 Hz, H-2), 3.68-3.66 (m, $J_{5,6b}$ = 5.3 Hz, $J_{6a,6b}$ = 9.0 Hz, 2H, H-6a, H-3), 3.55 (dd, $J_{5,6b}$ = 5.3 Hz, $J_{6a,6b}$ = 9.0 Hz, 1H, H-6b); ^{13}C NMR (176 MHz, $CDCl_3$) δ =169.8 (C-1), 139.6, 139.2, 138.9, 138.8, 138.1 (d, $^2J_{C,P}$ = 6.9 Hz), 138.0 (d, $^2J_{C,P}$ = 6.9 Hz), (6 quaternary aromatic C), 129.8-128.1 (30C, 6 × Ph), 96.4 (d, $^1J_{C,P}$ = 192.8 Hz, C-1′), 83.0 (C-5), 79.7 (C-3), 77.9 (d, $^3J_{C,P}$ = 13.3 Hz,

*C*HC=C-P, C-2), 73.98 (C-4), 76.23, 75.96, 75.14 (4 × *C*H_2Ph), 69.06 (C-6), 68.50 (d, $^2J_{C,P}$ = 5.8 Hz, 1C, Ph*C*H_2OP), 68.12 (d, $^2J_{C,P}$ = 5.6 Hz, 1C, Ph*C*H_2OP); $^{31}P\{^1H\}$ NMR (202.5, $CDCl_3$) δ = 18.70 (s, 1P) ppm. HRMS (ESI, positive mode): found $(M + Na)^+$ 819.3057. $C_{49}H_{49}O_8P$ requires $(M + Na)^+$ 819.3063.

2,3,4,6-Tetra-*O*-benzyl-C-(1′*R*-fluoro-dibenzylphosphonomethyl)-α-D-galactopyranose (5) and 2,3,4,6-tetra-*O*-benzyl-C-(1′*S*-fluoro-dibenzylphosphonomethyl)-α-D-galactopyranose (6)

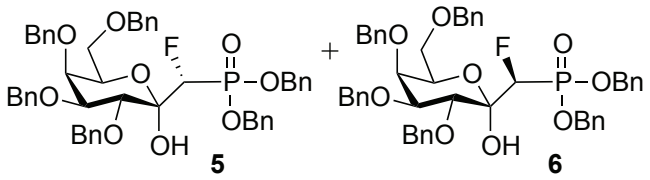

To a solution of **4** (2.40 g, 3.04 mmol) in anhydrous CH_3CN (30 mL) was added Selectfluor™ (2.13 g, 6.12 mmol) at rt and stirred for 12 h. Following the addition of H_2O (10 mL) the mixture was heated to 70 °C and stirred for an additional 2 h. The solution was poured into H_2O (30 mL) and extracted with EtOAc (3 × 50 mL). The combined organic extracts were dried with anhydrous Na_2SO_4, filtered and evaporated to dryness under reduced pressure. The remaining diastereomeric mixture was purified using silica gel flash chromatography (3:7 EtOAc:hexanes) to afford **5** followed by **6** as colourless oils. **5** (4:6 EtOAc:hexanes, Rf product = 0.83) (1.13 g, 1.36 mmol, 45%); ^1H NMR (700 MHz, $CDCl_3$) δ =7.32-7.28 (m, 30H, 6 × Ph), 5.23 (s, anomeric OH), 5.19 (d, 2H, *J* = 8.45 Hz, C*H*$_2$Ph), 5.05 (m, 4 H, 2 × C*H*$_2$Ph), 5.02, 4.92 (dd, $^2J_{H,F}$ = 45.85 Hz, $^2J_{H,P}$ = 4.9 Hz, 1H, H-1′), 4.73 (s, 2H, C*H*$_2$Ph), 4.68, 4.64 (ABq, 2H, J_{AB} = 11.5 Hz, C*H*$_2$Ph), 4.30 (dd, $J_{4,5}$ = 0.92 Hz, $J_{5,6a}$ = 6.41 Hz, 1H, H-5), 4.26 (dd, $J_{2,3}$ = 9.37 Hz, $^4J_{2,F}$ = 2.19 Hz, 1H, H-2), 4.28, 4.27 (ABq, 2H, J_{AB} = 12 Hz, C*H*$_2$Ph), 4.11 (dd, $J_{2,3}$ = 9.37 Hz,

$J_{3,4}$ = 2.78 Hz, 1H, H-3), 3.96 (dd, $J_{3,4}$ = 2.78 Hz, $J_{4,5}$ = 0.92 Hz, 1H, H-4), 3.49 (dd, $J_{5,6a}$ = 6.41 Hz, $J_{6a,6b}$ = 9.40 Hz, 1H, H-6a), 3.42 (dd, $J_{5,6b}$ = 6.41 Hz, $J_{6a,6b}$ = 9.40 Hz, 1H, H-6b); ^{13}C NMR DEPT135 (125 MHz, $CDCl_3$) δ = 128.4-127.6 (30H, 6 × Ph), 87.4 (dd, $^1J_{C,F}$ = 202.37 Hz, $^1J_{C,P}$ = 158.75 Hz, C-1′) 80.2 (d, C-5), 75.6 (CH$_2$Ph), 74.9 (C-3), 74.5 (CH$_2$Ph), 74.4 ($^4J_{C,P}$ = 8.89 Hz, C-2), 73.3 (CH$_2$Ph), 72.9 (CH$_2$Ph), 71.0 (C-4), 69.8 (d, $^3J_{C,P}$ = 5.7 Hz, PhCH$_2$OP), 69.2 (C-6), 68.2 (d, $^3J_{C,P}$ J = 6.6 Hz, PhCH$_2$OP); ^{31}P{^{1}H} NMR (202.5, $CDCl_3$) δ = 18.26 (d, $^2J_{P,F}$ = 68.75 Hz, 1P); ^{19}F NMR (282 MHz, $CDCl_3$) δ = -211(dd, $^2J_{P,F}$ = 68.75 Hz, $^2J_{F,H\text{-}1'}$ = 45.85 Hz, $^4J_{2,F}$ = 2.19 Hz, 1F) ppm; HRMS (ESI, positive mode): found $(M + Na)^+$ 855.3069. $C_{49}H_{50}FO_9P$ requires $(M + Na)^+$ 855.3074.

6 (4:6 EtOAc–hexanes, Rf product = 0.93) (451 mg, 0.54 mmol, 18%). ^{1}H NMR (700 MHz, $CDCl_3$) δ =7.39-7.19 (m, 30H, 6 × Ph), 6.06 (d, J = 9.99 Hz, anomeric OH), 5.17-5.06 (m, 5H, 2 × CH_2Ph, H-1′), 5.01 (d, J =11.5, 2H, CH_2Ph) 4.78, 4.55 (ABq, 2H, J_{AB} = 10.5 Hz, CH_2Ph h), 4.73, 4.48 (ABq, 2H, J_{AB} = 11 Hz, CH_2Ph), 4.34, 4.27 (ABq, 2H, J_{AB} = 5 Hz, CH_2Ph), 4.30 (quartet, J = 11.67 Hz, 1H, H-5), 4.02 (d, J = 1.70 Hz, 1H, H-4), 3.97 (dd, $J_{2,3}$ = 9.94 Hz, $^4J_{H,F}$ = 2.11 Hz, 1H, H-2), 3.48 (dd, J = 6.45 Hz, 2H, H-6a, H-6b); ^{31}P{^{1}H} NMR (202.5, $CDCl_3$) δ = 15.5 (d, $^2J_{P,F}$ = 68.75 Hz, 1P); ^{19}F NMR (282 MHz, $CDCl_3$) δ = -219.9 (dd, $^2J_{P,F}$ = 68.75 Hz, $^2J_{F,H\text{-}1'}$ = 45.85 Hz, 1F) ppm; HRMS (ESI, positive mode): found $(M + Na)^+$ 855.3069. $C_{49}H_{50}FO_9P$ requires $(M + Na)^+$ 855.3074.

General deprotection procedure (3, 7, and 8).

To a solution of globally benzylated ketose phosphonates (**2**, **5**, or **6**; 51 mg, 55 mg, or 30 mg, respectively) in 1:1 MeOH:EtOAc (3 mL) was added palladium on carbon (10% w/w) (0.1 equivalents) and degassed under vacuum. The reaction mixture was then stirred

vigorously under hydrogen gas at 1 atm. pressure for 18 h. The suspension was then filtered and condensed. The resultant residue was immediately dissolved in H_2O (2 mL) and extracted with EtOAc (2 × 2 mL). The aqueous fraction was adjusted to pH 8 with NH_4OH (0.2 mM) and lyophilized. The crude solids were dissolved in a minimal amount of water (~1-2 ml) and passed through a Sephadex® LH-20 resin, fractions found to contain compound using NMR were combined and lyophilized to afford compound **3** (10.11 mg, 63%), **7** (14.57 mg, 73%), and **8** (3.71 mg, 35%) as colourless foams.

Ammonium-C-(1′-phosphonomethyl)-α-D-galactopyranoside (3)

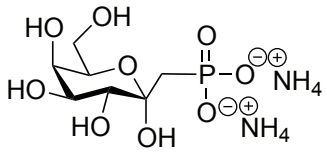

3

Major compound: ^{1}H NMR (500 MHz, D_2O) δ =3.97 (m, 1H, H-4), 3.84 (dd, J = 3.38 Hz, J =1.07 Hz, 1H, H-2), 3.70 (dd, $J_{5,6b}$ = 10.40 Hz, J =3.34, 1H, H-5), 3.66 (d, J = 7.98 Hz, 1H, H-6a), 3.59 (m, 1H, H-3), 3.51 (d, $J_{5,6b}$ =10.06 Hz, 1H, H-6b) 2.28 (dd, J = 17.44 Hz, 15.55 1H, H-1′) 2.08 (dd, J = 16.72 Hz, 15.5 Hz 1H, H-1′); ^{13}C NMR (176 MHz, D_2O) δ = 98.74 (m, $^2J_{C,P}$ = 6.6 Hz, C-1), 72.6 (C-5), 71.3 (d, $^3J_{C,P}$ = 3.0 Hz, C-2) 71.0 (C-4) 63.0 (C-3), 60.7 (C-6), 37.5 (d, $^1J_{C,P}$ = 127 Hz, C-1′) ^{31}P{^{1}H} NMR (202.5, D_2O) δ =20.62 (s, 1P) ppm; HRMS (ESI, negative mode): found $(M-H)^-$ 273.0381. $C_7H_{15}O_9P$ requires $M-H)^-$ 273.0383.

Ammonium-C-(1′*R*-Fluoro-phosphonomethyl)-α-D-galactopyranoside (7)

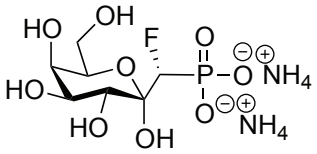

7

Major compound: ^{1}H NMR (500 MHz, D_2O) δ =4.05 (dd, J =7.90 Hz, 1H, H-1′), 3.97 (m, 1H, H-2), 3.68 (d, J = 8.06 Hz, 1H), 3.60 (dd, J =3.02 Hz, J = 14.67 Hz, 1H), 3.63 (d, J =16.38 Hz, 1H), 3.45 (d, J = 10.10 Hz, 1H), 2.15 (dd, J = 17.44 Hz, 15.5, 1H, H-6a) 1.90 (dd, J = 16.72 Hz, 15.5 Hz 1H, H-6b) (found 8H, expected 7H); ^{13}C NMR (176 MHz, D_2O) δ = 98.74 (m, $^{2}J_{C\text{-}P}$ = 6.6 Hz, C-1), 72.6 (s, C-5), 71.3 (d, $^{3}J_{C\text{-}P}$ = 3.0 Hz C-2) 71.0 (C-4) 63.0 (d, C-3), 60.7(C-6), 37.5 (d, $^{1}J_{C\text{-}P}$ = 127 Hz, C-1′) ^{31}P{^{1}H} NMR (202.5, $CDCl_3$) δ =11.92 (s, 1P) ppm; ^{19}F NMR (282 MHz, $CDCl_3$) δ = -207 (dd, $^{2}J_{P\text{-}F}$ = 68.75 Hz, $^{2}J_{F\text{-}H\text{-}1'}$ = 45.85 Hz, $^{4}J_{2\text{-}F}$ = 2.19 Hz, 1F) ppm; HRMS (ESI, negative mode): found (M + H)$^-$ 291.0287. $C_7H_{13}FO_9P$ requires M –H)$^-$ 291.0280.

Ammonium-C-(1′*S*-Fluoro-phosphonomethyl)-α-D-galactopyranose (8)

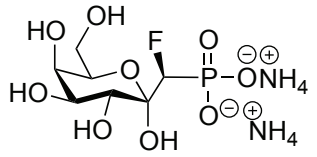

8

Major compound: ^{1}H NMR (500 MHz, D_2O) δ = 4.70 (dd, $^{2}J_{H,F}$ = 44.6 Hz, $^{2}J_{H,P}$ = 6.5 Hz 1H, H-1′), 4.07 (dd, $J_{2,3}$ = 7.70 Hz, $^{4}J_{H,F}$ = 3.11 Hz 1H, H-2), 3.92 (d, J = 2.80 Hz, 1H, H-4), 3.83 (m, 3H, H-3, H-5, H-6a), 3.65 (dd, J =12.4 Hz, J = 3.35 Hz 1H, H-6b), ^{13}C NMR (176 MHz, D_2O) δ = 100.25 (d, $^{2}J_{C,P}$ = 19 Hz, C-1′), 74.3 (C-5), 72.6 (C-3), 72.2 (C-4), 69.5 (C-2), 64.0 (C-6) ppm; ^{31}P{^{1}H} NMR (202.5, D_2O) δ =12.48 (d, $^{2}J_{P,F}$ = 65.35 Hz 1P) ppm; ^{19}F{^{1}H} NMR (282 MHz, D_2O) δ = -211(dd, $^{2}J_{P,F}$ = 65.35 Hz, 1F) ppm; HRMS (ESI, negative mode): found $(M-H)^-$ 291.0287. $C_7H_{13}FO_9P$ requires $(M-H)^-$ 291.0280.

2,3,4,6-Tetra-*O*-benzyl-C-(1′α,α-difluoro-diethylphosphonomethyl)-α-D-galactopyranose (9)

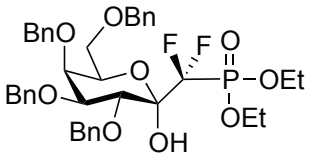

9

To a stirring solution of diisopropylamine (1.27 mL, 9.70 mmol) in THF (3 mL) at –78 °C was added *n*-BuLi (3.65 mL, 9.70 mmol, 2.5 M in hexanes). The resulting solution was warmed to 0 °C for 30 min. The resultant LDA was then cooled to –78 °C and an equitemperature solution of diethyl difluoromethyl phosphonate (0.92 mL, 9.70 mmol) in THF (4 mL) was added and stirred for 15 min. A solution of lactone **2** (1.04 g, 1.94 mmol) in THF (4 mL) was added and the resulting solution was stirred for 30 additional min at –78 °C. The reaction was quenched with saturated NH_4Cl (aq.) and extracted with diethyl ether (3 × 50 mL). The combined organic layers were dried with anhydrous Na_2SO_4, filtered and concentrated. The remaining residue was purified using silica gel

flash chromatography (3:7 EtOAc:hexanes) to afford **9** as a pale yellow oil (3:7 EtOAc:hexanes, R*f* product = 0.42) (723 mg, 1.00 mol, 52%). ^{1}H NMR (500 MHz, $CDCl_3$) δ = 7.41-7.30 (m, 20 H, 4 × Ph), 5.09 (s, 1H, anomeric OH), 5.07, 4.66 (ABq, 2H, J_{AB} = 12.5 Hz, C*H*$_2$Ph), 4.92, 4.83 (ABq, 2H, J_{AB} = 11 Hz, C*H*$_2$Ph), 4.83, 4.77 (ABq, 2H, J_{AB} = 11.5 Hz, C*H*$_2$Ph), 4.49, 4.45 (ABq, 2H, J_{AB} = 11.5 Hz, C*H*$_2$Ph), 4.39 (m, 4H, 2 × OC*H*$_2$CH$_3$), 4.28 (m, 1H, H-2), 4.07 (d, J = 2.78 Hz, 1H, H-5), 4.05 (m, 1H, H-3), 3.63 (d, $^{2}J_{6a,6b}$ = 6.17 Hz, 2H, H-6a, H-6b), 1.41 (m, 3H, OCH$_2$*CH*$_3$), 1.35 (m, 3H, OCH$_2$*CH*$_3$); ^{13}C NMR DEPT135 (176 MHz,$CDCl_3$) δ =138.0, 137.8, 137.2, 136.8 (4 × quaternary aromatic C), 128.3, 127.4 (30C, 6 × PH), 96.9 (C-1′), 80.3 (C-5), 75.2 (*C*H$_2$Ph), 74.5 (C-3), 74.4 (*C*H$_2$Ph), 74.3 (C-2), 73.2 (*C*H$_2$Ph), 73.1 (*C*H$_2$Ph), 70.5 (C-4), 68.4 (C-6), 65.2 (d, $^{2}J_{C,P}$ = 6.5 Hz, P-O*C*H$_2$) 65.0 (d, $^{2}J_{C,P}$ = 6.4 Hz, P-O*C*H$_2$), 16.3 (s, P-OCH$_2$*C*H$_3$), 16.2 (s, P-OCH$_2$*C*H$_3$);^{31}P{^{1}H} NMR (202.5, $CDCl_3$) δ =7.18 (dd, $^{2}J_{P,F}$ = 97.0 Hz, 1P) ppm; ^{19}F NMR (282 MHz, $CDCl_3$) δ = -119.1 (dd, $^{2}J_{P,F}$ = 97.0 Hz, $^{2}J_{F,F}$ = 305 Hz, 1F), -119.9 (dd, $^{2}J_{P,F}$ = 97.0 Hz, $^{2}J_{F,F}$ = 305 Hz, 1F) HRMS (ESI, positive mode): found (M + Na) 749.2661. $C_{39}H_{45}F_2O_9P$ requires $(M + Na)^+$ 749.2667.

Ammonium-C-(1′α,α-difluoro-phosphonomethyl)-α-D-galactopyranose (10)

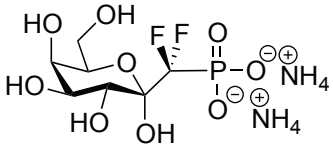

10

A stirring solution of **9** (102 mg, 0.16 mmol) in anhydrous DCM (2 mL) at 0 °C was treated with TMSI (0.75 mL, 4.5 mmol) and allowed to warm to rt over 4h. The reaction was quenched with methanol (2 mL) and concentrated. The resultant residue was dissolved in H_2O (15 mL) and washed with diethyl ether (10 ×10 mL). The aqueous layer was passed through a Dowex (H^+) ion exchange resin. The acidic aqueous fractions were combined and adjusted to pH 8 with NH_4OH (0.2 M) and lyophilized to afford compound **10** (26.9 mg, 54%). Major compound: ^{1}H NMR (500 MHz, D_2O) δ =4.29 (d, J = 9.13 Hz, 1H, H-2), 4.15 (dd, J = 8.36 Hz, J = 7.70 Hz, 1H, H-4), 3.78 (m, 3H, H-3, H-5, H-6a), 3.62 (dd, J =11.65 Hz, J = 6.68 Hz, 1H, H-6b) ppm; ^{13}C NMR (176 MHz, D_2O) δ = 79.8 (C-5), 75.0 (C-2), 73.7 (C-3), 71.9 (C-4) 62.1 (C-6) ppm; ^{31}P{^{1}H} NMR (202.5, D_2O) δ = 4.84 (quartet, $^2J_{P,F}$ = 77.90 Hz, 1P) ppm; ^{19}F NMR (282 MHz, D_2O) δ = -124.81 (dd, $^2J_{P,F}$ = 77.90 Hz, $^2J_{F,F}$ = 300 Hz, 1F) -126.6 (dd, $^2J_{P,F}$ = 77.90 Hz, $^2J_{F,F}$ = 300 Hz, 1F) ppm; HRMS (ESI, positive mode): found $(M + H)^-$ 309.0192. $C_7H_{12}F_2O_9P$ requires $(M + H)^-$ 309.0192.

2,3,4,6-Tetra-*O*-benzyl-C-(1′-dimethylphosphonomethyl)-α-D-galactopyranose (11)

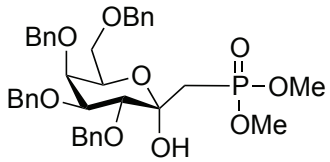

11

To a stirring solution of dimethyl methylphosphate (2.001 g, 16.0 mmol) in anhydrous THF (30 mL) at -78 °C, was added *n*-BuLi (7.22 mL, 16.0 mmol, 2.5 M in hexanes)

dropwise. The reaction was stirred for 30 min before adding **1** (3.090 g, 5.74 mmol, in 15.0 mL THF) dropwise. The resultant solution was then allowed to warm to rt while stirred for a further 2 h. The reaction was quenched with saturated NH_4Cl (45.0 mL). The organic layer was then washed with H_2O (50 mL). The aqueous layers were combined and extracted with DCM (2 × 50 mL), dried with anhydrous Na_2SO_4, filtered and concentrated. The remaining residue was purified using silica gel flash chromatography (35:65 EtOAc:hexanes) to afford **11** as a pale yellow oil (3:7 EtOAc:hexanes, R_f product = 0.29) (2.550 g, 3.848 mmol, 67%). Spectroscopic data was consistent with previous literature.[66]

3,4,5,7-Tetra-O-benzyl-1,2-dideoxy-D-glucohept-1-enitol (16)

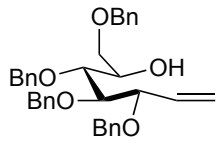

16

To a suspension of methyltriphenylphosphonium bromide (6.001 g, 0.011 mol) in anhydrous THF (150 mL) at −78 °C was added *n*-BuLi (4.5 mL, mol, 2.5 M in hexanes) dropwise. The resultant orange ylide solution was allowed to warm to rt over 30 min. In a separate flask also at −78 °C, a solution of 2,3,4,6-tetra-*O*-benzyl-D-glucopyranose in anhydrous THF was stirred and *n*-BuLi (12.5 mL, mol, 2.5 M in hexanes) was added dropwise. This solution was warmed to rt over 20 min and transferred to the ylide solution via cannula.

Upon complete transfer, the combined reaction mixture was stirred at 45 °C for 2 h. Acetone (130 mL) was added and the mixture was stirred for an additional 2 h. The reaction was evaporated to dryness under reduced pressure, dissolved in brine (400 mL), and extracted with diethyl ether (3 × 300 mL). The combined organic extracts were dried with anhydrous Na_2SO_4, filtered and concentrated. The remaining residue was purified using silica gel flash chromatography (2:8 EtOAc:hexanes) to afford **16** as a colourless liquid (2:8 EtOAc:hexanes, R_f product = 0.40) (5.3773 g, 9.98 mmol, 90%) NMR was consistent with previous literature.[8, 67]

_C_-(1-Deoxy 2,3,4,6-Tetra-_O_-benzyl-α-D-glucopyranosyl) methyl mercury(II) chloride (17)

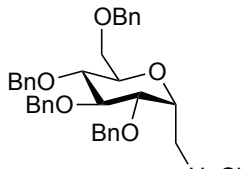

17

To a stirring solution of mercuric trifluoroacetate (4.258 g, 9.96 mmol) in anhydrous THF (100 mL) at rt was added **14** (5.377 g, 9.96 mmol, dissolved in anhydrous THF (50 mL)). After 18 h, KCl (200 mL, 0.8 M) was added and the mixture was allowed to stir for a further 2 h before the reaction was condensed, resulting in a single aqueous phase. The aqueous phase was subsequently extracted with DCM (3 × 30 mL). The combined organic extracts were dried with anhydrous Na_2SO_4, filtered and concentrated. The resulting oil was purified using silica gel flash chromatography (3:7 EtOAc:hexanes) yielding **17** (2:8 EtOAc:hexanes, R_f product = 0.27, 60%) (4.620 g, 5.97 mmol).

Spectroscopic data was consistent with previous literature.[8] In the event that **17** was to be used to synthesize **18,** crude product **17** was not purified using column chromatography.

_C_-(1-Deoxy 2,3,4,6-Tetra-_O_-benzyl-α-D-glucopyranosyl) iodomethane (18)

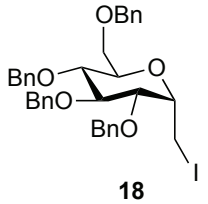

18

Iodine (0.576 g, 4.50 mmol) and **17** (2.001 g, 2.59 mmol) were dissolved in anhydrous DCM (50 mL) at rt and stirred for 1.5 h. Aqueous $Na_2S_2O_3$ (10%, 15 mL) was added and the biphasic solution was stirred vigorously for 15 minutes. The organic layer was collected and washed with aqueous KI (5%, 30 mL) and brine (30 mL), dried with anhydrous Na_2SO_4, filtered and concentrated. The remaining residue was purified using silica gel flash chromatography (1:9 EtOAc:hexanes) to afford **18** as a white solid (2:8 EtOAc:hexanes, R_f product = 0.65) (1.203 g, 1.87 mmol, 70%) The spectroscopic data was consistent with previous literature.[8]

2,6-Anhydro-3,4,5,7-Tetra-_O_-benzyl-1-deoxy-D-glucohept-1-enitol (25)

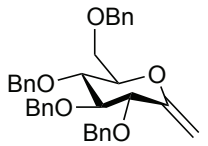

25

To as suspension of KO_2 (1.66 g, 18.1 mmol) and 18-crown-6 (4.77 g, 18.1 mmol) in anhydrous DMSO (40.0 mL) at rt, was added a solution of **15** (3.00 g, 4.52 mmol, 40 mL anhydrous THF) dropwise and stirred for 3 h. Brine (20 mL) was added and the THF was removed *in vacuo*. The remaining aqueous solution was extracted with EtOAc (3 × 100 mL). The combined organic extracts were washed with brine (50 mL), dried with anhydrous $MgSO_4$, filtered and condensed. The remaining residue was purified using silica gel flash chromatography (2:8 EtOAc:hexanes) to afford **25** as a colourless liquid (2:8 EtOAc:hexanes, R_f product = 0.60). ^{1}H NMR was consistent with previous literature.[40]

***C*-(1-Deoxy 2,3,4,6-Tetra-*O*-benzyl-α-glucopyranosyl) methanol (26)**

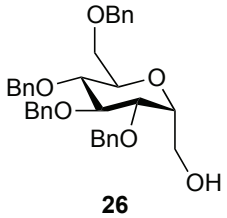

26

This reaction was not preformed under a nitrogen atmosphere. A solution of **17** (1.001 g, 1.29 mmol) was dissolved in anhydrous DCM (60 mL) and anhydrous DMF (40 mL) in a wide-mouth 120 mL jar and stirred while a vigorous supply of O_2 gas was delivered via a gas dispersion tube (Corning, 30mm, extra-coarse porosity). After oxygenation for 45 minutes, $NaBH_4$ (0.423 g, 11.1 mmol) was added in small aliquots to control the resulting exothermic reaction. After 2 h, the O_2 supply was removed and the reaction was quenched with a saturated aqueous solution of NH_4Cl and extracted into diethyl ether (3 ×

50 mL). The organic layers were combined, washed with water, dried with $MgSO_4$, filtered and condensed. The remaining crude oil was purified using silica gel flash chromatography (4:6 EtOAc:hexanes) to afford **26** as clear viscous oil (3:7 EtOAc:hexanes, R_f product = 0.21) (0.320 g, 0.577 mmol, 46%). HRMS (ESI, positive mode): found $(M + Na)^+$ 577.2561. $C_{35}H_{36}O_6P$ requires $(M + Na)^+$ 577.2566. Spectroscopic data was consistent with the literature.[40]

_C_-(1-Deoxy 2,3,4,6-Tetra-_O_-benzyl-α-D-glucopyranosyl) methanal (19)

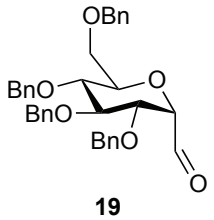

19

A stirring solution of **18** (50 mg, 0.090 mmol) and $NaHCO_3$ (76 mg, 0.8991 mmol) in anhydrous DCM (2 mL) was treated with DMP (0.038 g, 0.0903 mmol) and stirred at rt for 1.5 h. The suspension was then dissolved with Et_2O (5 mL) and condensed and immediately brought up in a solution of saturated aqueous $NaHCO_3$ (5 mL) containing NaS_2O_3 (10%) and extracted with EtOAc (2 × 10 mL), washed with H_2O (10 mL) and brine (10 mL), dried with $MgSO_4$, filtered and condensed. Spectroscopic data was consistent with the literature.[68]

2,3,4,6-Tetra-_O_-benzyl-C-(1′-hydroxy-diethylphosphonomethyl)-α-D-glucopyranoside (20)

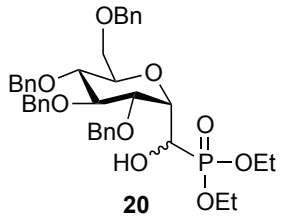

20

Method A. To a stirring solution of diethyl phosphite (0.015 mL, 0.12 mmol) in THF (2 mL) at -78 °C was added LiHMDS (20 mg, 0.12 mmol) as a pre-cooled (-78 °C) THF solution (1 mL). The resultant solution was stirred for five minutes before the addition of **19** (0.060 g, 0.11 mmol), as a THF solution (2 mL) via cannula. Upon complete transfer, the mixture was stirred for 10 minutes at -78 °C. It was then quenched with saturated aqueous NH_4Cl (5 mL) and allowed to warm to rt. The biphasic solution was then extracted with Et_2O (2 × 10 mL) dried with $MgSO_4$, filtered and condensed. The remaining crude oil was purified using silica gel flash chromatography (4:6 EtOAc:hexanes) to afford the diastereomeric mixture **20** as viscous oil (3:7 EtOAc:hexanes, R_f product = 0.21) (0.016 g, 0.2286 mmol, 21%).

Method B. To a stirring solution of **19** (34 mg, 57.0 mmol) and diethyl phosphite (0.090 mL, 63.0 mmol) in THF (3 mL) at 0 °C was added DBU (0.100 mL, 63.0 mmol). The reaction was allowed to warm to rt over 30 minutes at which point the solvent was evaporated. The remaining residue was dissolved in DCM (10 mL) and washed with aqueous HCl (1 M), dried, and condensed. The remaining crude oil was purified using silica gel flash chromatography (4:6 EtOAc:hexanes) to afford the diastereomeric mixture **20** as viscous oil (3:7 EtOAc:hexanes, R_f product = 0.21) (15 mg, 0.0210 mmol, 34%). HRMS (ESI, positive mode): found $(M + Na)^+$ 713.2850. $C_{39}H_{47}O_9P$ requires $(M + Na)^+$ 713.2590. ^1H NMR (500 MHz, $CDCl_3$) δ = 7.39-7.19 (m, 20H, 4 × Ph), 4.85, 4.67 (ABq,

2H, J_{AB} = 11.5 Hz, CH_2Ph), 4.80, 4.57 (ABq, 2H, J_{AB} = 12 Hz, CH_2Ph), 4.61, 4.52 (ABq, 2H, J_{AB} = 12.5 Hz, CH_2Ph), 4.74 (dd, J = 11.4 Hz, 4.25 Hz, 1H, H-1) 4.25 (m, 2H, H-5, H-2), 4.17 (m, 4H, 2 × OCH_2CH$_3$), 4.13 (m, 1H, H-4), 3.77 (m, 3 H, H-6a, H-6b, H-3), 3.72, 3.53 (ABq, 1H, J_{AB} = 5 Hz, H-1′), 2.88 (dd, 1H, O*H*), 1.36 (m, 6H, 2 × OCH$_2$CH_3) ppm; ^{31}P{^{1}H} NMR (202.5, CDCl$_3$) δ = 22.60 (s, 1P) ppm; LRMS (ESI, positive mode) found $(M + Na)^+$ 713.0. $C_{39}H_{47}O_9P$ requires $(M + Na)^+$ 713.2.

Ammonium-C-(1′-hydroxy-diethylphosphonomethyl)-α-D-glucopyranoside (21)

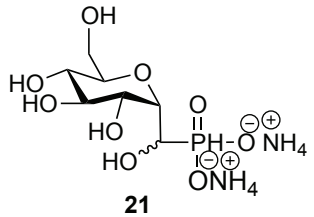

21

The diastereomeric mixture **20** (25 mg, 0.0363 mmol) was dissolved in EtOAc:MeOH (1:1, 5 mL) and poured over palladium on carbon (10% w/w) (0.1 equivalents) in a glass Parr hydrogenolysis apparatus. The resultant suspension was then degassed, and shaken at 55 psi for five hours. The suspension was filtered over celite and condensed. The remaining residue was dissolved in water and adjusted to pH 8 with 0.2 mM NH_4OH, and lyophilized to yield the diastereomeric mixture **21** as a colourless foam (7.4 mg, 70%).^{1}H NMR (500 MHz, D_2O) δ =4.19 (dd, 1H), 4.03 (m, 4H), 3.82 (m, 5H), 3.68 (m, 4H), 3.3 (m, 2H) ppm (found 16H, expect 16H); ^{31}P{^{1}H} NMR (202.5, D_2O) δ =16.05 (s, 1P), 15.94 (s, 1P) ppm; LRMS (ESI, negative mode): found $(M - H)^-$ 273.10. $C_7H_{15}O_9P$ requires $M - H)^-$ 273.15.

Bibliography

(1) Baddiley, J.; Michelson, A. M.; Todd, A. R., *Nature* **1948**, *161*, 761.

(2) Blackburn, M. G., *New J. Chem.* **2010**, *34*, 784-794.

(3) Engel, R., *Chem. Rev.* **1977**, *77*, 349-367.

(4) Cipolla, L.; La Ferla, B.; Nicotra, S. F., *Carbohydr. Polym.* **1998**, *37* (3), 291-298.

(5) Han, L.; Hiratake, J. Kamiyama, A.; Sakara, K. *Biochemistry* **2007**, *46* (5), 1432-1447.

(6) Clercq, E., *Biochem. Pharmacol.* **2007**, *73*, 911-922.

(7) Forget, S. M.; Bhattasali, D.; Hart, V. C.; Cameron, T. S.; Syvitshi, R. T.; Jakeman, D. L., *Chem. Sci.* **2012**, *3*, 1866-1878.

(8) Beaton, S. A.; Huestis, M. P.; Sadeghi-Khomami, A.; Thomas, N. R.; Jakeman, D. L., *Chem. Commun.* **2009**, 238-240.

(9) Vasella, A.; Baudin, G.; Panza, L., *Heteroatom. Chem.* **1991**, *2*, 151-161.

(10) Romanenko, V. D.; Kukhar, V. P., *Chem. Rev.* **2006**, *106*, 3868-3935.

(11) Blackburn, M. G., *Chem. Ind.* **1981**, 134-138.

(12) Blackburn, M. G., *J. Chem. Soc. Perkin Trans. 1* **1987**, 181-186.

(13) Nicotra, S. F., Synthesis of C-glycosides and biological interest. In *Glycoscience Synthesis of Substrate Analogs and Mimetics*, **1997**, 55-83.

(14) Pertusati, F.; Serpi, M.; McGuigan, C., *Antivir. Chem. Chemother.* **2012**, *22*, 181-203.

(15) Jessen, H. J.; Schulz, T.; Balzarini, J.; Meier, C., *Angew. Chem. Int. Ed.* **2008**, *47*, 8719-8722.

(16) Borman, S., Glycoslyation Engineering. *Chem. Eng. News* **2006**, *84*, 13-22.

(17) Lowary, T. L., *Carbohydr. Res.* **2006**, *341*, 1207.

(18) Thorson, J. S.; Hosted, T. J. Jr.; Jaing, J.; Biggins, J. B.; Ahlert, J., *Curr. Org. Chem.* **2001**, *5*, 139-167.

(19) Thorson, J. S.; Moretti, R., *J. Biol. Chem.* **2007**, *282*, 16942-16947.

(20) Gold, H.; van Delft, P.; Meeuwenoord, N.; Codée, J. D.; Filippov, D. V.; Eggink, G.; Overkleeft, H. S.;van der Marel, G. A., *J. Org. Chem.* **2008**, *73*, 9458-9460.

(21) Griffin, B. S.; Burger, A., *J. Am. Chem. Soc.* **1956**, *78*, 2336-2338.

(22) Whistler, R. L.; Wang, C. C., *J. Org. Chem.* **1968**, *33*, 4455-4458.

(23) Beaton, S. A.; Jakeman., D. L., *unpublished work.* **2010**.

(24) Caravano, A.; Dohi, H.; Sinay, P.; Vincent, S. P., *Chem. Eur. J.* **2006**, *12*, 3114-3123.

(25) Barlow, J.; Girvin, M.; Blanchard, J., *J. Am. Chem. Soc.* **1999**, *121*, 6968-6969.

(26) Partha, S. K.; Sadeghi, A.; Slowski, K.; Toshihihisa, K.; Thomas, N. R.; Jakeman, D. L.; Sanders, D. A. R., *J. Mol. Biol.* **2010**, *403*, 578-590.

(27) Albright, J. D.; Goldman, L., *J. Am. Chem. Soc.* **1967**, *89*, 2416-2423.

(28) Meyer, O.; Grosdemange-Billiard, C.; Tritsch, D.; Rohmer, M., *Org. Biomol. Chem.* **2003**, *1* (24), 4367-4372.

(29) Mohapatra, D. K.; Bhattasali, D.; Gujar, M. K.; Khan, M. I.; Shashidhara, K. S., *J. Org. Chem.* **2008**, *36*, 6213-6224.

(30) Hartung, W.; Simonoff, R., *Org. Reactions* **1953**, *7*, 263.

(31) Stonehouse, J. Adell, P.; Keeler, J.; Shaka, A. J., *J. Am. Chem. Soc.* **1994**, *116*, 6037-6038.

(32) Bhattasali, D.; Jakeman, D. L., *unpublished work.* **2012**.

(33) Becker, S.; Schnackerz, K.; Schinzel, R., *Biochim. Biophys. Acta, Gen. Subj.* **1995**, *1243*, 381.

(34) Pradere, U.; Clavier, H.; Roy, V.; Nolan, S. P.; Agrofoglio, L. A., *Eur. J. Org. Chem.* **2011**, 7324-7330.

(35) Pougny, J.-R.; Nassr, M. A.; Sinay, P., *J. Chem. Soc.* **1981**, 357-358.

(36) Johnson, A. P., Pelter, A., *J. Chem. Soc.* **1964**, 520-522.

(37) Lui, J.; Dong, X.; Meng, S.; Xiao, J.; Cheng, L., *Carbohydr. Res.* **2006**, *341*, 2653-2657.

(38) Kehler, J.; Ebert, B.; Dahl, O; Krogsgaard-Larsen, P., *J. Chem. Soc., Perkin Trans. 1* **1998**, 3241-3243.

(39) Carley, S.; Brimble, M. A., *Org. Lett.* **2009**, *3*, 563-566.

(40) RajanBabu, T. V.; Reddy, G. S., *J. Org. Chem.* **1986**, *51*, 5458-5461.

(41) Hill, C. L.; Whitesides, G. M., *J. Am. Chem. Soc.* **1974**, *96*, 870.

(42) Reiner, M.; Schmidt, R. R., *Tetrahedron: Asymmetry 11* **2000**, 319-335.

(43) Caplan, N. A.; Pogson, C. I.; Hayes, D. J.; Blackburn, G. M., *J. Chem. Soc., Perkin Trans. 1* **2000**, 421-437.

(44) Berkowitz, D. B.; Bose, M.; Pfannenstiel, T. J.; Doukov, T., *J. Org. Chem.* **2000**, *65* (15), 4498-4508.

(45) Pàmies, O.; Bäckvall, J.-E., *J. Org. Chem.* **2003**, *68,* 4815-4818.

(46) Forget, S. M.; Jakeman, D. L, *unpublished work.* **2011**.

(47) Choumane, M.; Banchet, A.; Probst, N.; Gerard, S.; Ple, K.; Haudrechy, A., *C. R. Chimie* **2011,** *14*, 235-273.

(48) Wang, Z.; Shao, E. H.; Lacroix, E.; Wu, S. H.; Jennings, H. J.; Zou, W., *J. Org. Chem.* **2003**, *68*, 8097.

(49) Blankenfeldt, W.; Asuncion, M.; Lam, J. S.; Naismith, J. H., *EMBO J.* **2000**, *19*, 6652-6663.

(50) Barton, W. A.; Lesniak, J.; Biggins, J. B.; Jeffery, P. D.; Jiang, J.; Rajashankar, K. R.; Thorson, J. S.; Nikolov, D. B., *Nat. Struct. Biol.* **2001**, *8*, 545-552.

(51) Tsuboi, K. K.; Fukunaga, K.; Petricciani, J. C., *J. Biol. Chem.* **1969**, *244*, 1008-1015.

(52) Sheu, K.-F. R.; Richard, J. P.; Frey, P. A., *Biochemistry* **1979**, *18*, 5548-5556.

(53) Mizanur, R. M.; Zea, C. J.; Pohl, N. L., *J. Am. Chem. Soc.* **2004**, *126*, 15993-15998.

(54) Jakeman, D. L.; Young, J. L.; Huestis, M. P.; Peltier, P; Daniellou, R.; Nugier-Chauvin, C.; Ferrieres, V., *Biochemistry* **2008**, *47*, 8719-8725.

(55) Huestis, M. P.; Aish, G. A.; Hui, J. P. M.; Soo, E. C.; Jakeman, D. L., *Org. Biomol. Chem.* **2008**, *6*, 477-484.

(56) Timmons, S. C.; Mosher, R. H.; Knowles, S. A.; Jakeman, D. L., *Org. Lett.* **2007**, *9*, 857-860.

(57) Wedekind, J. R.; Frey, P. A.; Rayment, I., *Biochemistry* **1996**, *35*, 11560-11569.

(58) Errey, J.C.; Mukhopadhyay, B.; Kartha, K. P. R.; Field, R. A., *Chem. Commun.* **2004**, 2796-2707.

(59) Peng, J. W.; Jonathan, M.; Abdul-Manan, N., *Prog. Nucl. Magn. Reson. Spectrosc* **2004**, *44*, 225-256.

(60) Otting, G., *Annu. Rev. Biophys.* **2010**, *39*, 387-405.

(61) Lui, Z.; Zhang, J.; Chen, X.; Wang, P. G., *ChemBioChem* **2002**, *3*, 348-355.

(62) Wedekind, J. R.; Frey, P. A.; Rayment, I., *Biochemistry* **1995**, *34*, 11049-11061.

(63) Jaing, J. Q.; Briggs, J. B.; Thorson, J. S., *J. Am. Chem. Soc.* **2000**, *122*, 6803.

(64) Waschke, D.; Thimm, J.; Thiem, J., *Org. Lett.* **2011**, *13*, 3628.

(65) Dondoni, A.; Scherrmann, M.-C., *J. Org. Chem.* **1994**, *59*, 6404-6412.

(66) Dondoni, A.; Marra, A. Pasti, C., *Tetrahedron: Asymmetry* **2000**, *11* (1), 305-317.

(67) Martin, O. R.; Saavedra, O. M.; Xie, F.; Liu, L.; Picasso, S.; Vogel, P.; Kizu, H.; Asano, N., *Bioorg. Med. Chem.* **2001**, 1269-1278.

(68) Kobertz, W. R.; Bertozzi, C. R.; Bednarski, M. D., *Tetrahedron Lett.* **1992**, *33*, 737-740.

Appendix 1. Selected NMR Spectra and Crystallographic Data

^{1}H NMR. 2,3,4,6-Tetra-*O*-benzyl-C-(1′-dibenzylphosphonomethyl)-α-D-galactopyranose **(2)**

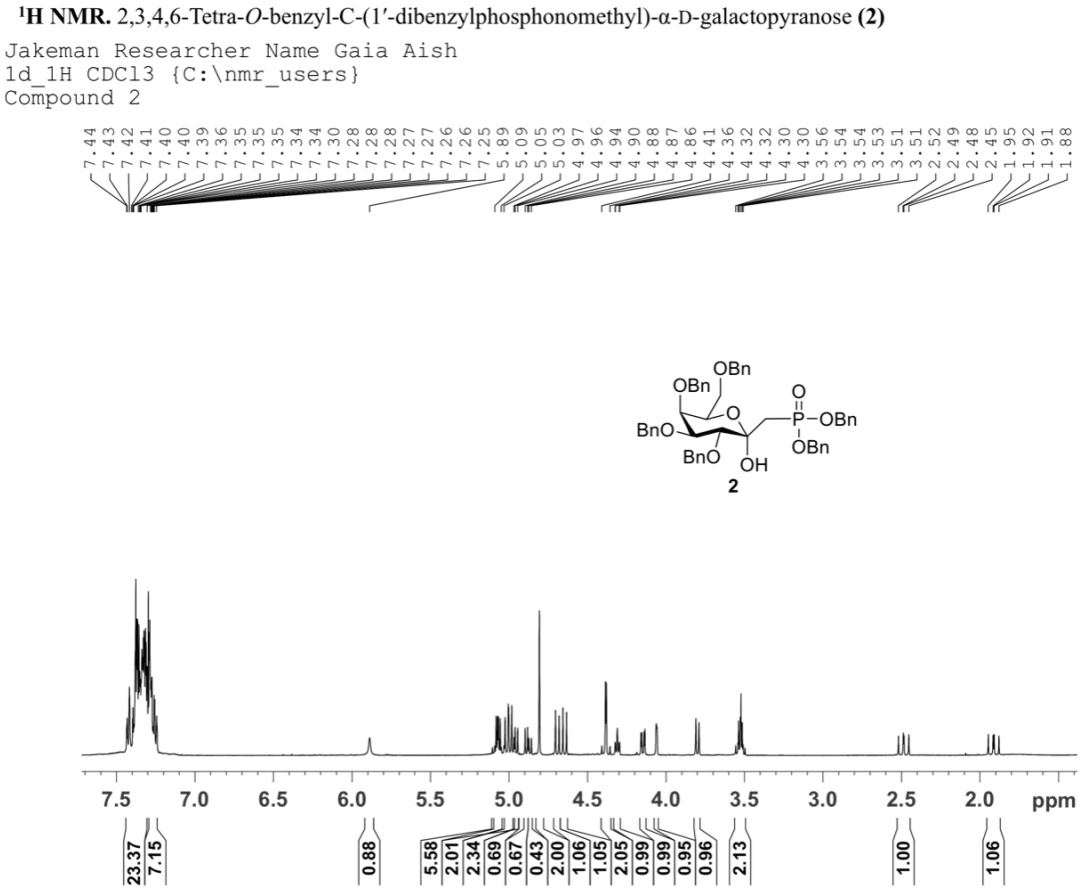

^{31}P NMR. 2,3,4,6-Tetra-*O*-benzyl-C-(1′-dibenzylphosphonomethyl)-α-D-galactopyranose **(2)**

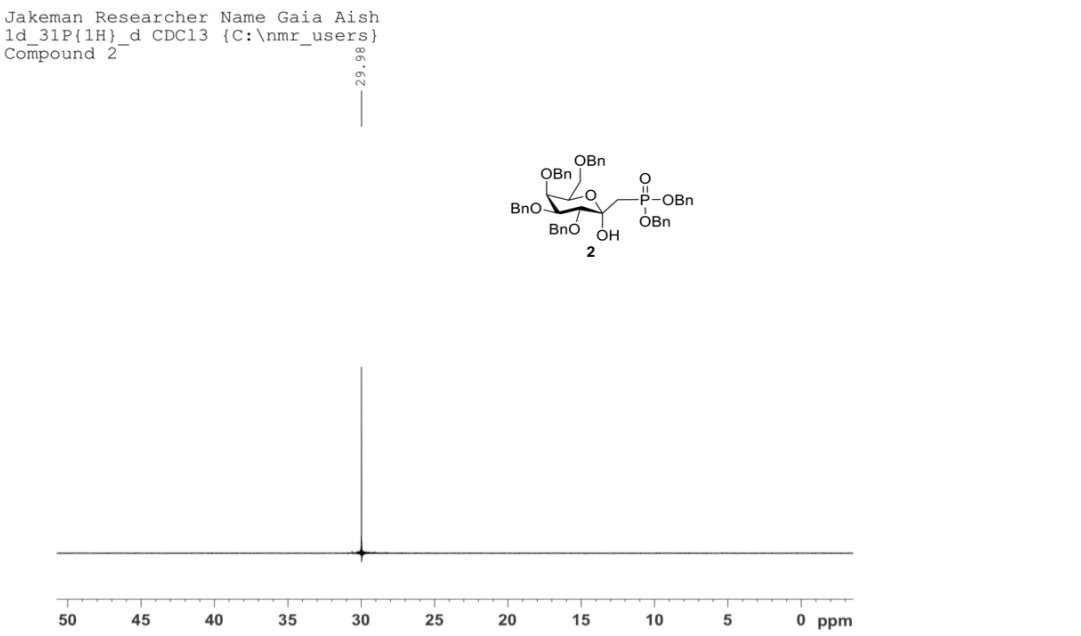

^{13}C NMR. 2,3,4,6-Tetra-*O*-benzyl-C-(1′-dibenzylphosphonomethyl)-α-D-galactopyranose **(2)**

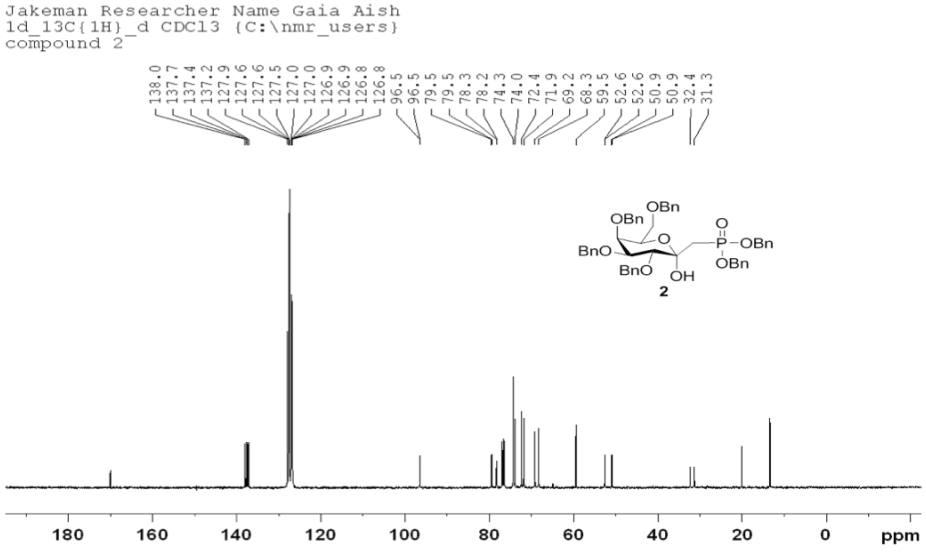

^{1}H NMR. Ammonium-C-(1′-phosphonomethyl)-α-D-galactopyranoside **(3)**

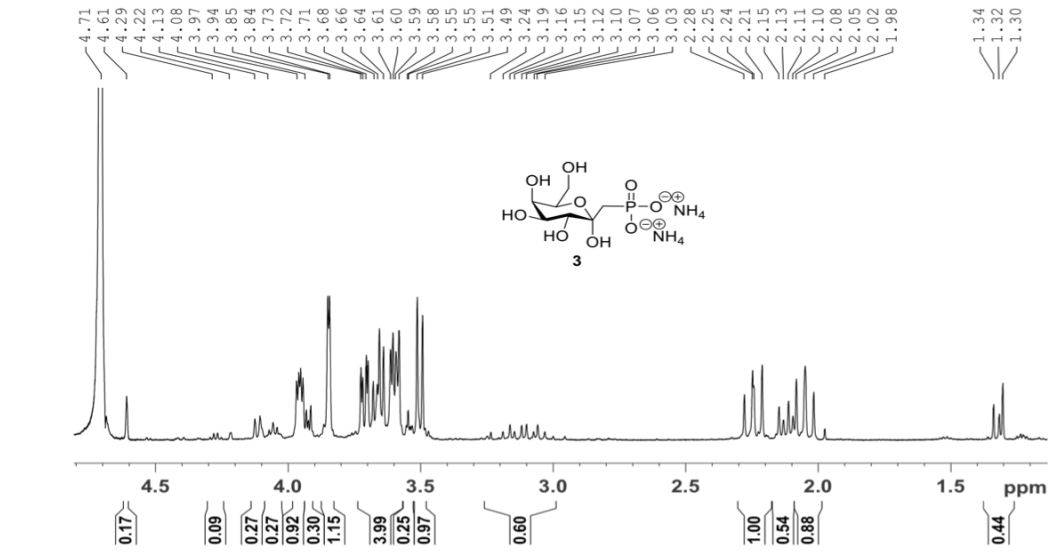

^{31}P NMR. Ammonium-C-(1′-phosphonomethyl)-α-D-galactopyranoside **(3)**

```
Jakeman Researcher Name Gaia Aish
1d_31P{1H}_d D2O {C:\nmr_users}
compound 3
```

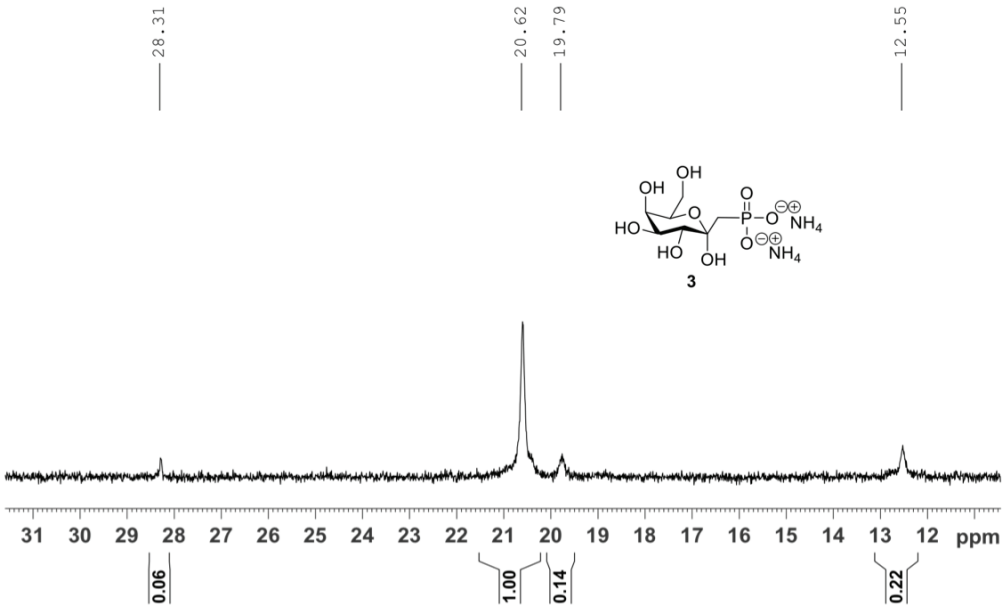

^{13}C NMR. Ammonium-C-(1′-phosphonomethyl)-α-D-galactopyranoside **(3)**

```
User Name gaia
Solvent d20
Sample Size ~ 5mg
gallckphos after LH20
imb_CARBON D2O
compound 3
```

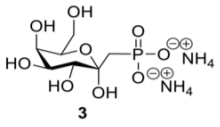

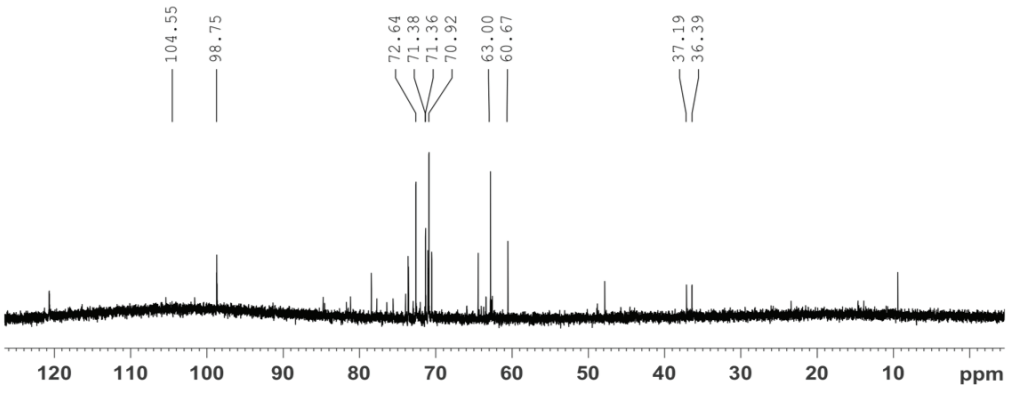

^{1}H NMR. Dibenzyl (Z)-C-(1′-deoxy-2,3,4,6-Tetra-*O*-benzyl-D-galactopyranosyl-2-ylidene) methanephosphonate **(4)**

```
gaia aish
exogycal
imb_PROTON CDCl3
compound4
```

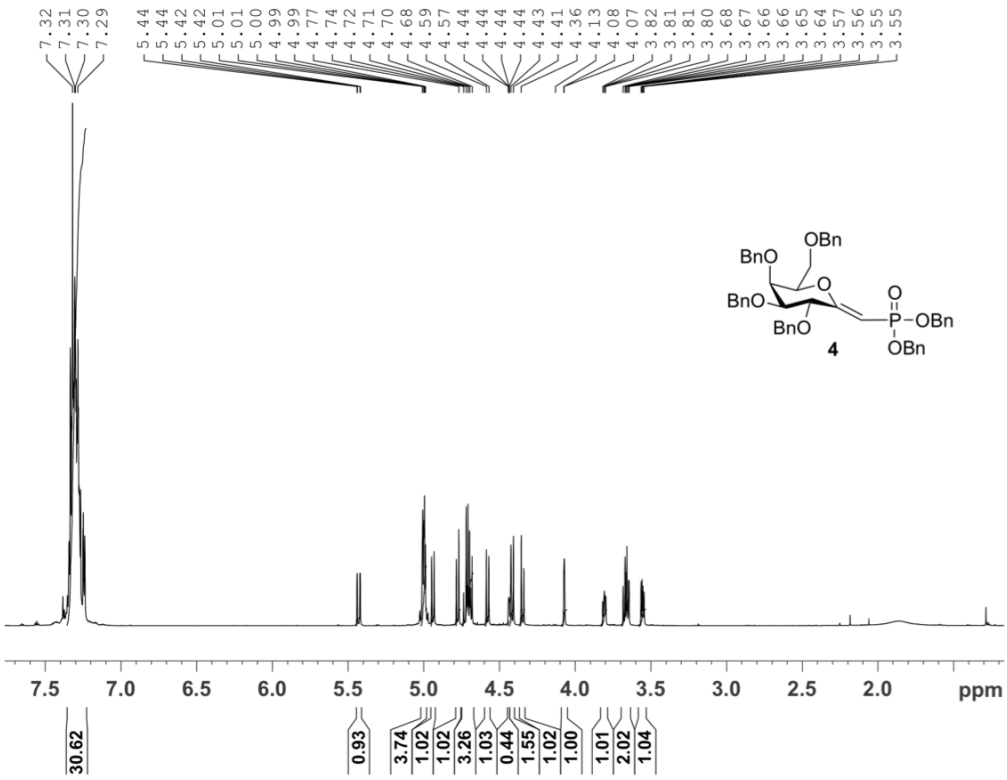

^{31}P NMR. Dibenzyl (Z)-C-(1′-deoxy-2,3,4,6-Tetra-*O*-benzyl-D-galactopyranosyl-2-ylidene) methanephosphonate **(4)**

```
Jakeman Researcher Name Gaia Aish
1d_31P{1H}_d CDCl3 {C:\nmr_users}
compound 4
```

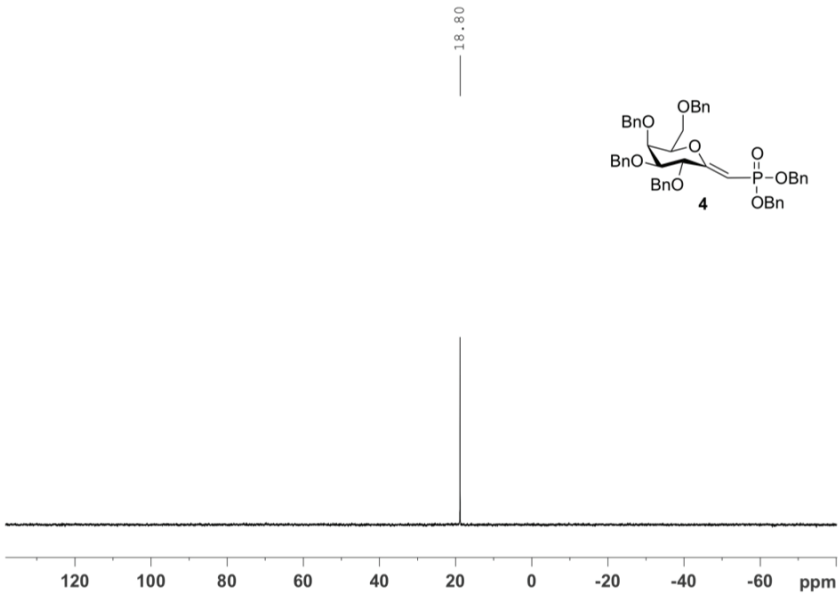

^{31}P NMR. Dibenzyl (Z)-C-(1′-deoxy-2,3,4,6-Tetra-*O*-benzyl-D-galactopyranosyl-2-ylidene) methanephosphonate **(4)**

```
Jakeman Researcher Name Gaia Aish
1d_31P{1H}_d CDCl3 {C:\nmr_users}
compound 4
```

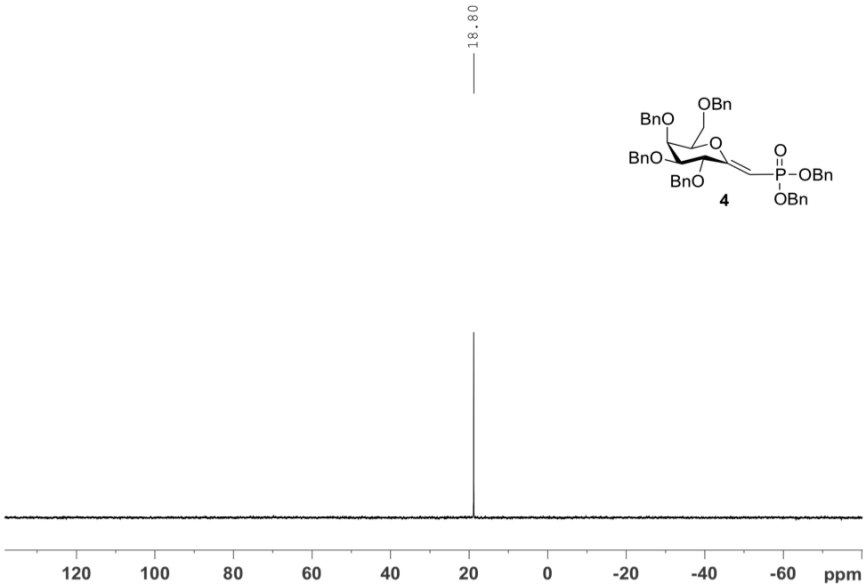

^{13}C NMR. Dibenzyl (Z)-C-(1′-deoxy-2,3,4,6-Tetra-*O*-benzyl-D-galactopyranosyl-2-ylidene) methanephosphonate **(4)**

```
Gaia Aish
imb_CARBON CDCl3
compound 4
```

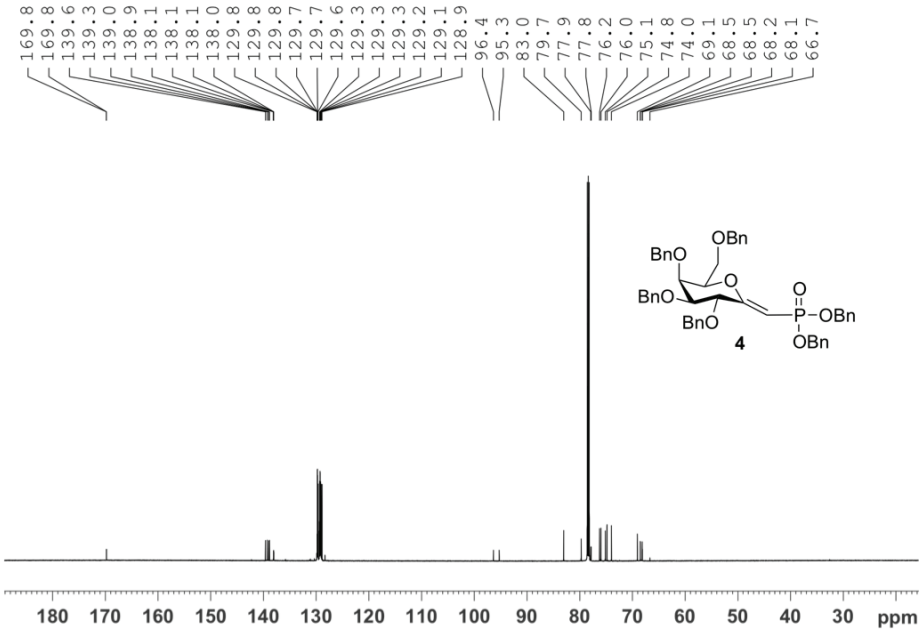

^{31}P NMR. 2,3,4,6-Tetra-*O*-benzyl-C-(1′*R*-Fluoro-dibenzylphosphonomethyl)-α-D-galactopyranose **(5)**

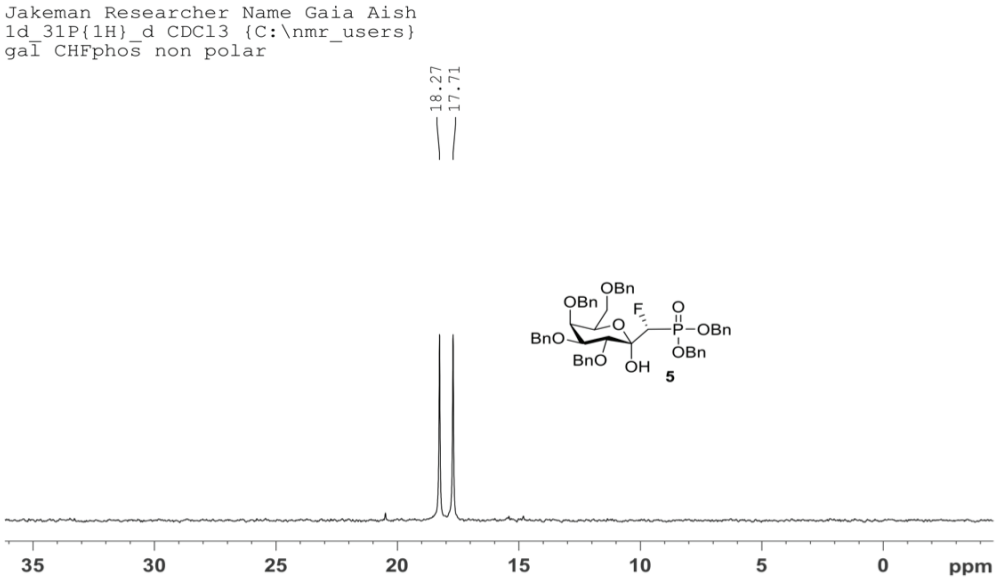

^{1}H NMR. 2,3,4,6-Tetra-*O*-benzyl-C-(1′*R*-Fluoro-dibenzylphosphonomethyl)-α-D-galactopyranose **(5)**

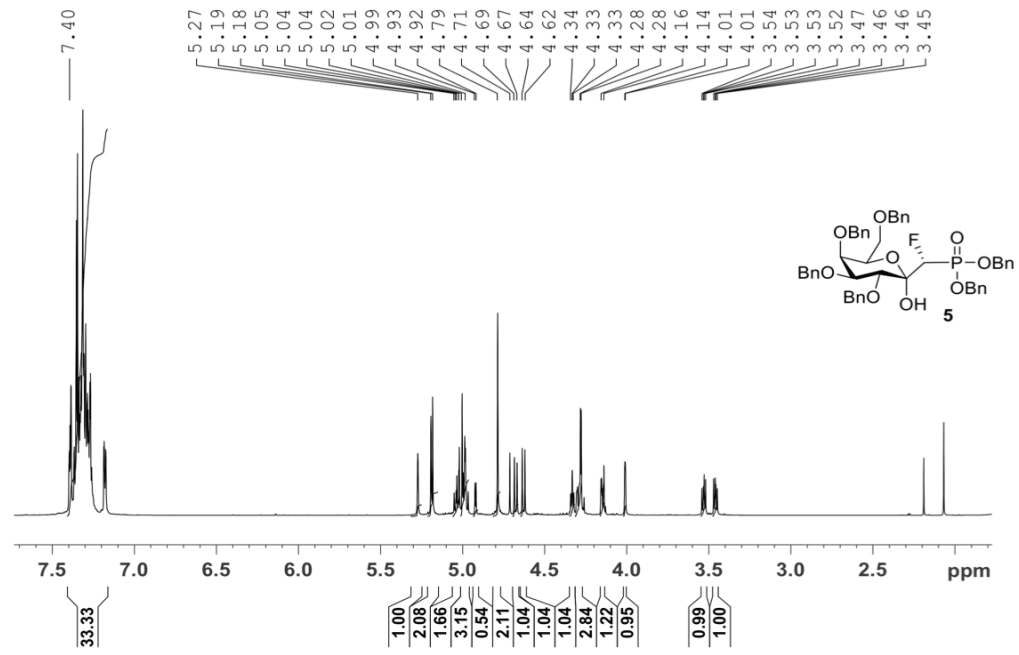

^{19}F NMR. 2,3,4,6-Tetra-*O*-benzyl-C-(1′*R*-Fluoro-dibenzylphosphonomethyl)-α-D-galactopyranose **(5)**

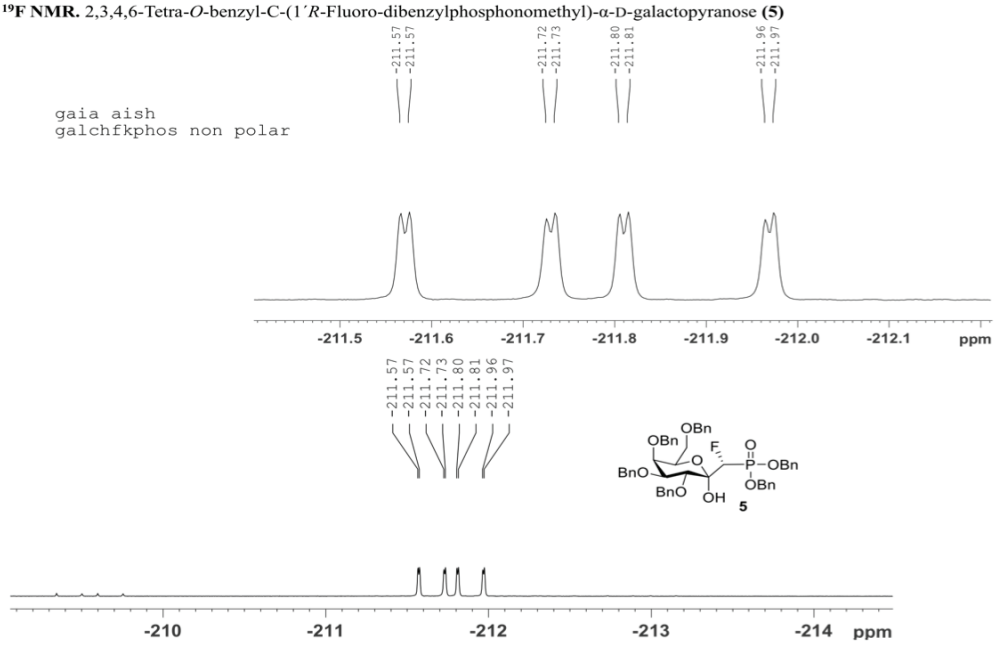

^{13}C DEPT NMR. 2,3,4,6-Tetra-*O*-benzyl-C-(1′*R*-Fluoro-dibenzylphosphonomethyl)-α-D-galactopyranose **(5)**

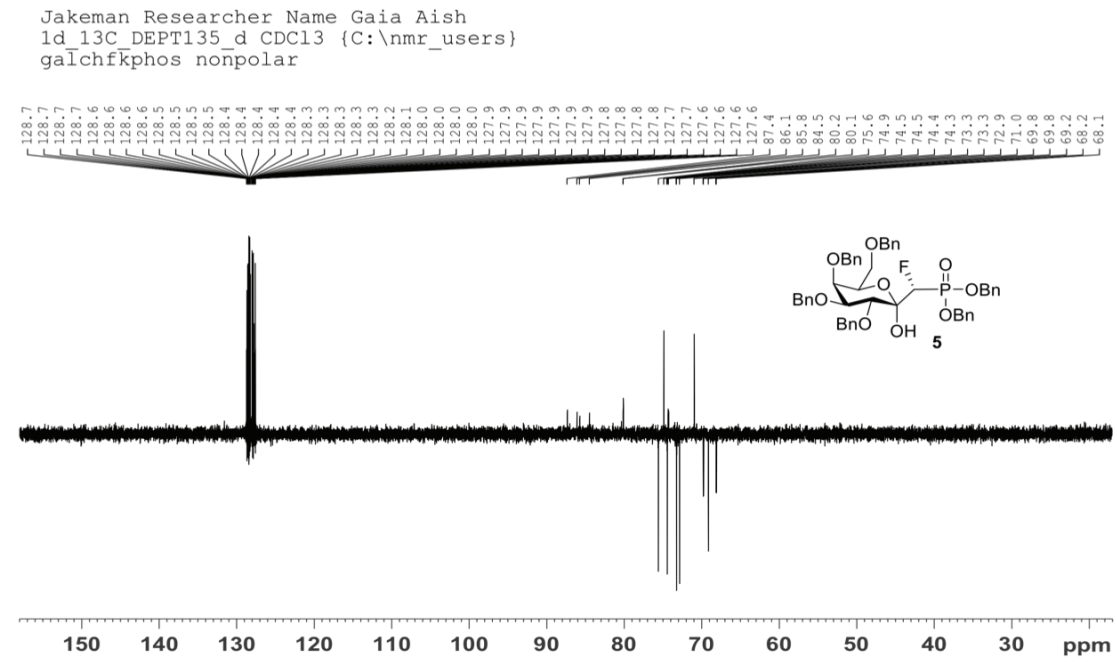

^{1}H NMR. 2,3,4,6-Tetra-*O*-benzyl-C-(1′*S*-Fluoro-dibenzylphosphonomethyl)-α-D-galactopyranose **(6)**

Jakeman Researcher Name Gaia Aish
1d_1H CDCl3 {C:\nmr_users}
galCHFkphos polar

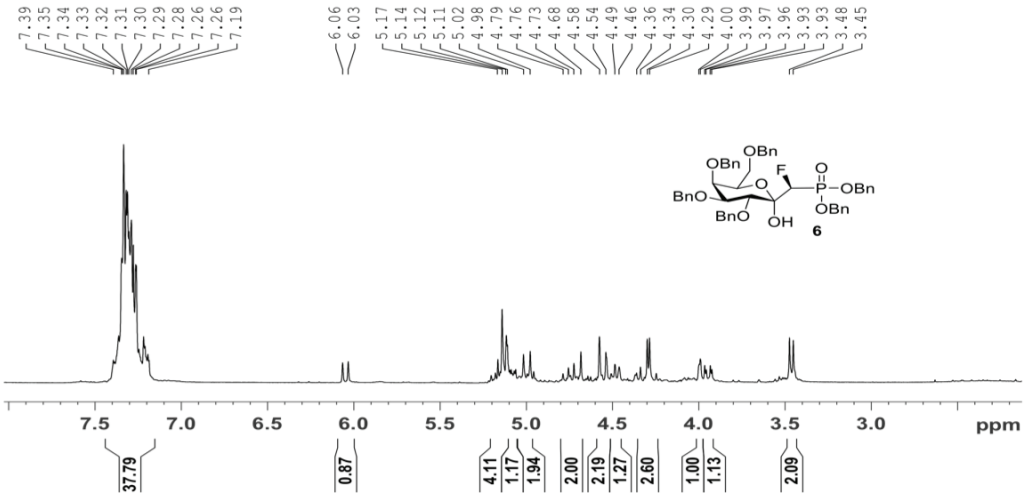

^{19}F DEPT NMR. 2,3,4,6-Tetra-*O*-benzyl-C-(1′*R*-Fluoro-dibenzylphosphonomethyl)-α-D-galactopyranose **(5)**

Gaia polar (8)

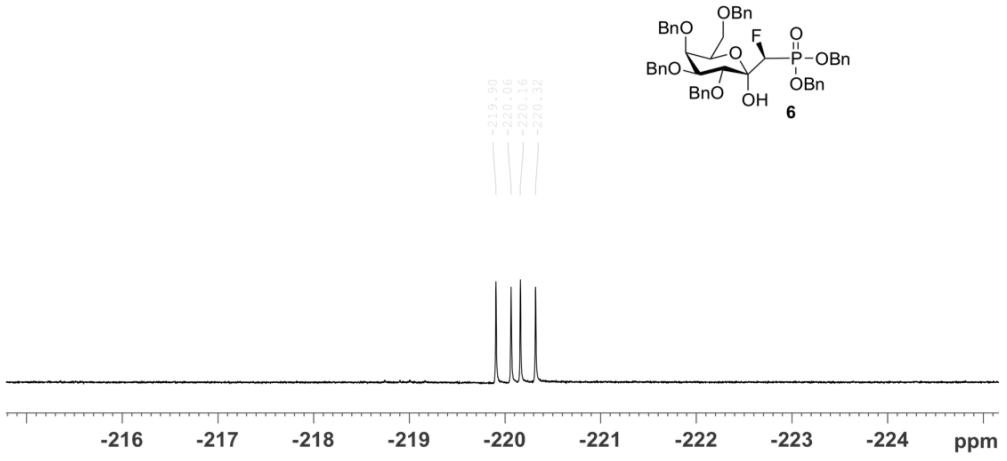

^{1}H NMR. Ammonium-C-(1′*R*-Fluoro-phosphonomethyl)-α-D-galactopyranoside **(7)**

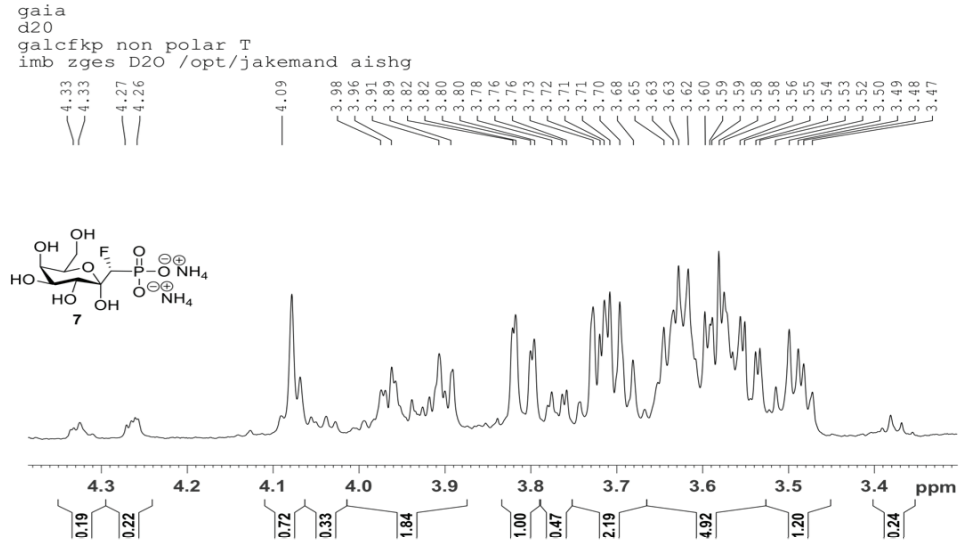

19F NMR. Ammonium-C-(1′*R*-Fluoro-phosphonomethyl)-α-D-galactopyranoside **(7)**

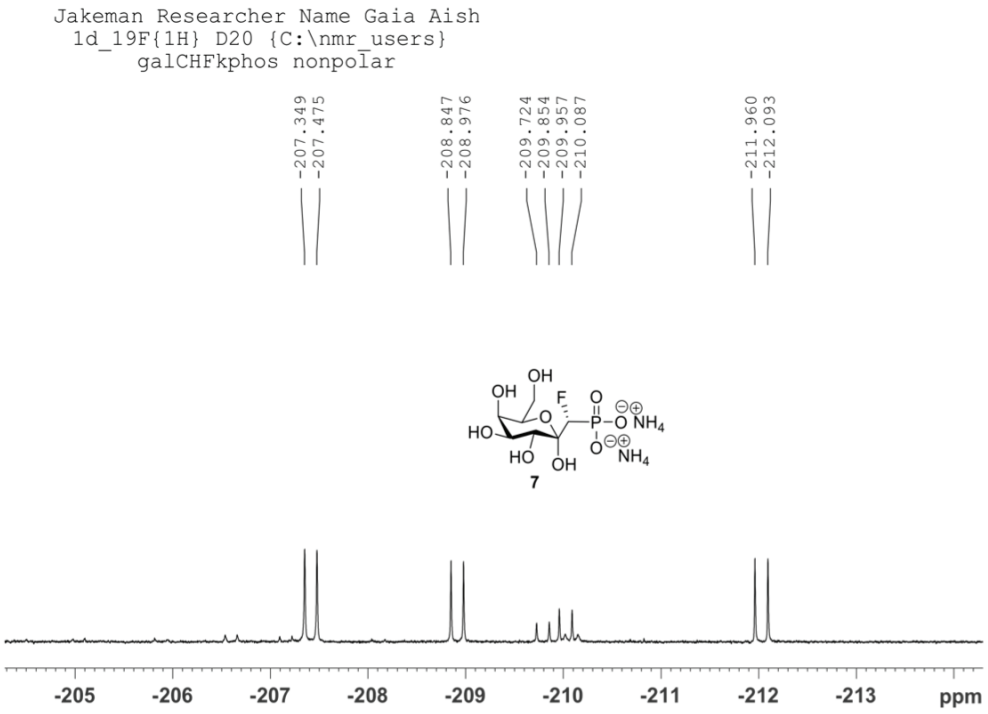

^{31}P NMR. Ammonium-C-(1′*R*-Fluoro-phosphonomethyl)-α-D-galactopyranoside **(7)**

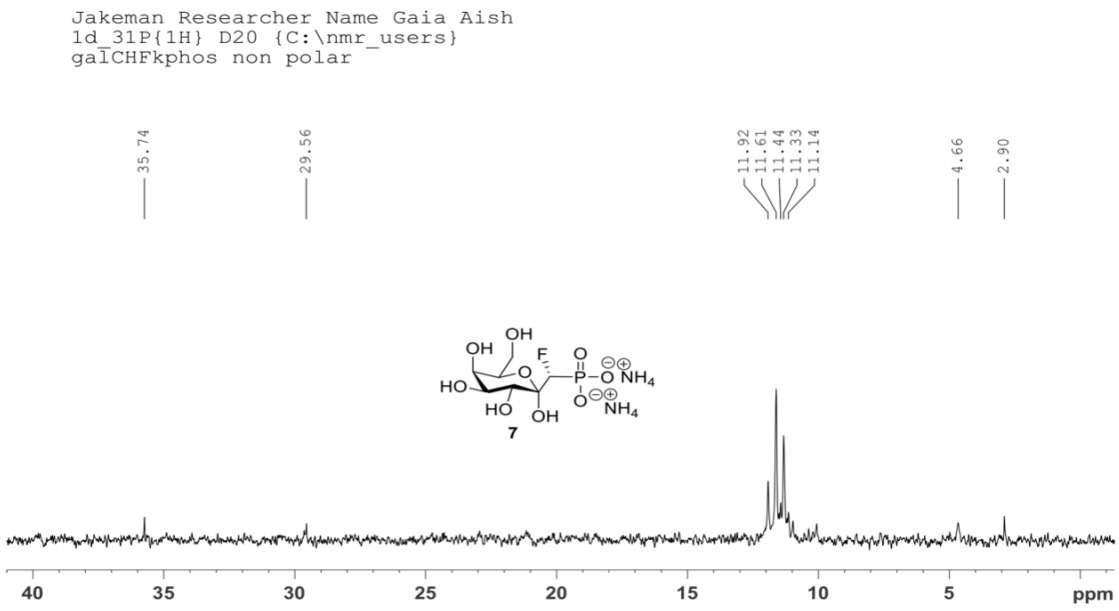

^{1}H NMR. Ammonium-C-(1′*S*-Fluoro-phosphonomethyl)-α-D-galactopyranose **(8)**

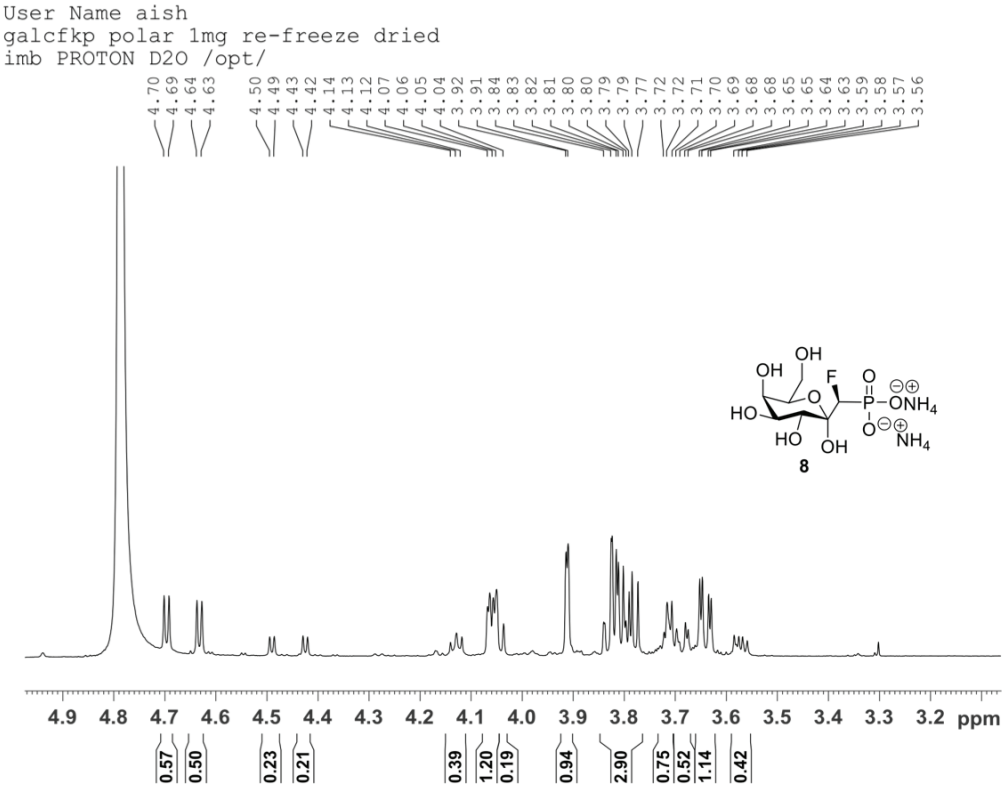

^{19}F NMR. Ammonium-C-(1′*S*-Fluoro-phosphonomethyl)-α-D-galactopyranose **(8)**

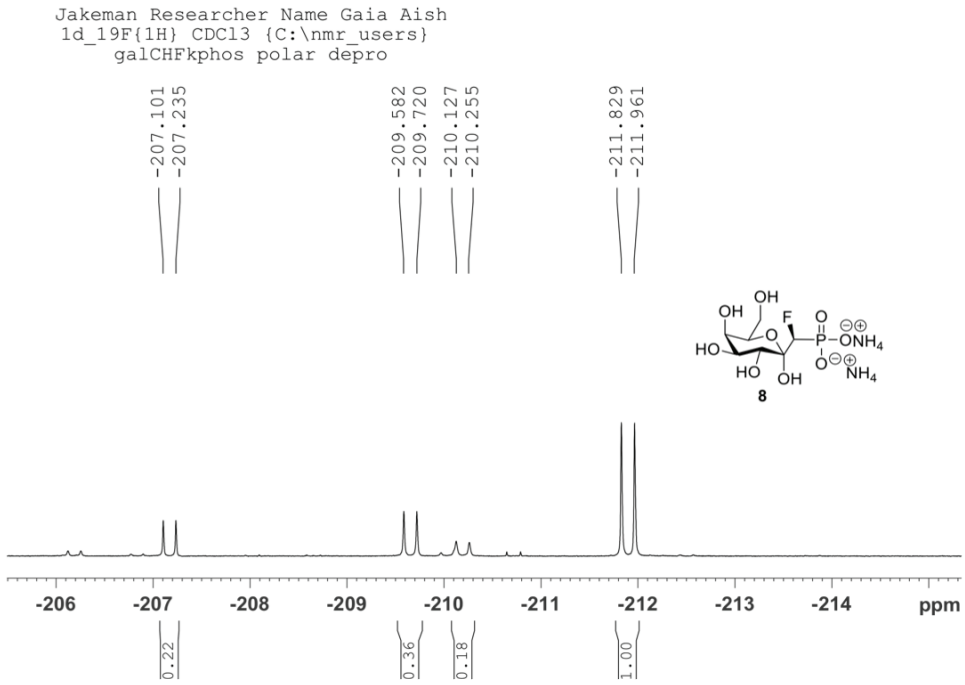

^{31}P NMR. Ammonium-C-(1′*S*-Fluoro-phosphonomethyl)-α-D-galactopyranose **(8)**

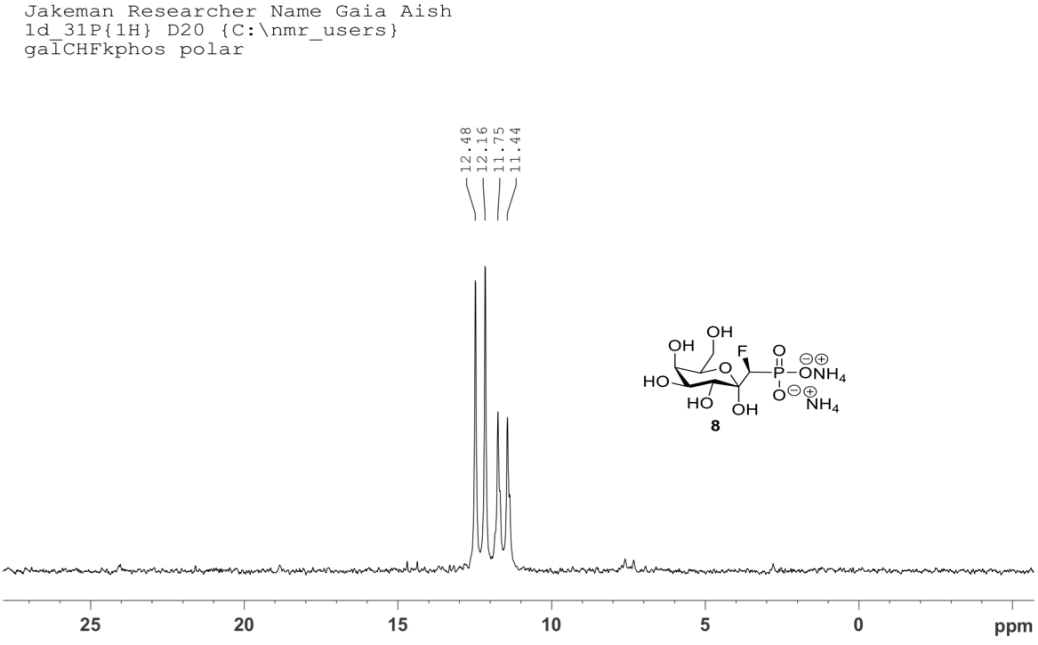

^{13}C NMR. Ammonium-C-(1′*S*-Fluoro-phosphonomethyl)-α-D-galactopyranose **(8)**

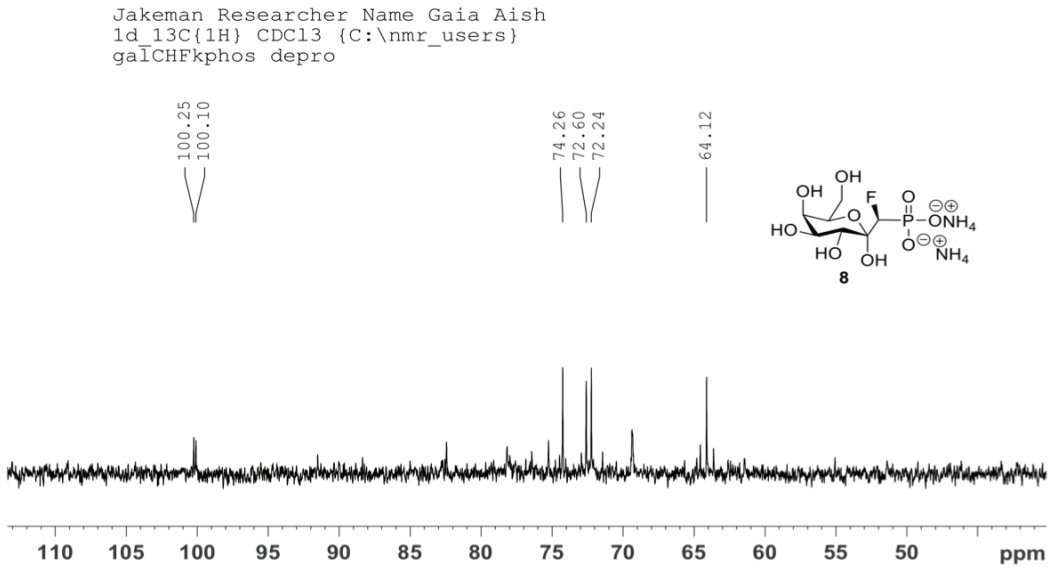

^{1}H NMR. 2,3,4,6-Tetra-*O*-benzyl-C-(1′-α,α-difluoro-diethylphosphonomethyl)-α-D-galactopyranose **(9)**

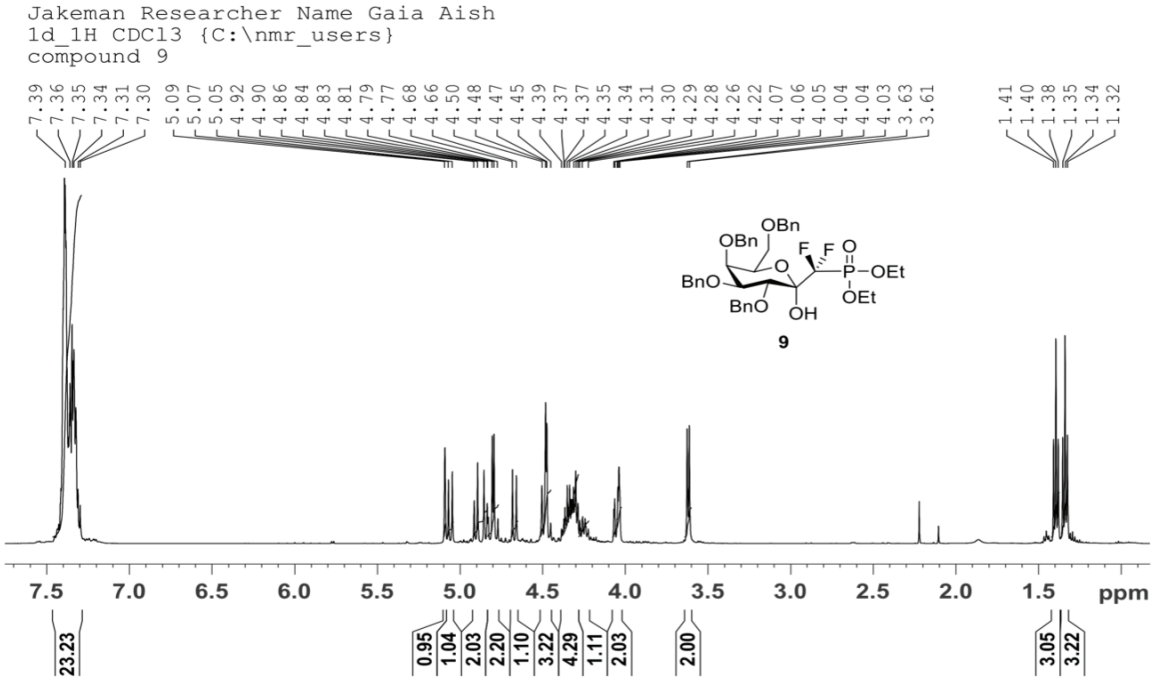

^{19}F NMR. 2,3,4,6-Tetra-*O*-benzyl-C-(1′-α,α-difluoro-diethylphosphonomethyl)-α-D-galactopyranose **(9)**

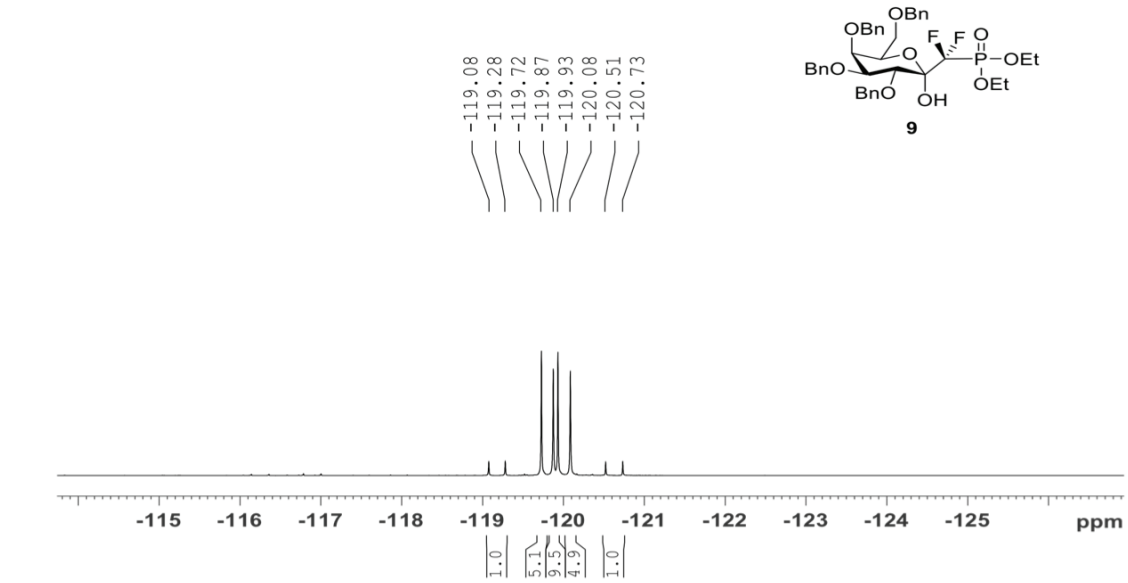

^{31}P NMR. 2,3,4,6-Tetra-*O*-benzyl-C-(1′-α,α-difluoro-diethylphosphonomethyl)-α-D-galactopyranose **(9)**

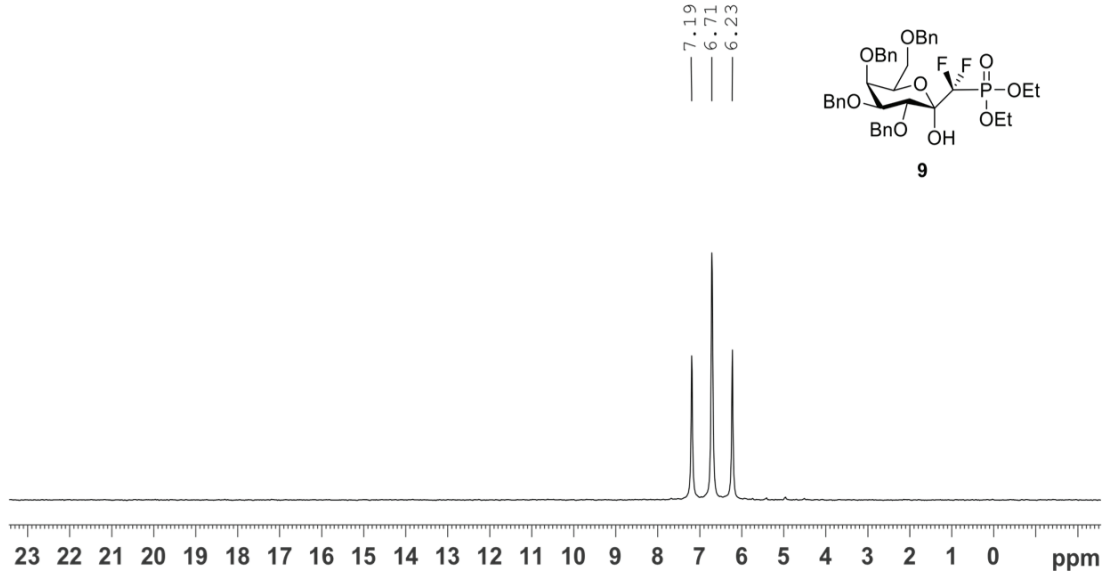

^{13}C NMR. 2,3,4,6-Tetra-*O*-benzyl-C-(1′-α,α-difluoro-diethylphosphonomethyl)-α-D-galactopyranose **(9)**

Jakeman Researcher Name Gaia Aish
1d_13C_DEPTQ135 CDCl3 {C:\nmr_users}
compound 9

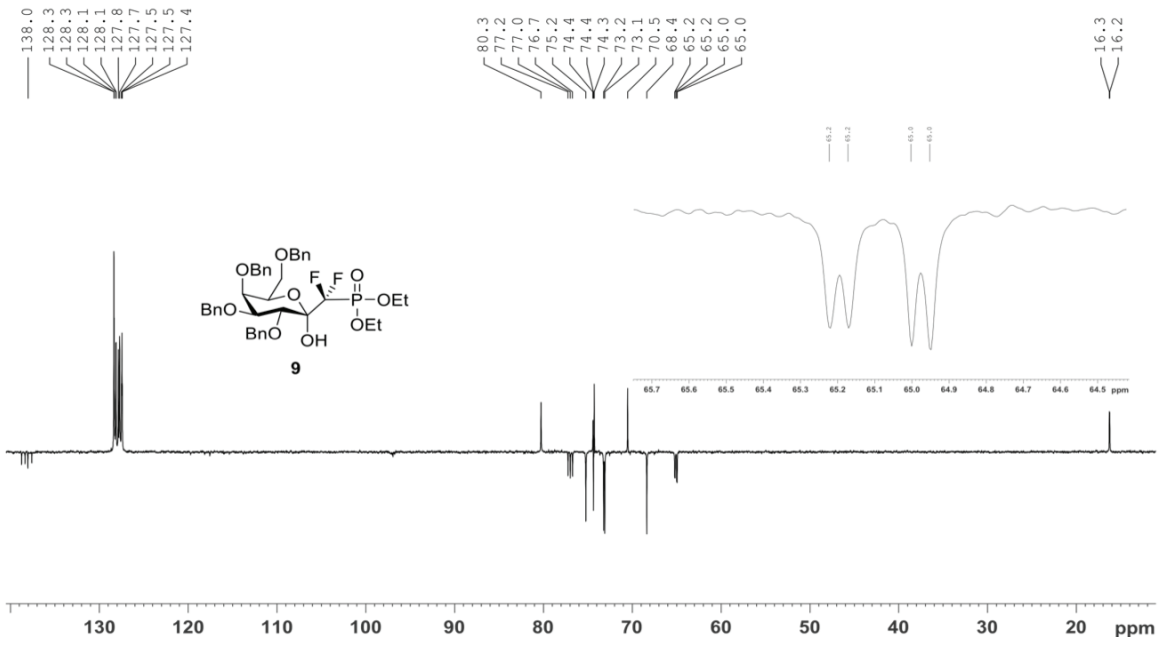

^{1}H NMR. Ammonium-C-(1′α,α-difluoro-phosphonomethyl)-α-D-galactopyranose **(10)**

Jakeman Researcher Name Gaia Aish
1d_1H D2O {C:\nmr_users}
compound 10

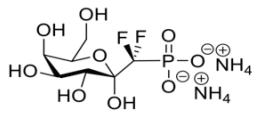

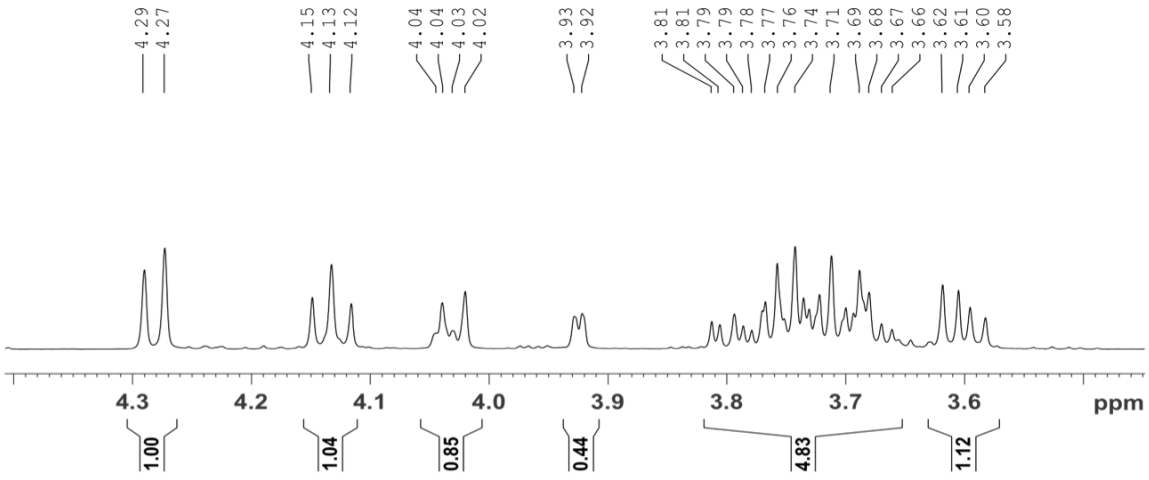

^{31}P NMR. Ammonium-C-(1′α,α-difluoro-phosphonomethyl)-α-D-galactopyranose **(10)**

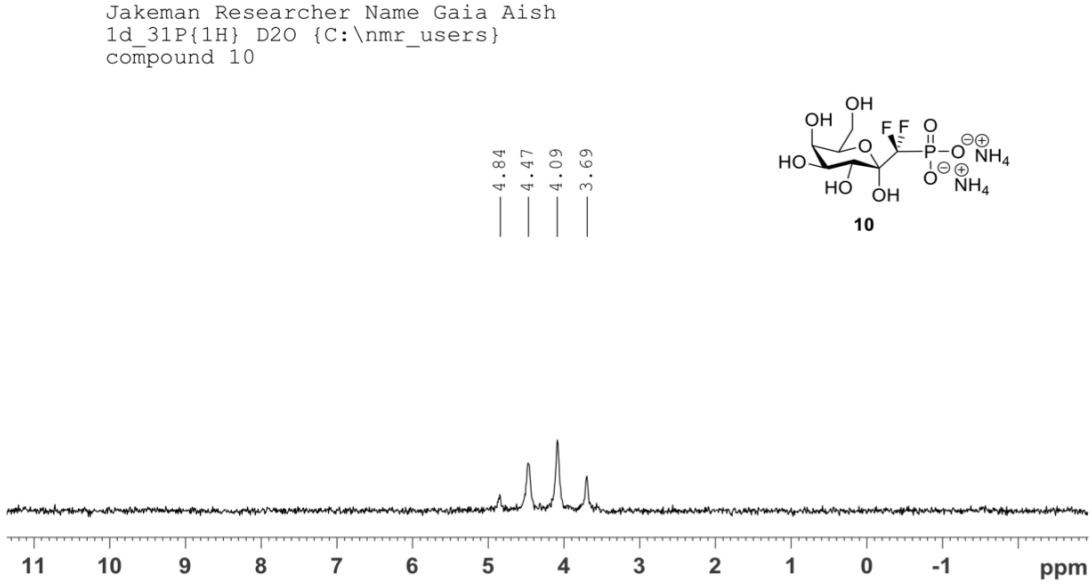

^{19}F NMR. Ammonium-C-(1′α,α-difluoro-phosphonomethyl)-α-D-galactopyranose **(10)**

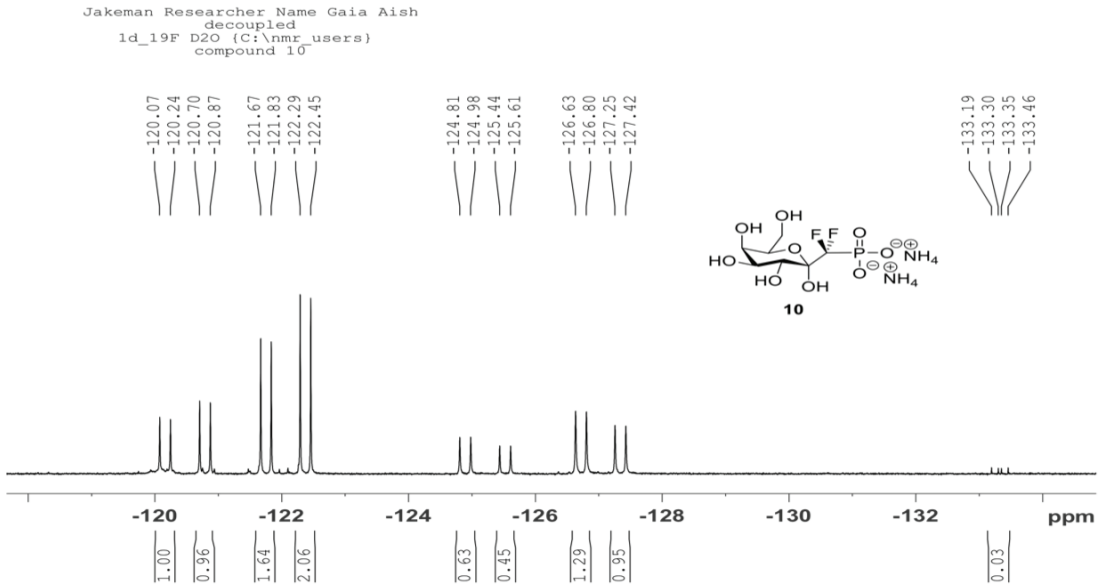

^{13}C NMR. Ammonium-C-(1′α,α-difluoro-phosphonomethyl)-α-D-galactopyranose **(10)**

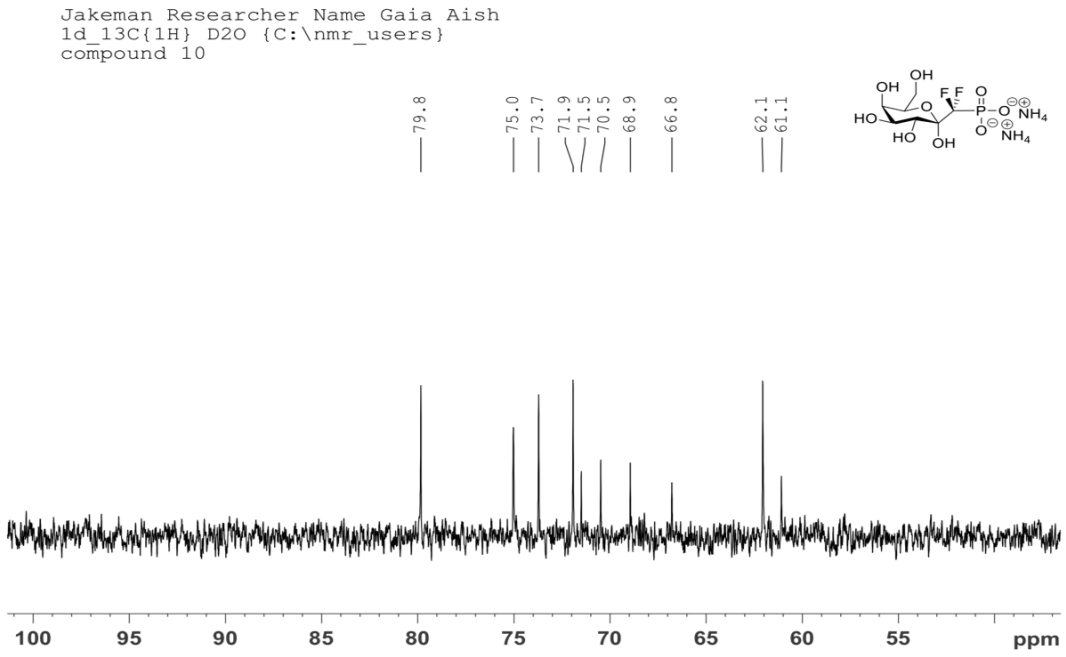

^{1}H NMR. 2,3,4,6-Tetra-*O*-benzyl-C-(1′-hydroxy-diethylphosphonomethyl)-α-D-glucopyranoside **(20)**

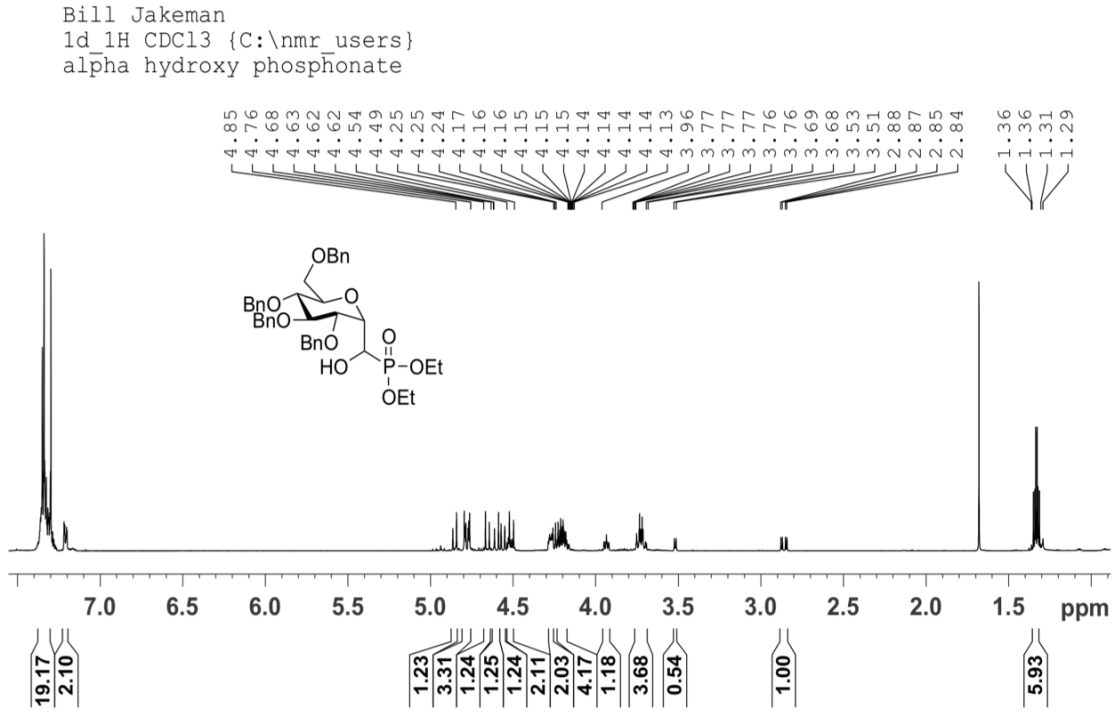

^{31}P NMR. 2,3,4,6-Tetra-*O*-benzyl-C-(1′-hydroxy-diethylphosphonomethyl)-α-D-glucopyranoside **(20)**

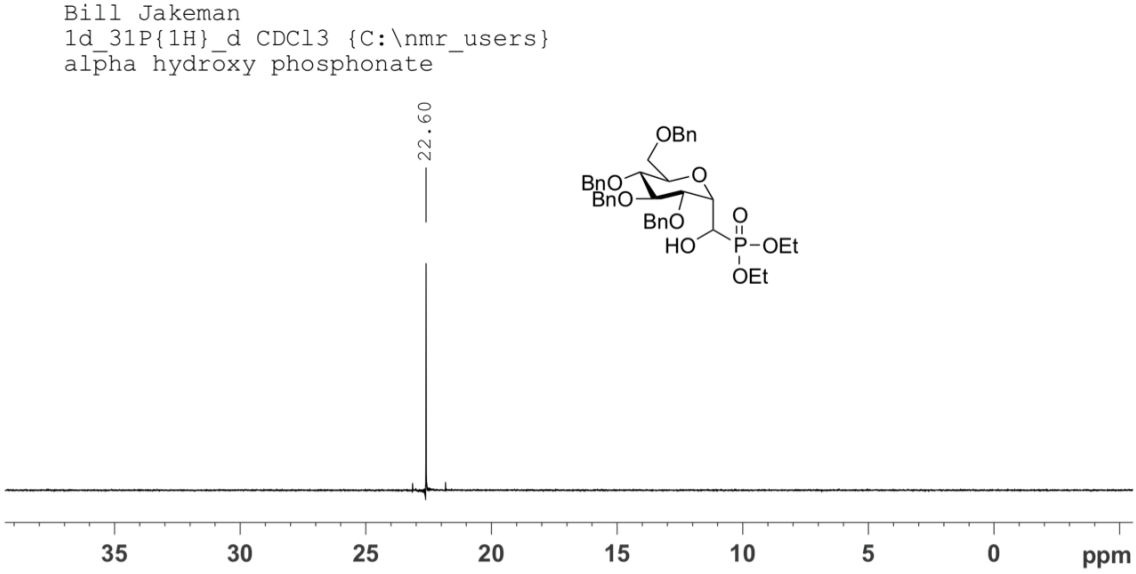

^{1}H NMR. Ammonium-C-(1′-hydroxy-diethylphosphonomethyl)-α-D-glucopyranoside **(21)**

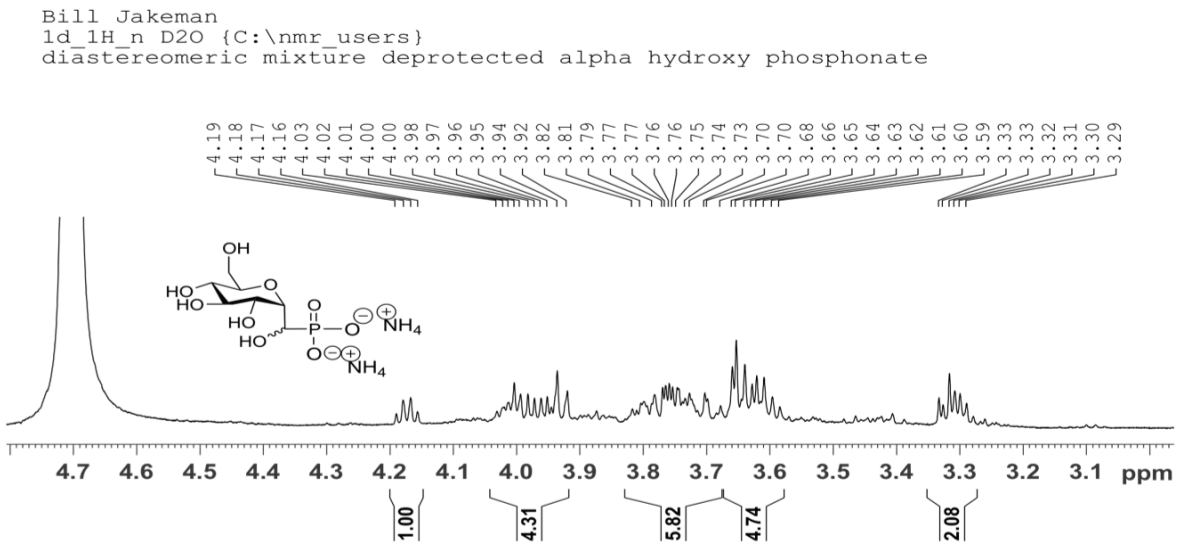

^{1}H NMR. Ammonium-C-(1′-hydroxy-diethylphosphonomethyl)-α-D-glucopyranoside **(21)**

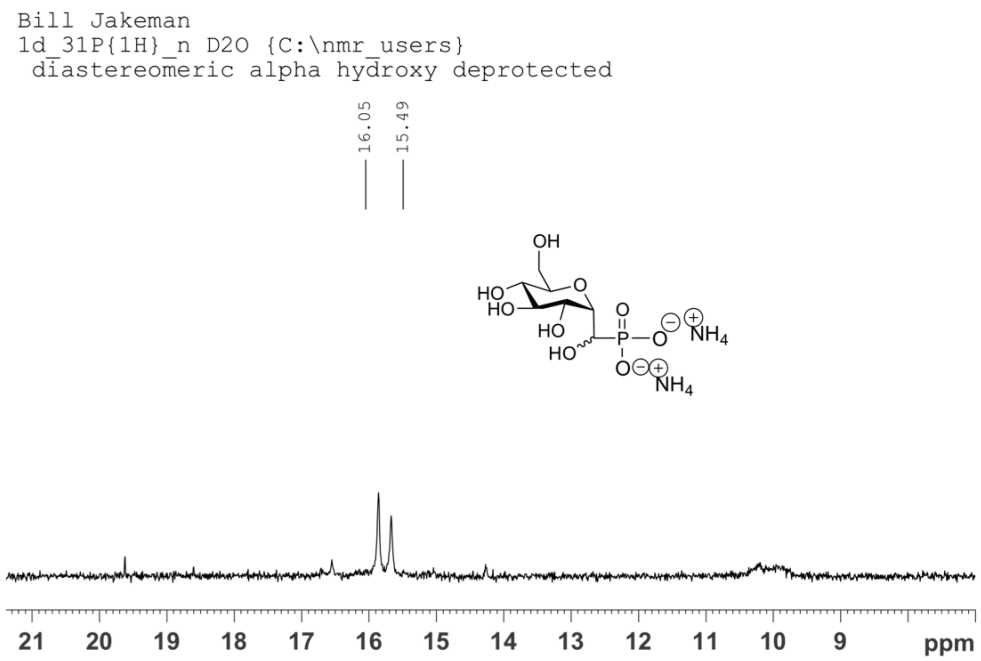

X-Ray Crystal Data. Experimental details.

A. Crystal Data

Empirical Formula	$C_{49}H_{52}O_9P$
Formula Weight	815.92
Crystal Color, Habit	colourless, needle
Crystal Dimensions	0.52 X 0.12 X 0.06 mm
Crystal System	monoclinic
Lattice Type	C-centered
Indexing Images	4 oscillations @ 3000.0 seconds
Detector Position	127.40 mm
Pixel Size	0.100 mm
Lattice Parameters	a = 29.8571(9) Å b = 5.6925(2) Å c = 26.8181(9) Å β = 112.3035(13) ^{o} V = 4217.0(2) Å^3
Space Group	C2 (#5)
Z value	4
D_{calc}	1.285 g/cm^3
F_{000}	1732.00
μ(MoKα)	1.230 cm^{-1}

B. Intensity Measurements

Diffractometer	Rigaku RAXIS-UNKNOWN
Radiation	MoKα (λ = 0.71070 Å) graphite monochromated
Data Images	24 exposures
ω oscillation Range	50.0 - 174.0^{o}
Exposure Rate	672.0 sec./^{o}
Detector Position	127.40 mm
Pixel Size	0.100 mm
$2\theta_{max}$	61.0^{o}
No. of Reflections Measured	Total: 13124 Unique: 9789 (R_{int} = 0.030) Friedel pairs: 3277
Corrections	Lorentz-polarization Absorption (trans. factors: 0.680 - 0.993)

C. Structure Solution and Refinement

Structure Solution	Direct Methods (SHELX97)
Refinement	Full-matrix least-squares on F
Function Minimized	Σ w (|Fo| - |Fc|)^2
Least Squares Weights parameters	Chebychev polynomial with 3 7.0098,-2.1306,5.2925,
$2\theta_{max}$ cutoff	52.0^o
Anomalous Dispersion	All non-hydrogen atoms
No. Observations (I>3.00σ(I))	5227
No. Variables	687
Reflection/Parameter Ratio	7.61
Residuals: R (I>3.00σ(I))	0.0499
Residuals: Rw (I>3.00σ(I))	0.0508
Goodness of Fit Indicator	1.147
Flack Parameter (Friedel pairs = 3277)	0.05(11)
Max Shift/Error in Final Cycle	0.000
Maximum peak in Final Diff. Map	0.57 e$^-$/Å^3
Minimum peak in Final Diff. Map	-0.29 e$^-$/Å^3